(4)

ERL-0449-SD

AR-005-365

DEPARTMENT OF DEFENCE

DEFENCE SCIENCE AND TECHNOLOGY ORGANISATION

SALISBURY

ELECTRONICS RESEARCH LABORATORY

SOUTH AUSTRALIA

SPECIAL DOCUMENT

ERL-0449-SD

LOCATING THE SOURCE OF LONG-DISTANCE RADIO DISTRESS SIGNALS FROM THE SOUTHERN OCEAN

G.L. GOODWIN

Approved for Public Release

AR-005-365

DEPARTMENT OF DEFENCE

DEFENCE SCIENCE AND TECHNOLOGY ORGANISATION

SALISBURY, SOUTH AUSTRALIA

ELECTRONICS RESEARCH LABORATORY

COMMUNICATIONS DIVISION

SPECIAL DOCUMENT

ERL-0449-SD

LOCATING THE SOURCE OF LONG-DISTANCE RADIO DISTRESS SIGNALS FROM THE SOUTHERN OCEAN

G.L. Goodwin

SUMMARY

This report summarises a feasibility study and strategy appropriate to search and rescue operations for ships or aircraft in distress in the Southern Ocean. The use of high frequency ionospherically-propagated radio transmissions is justified. Measurement of the direction of arrival of a radio signal facilitates ray-tracing through the ionosphere Characteristics of the F2 region mid-latitude ionisation trough are considered in detail. Because the trough is displaced towards Australia, its position must be known as near as practicable in real time for sufficiently accurate ray-tracing to be performed quickly enough after receipt of a distress signal. The differential Doppler technique using e.g. 150 and 400 MHz transmissions from NAVSAT (NNSS) satellites is recommended in locating the trough position.

DSTO ERL

POSTAL ADDRESS : Director, Electronic Research Laboratory
Box 1600, PO, Salisbury, South Australia, 5108

TABLE OF CONTENTS

A-1

LIST OF TABLES

LIST OF FIGURES

Page No.

LIST OF FIGURES (CONT.)

1. FOREWORD

The resources of the Australian Defence Forces can be called on as part of a search and rescue strategy in an expansive region adjacent to Australia, including the Southern Ocean extending south and southwest from Australia to Antarctica. The present report summarises a feasibility study carried out as part of the author's study programme during the period September, 1982 - March, 1983, while attached to the Ionospheric Studies Group at the Defence Research Centre, Salisbury (DRCS) on leave from the School of Physics of the South Australian Institute of Technology (S.A. Inst. of Tech.). A reasoned strategy is presented for search and rescue operations, together with a condensation of relevant background information.

This report was prepared in the context of a possible joint proposal between DRCS and the S.A. Inst of Tech. to apply radio direction-finding techniques and ionospheric ray tracing computations in determining the location (ship/plane) of long range radio distress signals. This proposal did not proceed because of changing priorities within the Defence Science and Technology Organisation (DSTO). However, Single Station Location (SSL) of HF distress signals propagating at latitudes containing the F2 region midlatitude trough continues to pose a real problem, the nature of which is examined in this report.

2. ABSTRACT OF CONTENTS

The study commenced with the premise that ships/'planes in distress will have available the normal means of radio communication.

It is concluded in Section 3 that over the next several years, at least, a search and rescue strategy should be based on the reception in Australia of long distance ionospherically-propagated transmissions at high frequency (H.F.) international distress frequencies (i.e. one or more of 2.182, 4.125 and 6.2155 MHz) since most ships/'planes have comparatively high power transmitters at these frequencies. An alternative, such as the use of low power emergency position indicating radio beacons (EPIRB), e.g. at 121.5 MHz to be received by near-polar orbiting search and rescue satellites (SARSAT), was in the proposal stage only, when this report was compiled.

In Section 4, it is assumed that the direction of arrival (azimuth and elevation) of ionospherically-propagated signals would be measured by means of at least one multi-element receiving aerial array in southern Australia. An extension of the existing DRCS RADFIN computer program would facilitate ray-tracing through the ionosphere, in computing the location of the signal source. Section 4 is mainly concerned with factors that limit the accuracy with which a signal source can be located. A limitation arises through a lack of directly observed ionospheric data over a wide expanse of Southern Ocean. A further limitation occurs because the south invariant magnetic pole (see Appendix 1) is displaced some 16 deg of latitude from the geographic pole towards Australia. This means that phenomena normally expected at high latitudes, occur nearer to Australia; in particular, the F2 region midlatitude trough of ionisation, a gross ionospheric feature, can occur at latitudes as far equatorward as the Australian continent. Although the trough can be modelled approximately, as considered in Section 4.3, its width, which can extend through 10 deg or more of invariant latitude (defined in Appendix 1), is unknown without direct measurement. In addition, the trough's mean position is a function of magnetic activity, and moves equatorwards under magnetically disturbed conditions; unfortunately, the trough's position cannot readily be estimated because the planetary K index (Kp), which is employed as an appropriate measure of magnetic activity, is not readily available until long

after required for computations. It is concluded that the accuracy of ray-tracing, and hence of signal source position location, will be severely restricted unless the midlatitude trough position and extent can be measured in approximately real time. The use of the Navy Navigation Satellite System (NNSS) and a differential Doppler technique (Section 7) are recommended to determine the trough position and latitudinal extent.

Section 5 summarises features of some satellite systems, with particular reference to their capacity, or otherwise, to serve in locating ships/'planes in distress. In particular, the MARISAT, proposed SARSAT, NNSS and Global Positioning System (GPS) systems of satellites are considered.

In Section 6, the characteristics of the midlatitude trough are discussed in detail. Its general location and features are considered, including the fact that although the trough is predominantly a winter night-time phenomenon, it can occur unpredictably at other times. The trough forms just equatorward of the auroral oval. As discussed in Appendix 3, an important factor in the trough's formation is the transport of excited N_2 equatorwards from the auroral region by thermospheric winds and by convection associated with magnetospherically produced electric fields. The excited N_2 undergoes reactions which remove ionised atomic oxygen and electrons from the F2 region.

The Doppler measurement of range is described in Appendix 2, providing background for Section 7 in which the differential Doppler technique is outlined. By means of this technique, changes in phase difference between coherent 150 and 400 MHz transmissions from a NNSS satellite are directly interpretable as changes in the ionospheric electron content along the ray path from satellite to receiver. This permits gross changes in electron content to be detected as the ray path encounters the trough edges, which allows the trough's position and extent to be determined.

Appendix 4 includes the results of preliminary computations of model midlatitude troughs, using a modified RADFIN program.

3. AUSTRALIAN EMERGENCY COMMUNICATION PROCEDURES

3.1 Introduction

The Department of Defence may be called on as part of the land/sea rescue strategy for a considerable area including the Australian continent, a large section of the Indian Ocean westwards of Australia and a region south and southwest of Australia to the pole. The southern region includes a vast expanse of the Southern Ocean which is the particular concern of the present report.

Figure 1 (Ref. 26; 1980) shows graphically that, following an alarm, there is an urgent need for land/sea rescue procedures to be initiated without delay, because the probability of human survival decreases rapidly with time. This figure presumably refers to "average" climatic conditions; under icy conditions at high latitudes, survival times could be considerably shorter.

The use of high and medium frequency distress signals should be effective in areas such as the Indian Ocean where there are many coastal stations in Australia, India and Africa, and numerous ships on well-used shipping lanes. These can all assist in applying direction-finding techniques to locate the source of a distress signal.

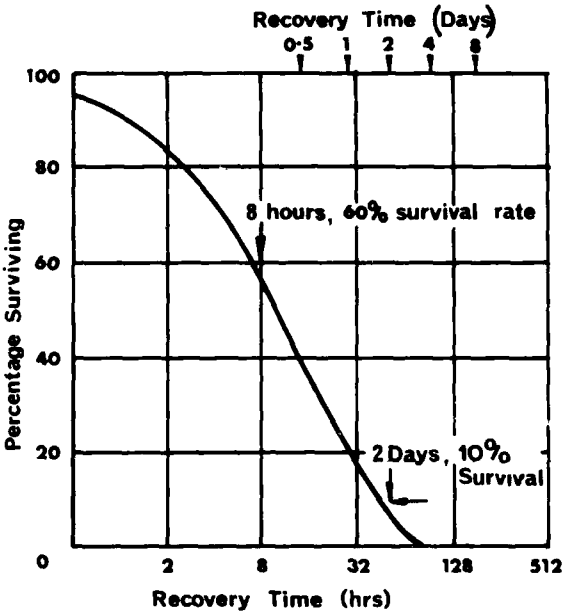

Figure 1. Probability of survival (%) is shown as a function of recovery time (from Refs. 26 and 60).

In contrast, much of the Southern Ocean carries little commercial shipping, and is also remote from coastal stations available for the reception of long-range distress signals. For this reason, searching operations in the Southern Ocean would rely heavily on direction-finding by means of long-distance transmissions in a region where published ionospheric characteristics are suspect because of the absence of directly observed ionospheric data. In particular, the properties of the mid-latitude "trough" of F-region ionisation (e.g. Ref. 22) discussed in Section 4.2 can cause gross errors in direction of arrival observations in Australia of radio signals propagated via the ionosphere from a source south of Australia. The characteristics of the trough are largely unmeasured at medium to high latitudes in the Southern Hemisphere, and must be inferred from (limited) Northern Hemisphere data (e.g. Ref. 39). Direct measurements of the trough position in the Southern Hemisphere would therefore be desirable, as a function of time of day, season, sunspot number and the planetary index (Kp) of magnetic activity.

Considering the size of this region, there are comparatively few coastal stations available. For both shipping and aircraft, distress signals would usually be long-range transmissions via the ionosphere at the international distress frequency, 2.182 MHz, or the supplementary frequencies, 4.125 and 6.2155 MHz. Maximum transmitted power is 400 W, but 25 W is a typical value for small craft. (The following discussion largely disregards transmitter/receivers operating at higher frequencies, since these are primarily for short-range communication and would not normally involve the ionosphere.)

Ref. 40 indicates emergency procedures for Australian shipping, that are also appropriate for aircraft. (A corresponding book is not available specifically for aircraft.)

Ships in distress rely heavily on other ship and shore stations receiving distress signals at one or more frequencies reserved for this purpose. Station operators are obliged to keep a record of particulars of all distress messages transmitted or received. A distress message should, if practicable, include the position (geographic latitude and longitude in degrees and minutes) of the craft in distress, or its position in relation to a well-known geographical feature. In the present discussion it is assumed that the ship/'plane location is either unknown or requires confirmation, so that the measures recommended in Section 4.1 need to be put into operation.

3.2 Medium and High Frequencies

Ship stations are expected to keep the maximum watch practicable on the international radiotelephone distress and calling frequency, 2.182 MHz, particularly during the three-minute "silence" periods reserved exclusively for distress signals, commencing on each hour and half-hour. The high frequencies (HF), 4.125 and 6.2155 MHz, are supplementary to 2.182 MHz for distress and safety purposes, and have a schedule of monitoring by the Australian Overseas Telecommunications Commission (OTC) shore stations. (All such stations keep watch on 6.2155 MHz within their station hours, which are at least 0500-1900 hours local time, while four stations, of which only Perth is relevant to the Southern Ocean, keep continuous watch during their hours of service.)

Where practicable, the distress ("Mayday") signal is preceded for one minute, by an alarm signal of two modulation frequencies transmitted alternately at 2200 and 1300 Hz.

The following propagation guide indicates the practical limitations in communication from ship-board at medium and high frequencies:
During daytime, when ionospheric D-region absorption is strong, 2 MHz communication is limited to approximately 80 to 160 km, depending on the ship's transmitter power and antenna efficiency; 2 MHz is the first choice of frequency for night-time communication via the ionosphere.
The normal day-time frequency is 4 MHz for distances of the order of 300 km, and for night-time communication when 2 MHz is unsatisfactory due to attenuation with distance or "static" noise.
For day-time communication, 6 MHz is used when long distances make 4 MHz unsatisfactory. The use of 6 MHz is not recommended at night on occasions when lower frequency communication is possible, because of the interference potentially caused and received with long distance 6 MHz transmissions.

Single sideband transmission at 2, 4 and 6 MHz is employed mainly by smaller ships, e.g. fishing vessels and non-commercial ("pleasure") yachts at maximum allowable transmitter powers of 400 W. In practice, small ship users normally purchase transmitters with 100 W peak envelope power which typically provide 25 W of aerial power; transmitted power must exceed 15 W to be acceptable to the Commonwealth Department of Communications. Small ships commonly have a "wire" (inverted L) aerial or a "whip" (approximately vertical) aerial if the ship has no mast. Several HF bands, nominally at 2, 4, 6, 8, 12, 16, 22, 25 and 27 MHz, are in general use; some bands are for Morse (i.e. amplitude modulation) and others involve single sideband transmissions, with peak envelope powers of 400 W. Their use is for long-range communication from both ships and aircraft. Big aircraft use continuously variable transceivers, whereas light aircraft often use 10 to 20 fixed frequencies.

Most big ships would normally operate at high powers in the medium frequency (MF) maritime band (410-512 kHz) for long-distance communication in telegraphy (Morse code) at a frequency which was returned to the earth by the ionosphere both in the day-time and at night. They would generally use 500 kHz (or else 2.182 MHz) for transmitting their own distress signals in telegraphy. Such ships, as well as shore stations, would have direction-finding equipment for identifying the directions of signals at these international distress frequencies, from other ships in distress.

In emergency operations, MF and HF transmitters on craft in distress are used as beacons for long-range transmissions over several hundred km to searching aircraft equipped with direction-finding facilities.

3.3 Very High Frequencies

The very high frequency (VHF) maritime mobile radiotelephone service operates with frequency modulation on channels in the ranges 156.375-156.80 MHz and 161.575-161.95 MHz providing a widely-used service for port authorities and commercial users, e.g. fishing boats, tugs and oil rigs, as well as for a growing non-commercial usage, e.g. for yachts. In particular, 156.80 MHz is allocated as an international distress and safety frequency and 156.375 MHz as a supplementary safety frequency. Ships at sea are expected to keep a listening watch on 156.80 MHz. The anticipated working range is low, being a maximum of 24 to 40 km for ship to shore communication, and 13 to 19 km for ship to ship, corresponding to a maximum ship transmitter power of 25 W, and substantially less actual power transmitted.

Large commercial 'planes over the Australian mainland, including flights to Tasmania, are in constant contact with air traffic control at one or other major airport, so that an aircraft's location would be known reasonably pecisely in case of emergency. These aircraft use VHF at 118 to 135.9 MHz at comparatively low powers of the order of several watts. Long wire transmitting-receiving aerials are commonly used in aircraft, e.g. from cockpit to tail, or, in light aircraft, a horizontal V-shaped aerial attached to the tail, cockpit and wing.

Emergency positions indicating radio beacons (EPIRB) are being progressively fitted, in a semipermanent fashion, to Australian ships and light aircraft. An EPIRB is a battery-operated low-power radio transmitter which sends a repetitive sawtooth-modulated emergency signal on both the international civil and military aircraft distress frequencies (121.5 and 243 MHz respectively). Maximum battery life is about 48 hours. "Hand held" EPIRBs are portable devices carried e.g. in a brief-case,which are more common in light aircraft and could be used, e.g. in rubber dinghies. The aerial is often a "whip" about 31 cm long (a quarter-wave at 243 MHz). Alternatively, flotation EPIRBs, e.g. attached to a life-raft by a tow-line, are carried by ships and aircraft on trans-oceanic flights.

It has been claimed (Ref. 26) that, world-wide, there are approximately 190,000 'planes and 2000 ships equipped with 121.5/243 MHz EPIRBs. This does not, however, reflect the situation for Australian 'planes on domestic flights which would, in general, not be equipped with EPIRBs; the exception would be for flights over some prescribed desolate areas of the Australian interior. EPIRBs would aid to searching aircraft, equipped with detection-finding facilities, in seeking marine and aviation casualties in and around Australia. The detectable range of an EPIRB transmission at sea is approximately 100 km, depending on the height of the searching aircraft and its receiver sensitivity.

A future possibility is the use of proposed SARSAT satellites, as considered in Section 3.2, to receive low-power EPIRB transmissions and to use Doppler techniques in locating the transmission source; this is, however, in the proposal stage only.

3.4 International Distress Frequencies - Summary

As detailed in the above discussion, international distress frequencies for "May day" calls are 2.182 MHz (at 400 W maximum power for SSB transmissions), 27.880 MHz (at 4 W power), 156.8 MHz (at 25 W power), as well as EPIRB at 121.5 and 243 MHz. Supplementary distress frequencies are 4.125 and 6.2155 MHz (at 400 W), 27.860 MHz (at 4 W) and 156.375 MHz (at 25 W). In addition, the 500 kHz band is commonly employed for distress signals.

For practical purposes, direction-finding for vessels in distress in the Southern Ocean and remote from the Australian coastline, would be restricted to HF (2.182, 4.125 and 6.2155 MHz) because of the comparatively high powers transmitted at these frequencies and the fact that they can be propagated over long distances via the ionosphere.

3.5 Radio Installations in Australian Shipping

Table 1, which gives information on the frequencies of transmitter-receivers installed in Australian ships, is a summary of data provided from the Adelaide office of the Radio Frequency Management Division, Australian Department of Communications. The third column indicates that in those States (Victoria, South Australia, Western Australia and Tasmania) with coastlines on the Southern Ocean, 5086 individual ships have HF installations at 2.182 MHz capable of long-range communications; in contrast the (generally smaller) ships which belong to clubs are equipped predominantly with 27 MHz equipment suitable for limited range coast and ship communication. It is noted that information in Table 1 is restricted to commercial and "pleasure" craft only.

TABLE 1. DISTRIBUTION OF COMMUNICATION FREQUENCIES IN AUSTRALIAN SHIPS

	INSTALLATION FREQUENCIES	VIC, SA, WA, TAS	NSW, QLD, NT, ACT
Ships (generally larger) equipped with radio-telephone installations which comply with the Wireless Telegraphy Act.	2.182 MHz and possibly also at other frequencies	5,086	5,280
	27 MHz	1,040	2,118
Ships (generally smaller) which belong to clubs, e.g. for pleasure, fishing.	27 MHz	7,289	11,705
	HF, VHF and UHF	92	29
	Undefined	2,206	213

4. DIRECTION OF ARRIVAL OF RADIO SIGNALS

4.1 A Facility for Locating Sources of HF Distress Signals

In order to locate the sources of HF radio distress signals at middle to high southern invariant geomagnetic latitudes, it is proposed that at least one multi-element receiving aerial array be established in southern Australia, e.g. near Adelaide, to act as a phase interferometer. The aerial outputs of the array would have different phases, and be combined to produce lobes of maximum reception in specified directions. This would allow both the azimuth and elevation of an incoming HF signal to be measured to a specific accuracy. One or more arrays of this kind are expected to be the basis of a facility whereby sources (ships/aircraft) of comparatively high power signals can be located rapidly in the Southern Ocean.

Errors can arise in HF direction-finding because of the occurrence of ionospheric irregularities which distort the otherwise smoothly "reflecting" ionosphere and cause ionospherically-propagated signals to deviate from great-circle paths and/or to be returned from unexpected heights. Normally, irregularities arise from three main

causes, namely travelling ionospheric disturbances, ionospheric tilts and sporadic E (e.g. Refs. 35 and 41). However, at the high invariant geomagnetic latitudes of the Southern Ocean, the mid-latitude trough, when it occurs, will produce steep gradients of electron density which could be the major source of errors in direction-finding at unpredictable times.

As part of the facility, it is proposed to set up a differential Doppler satellite-receiving system to obtain, almost in real time, the location of the F-region mid-latitude ionisation "trough" (discussed in detail in Section 4.4 and Appendix 4) in order to facilitate realistic computations of the ionospheric ray path between source and receiver.

In summary, the proposed facility would have the following advantages:

(a) It would permit rapid determination of the location of a craft transmitting HF distress signals in the Southern Ocean where remoteness from major shipping lanes and the lack of conveniently situated shore-receiving stations present severe difficulties in locating the source of any distress signal.

(b) HF transmissions, in particular the international distress frequency, 2.182 MHz, and the supplementary distress frequencies, 4.125 and 6.2155 MHz, are available from virtually all shipping and aircraft with long-distance communication facilities. A further advantage is that comparatively high power transmissions are employed, up to a maximum of 400 W.

(c) In the well-established Navy Navigation Satellite System (NNSS), five near-polar orbiting satellites provide very high frequency (VHF) transmissions at 150 and 400 MHz. This allows a set of ionospheric electron content measurements, and hence an update in the mid-latitude trough position, to be made at comparatively short mean time intervals of 82 min at a 35 deg latitude ground-receiving station.

(d) Use of NNSS satellites would have a further "spin-off" advantage in facilitating ionospheric research over the Southern Ocean. This is a region which is interesting because of its proximity to Australia, is complicated by the mid-latitude trough, and where the ionosphere has hardly been studied previously due to a lack of islands on which to establish land-based ionospheric sounding stations.

The highest latitude at which a trough might be observed in Adelaide using the differential Doppler technique is indicated from the following arguments. It is assumed that a representative trough has a peak elevation of about 450 km (justified in this sub-section below) and has an appreciable effect on total electron content measured from satellite signals passing through the ionospheric trough at elevations up to 450 km. (A trough with a rather greater peak elevation of 600 km is illustrated in Figure 2 from Ref. 11). It is further assumed that at elevation angles of 10 deg (and above) signals are received in Adelaide with strengths large enough to be useful. From geometry, a trough which was just observable at a 10 deg elevation angle would therefore occur at a geographic latitude approximately 13 deg south of Adelaide (lat. 35 S), i.e. at a geographic latitude approximately 48 S.

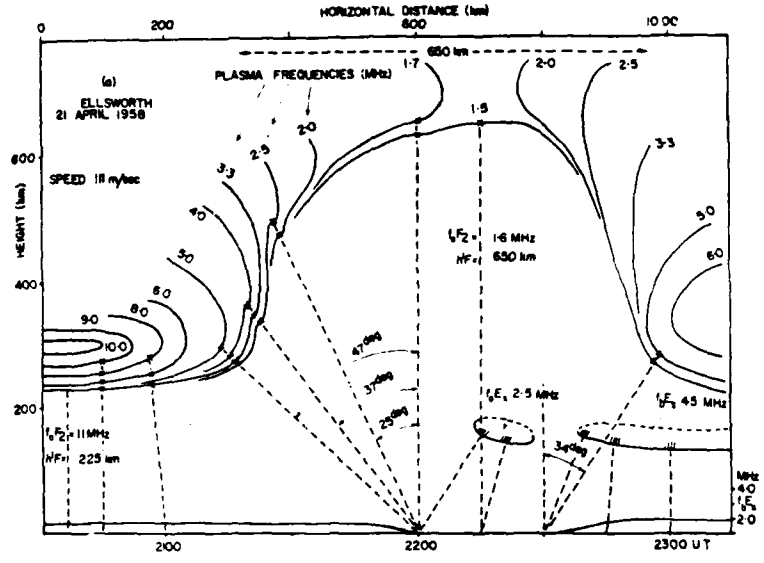

Figure 2. Distribution of Ionisation for Bottomside Trough on 21 April, 1958 (from Bowman (1969), Ref. 11 which is associated with Ref. 10).

As discussed in Section 4.1, the mean position of troughs is about 60 deg invariant latitude which, for Adelaide's longitude, corresponds to a geographic latitude of approximately 48 S; (see Figure 3). It follows that troughs which occurred approximately in the mean trough position would be observable in Adelaide. Furthermore, because of their appreciable latitudinal extent, troughs which were centred at higher latitudes but which extended through the 48 S invariant latitude should also be observable in Adelaide. Troughs should certainly be observable when they were located sufficiently equatorwards of the mean position so as to produce maximal effects on ionospherically-propagated transmissions from the Southern Ocean, which is the point of main concern in the present context.

In attempting to locate a craft in distress as rapidly as possible, the following procedure is proposed:

(a) Information that an HF distress signal has been received is forwarded, e.g. by OTC, without delay to the person responsible for operating the position-finding facility.

(b) The direction of arrival of the radio signal is measured in both azimuth and elevation, at a receiving station near Adelaide (and possibly elsewhere) using a highly directional multi-element crossed aerial array.

(c) A modification of the DRCS RADFIN ray-tracing program is employed to compute an estimate of the signal source position, which is to be relayed to the search and rescue authority. Currently, RADFIN computations are based on CCIR data in Ref. 14 constituting a representative ionosphere. These data require modification and improvement to form a composite model ionosphere, by superimposing on the CCIR data the best available definitive model of the mid-latitude trough, as devised by Halcrow and Nisbet (Ref. 39). In their model, the trough position is predicted in invariant geomagnetic co-ordinates (Appendix 1 and Ref. 7) by utilising the parameters, universal time, day of year (i.e. season), sunspot number and planetary K index (Kp) which is a measure of world-wide geomagnetic activity (Ref. 47).

In practice, Kp cannot reliably be obtained sooner than some four to six weeks after observation. In addition, Halcrow and Nisbet's model is based on ionospheric observations in the Northern Hemisphere where the north invariant geomagnetic pole is at approximately 80 deg N geographic latitude, in contrast to the south invariant pole at approximately 74 deg S geographic latitude (Ref. 28). The composite model ionosphere would be based on only an estimate of Kp. It can therefore be regarded only as a first approximation, but it is useful to insert into the program to obtain an initial estimate of the location of the signal source. This information is relayed to the search and rescue authority.

(d) Although the effect of the mid-latitude trough is greatest on winter nights, its effect at other times is also appreciable and unpredictable (Ref. 15). As a next step, direct observations of the location of the trough are therefore made by means of NNSS satellites in employing the differential Doppler effect. This permits a direct measurement of the trough position and latitudinal extent to be inserted into the program, to replace the estimated trough position previously computed within the program, from parameters which included an unreliable Kp value.

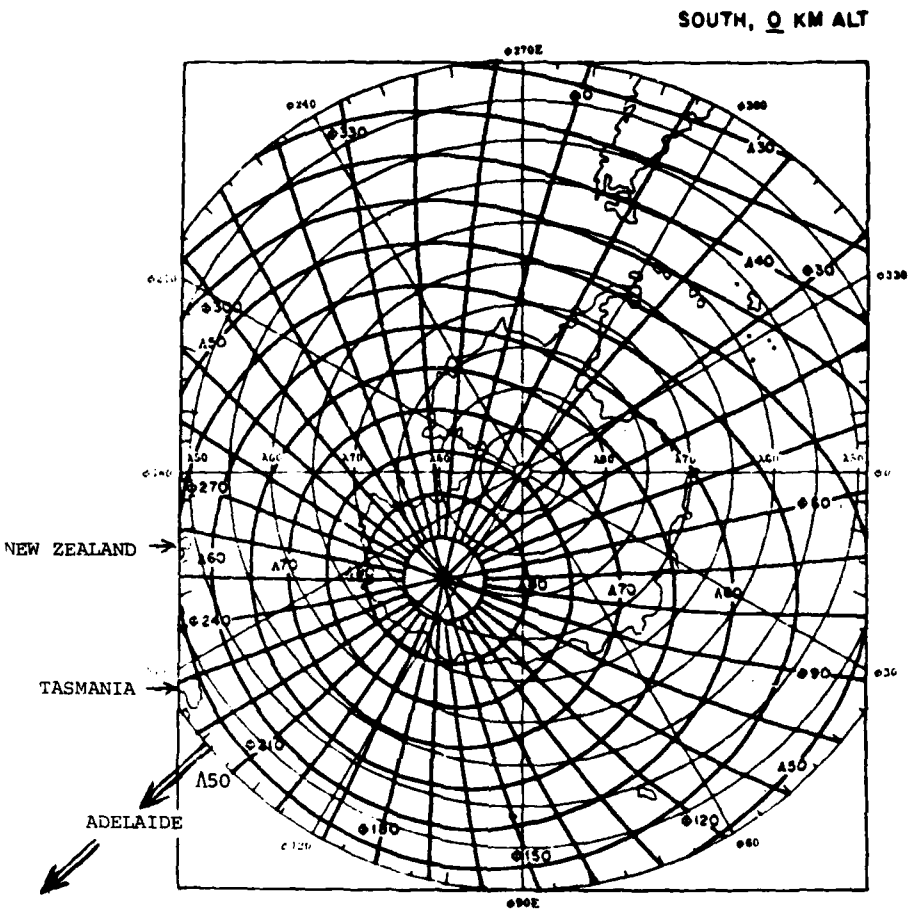

Figure 3. Invariant Geomagnetic Co-ordinates, Epoch 1969.75 (from Evans et al (1969), Ref. 28).

Furthermore, the variation in total electron content observed *during* the passage of a satellite could be translated into information on the vertical profile of ionospheric electron density in the trough. This should permit, for the Southern Hemisphere, the eventual improvement of the trough model currently available for the program (Ref. 39) which is based on Northern Hemisphere observations.

(e) The program, with the measured trough position included, is then employed to compute, more accurately, the location of the signal source; the information is relayed to the search and rescue authority.

4.2 Maximal Direction of Arrival Errors

The following comments are mainly restricted to propagation problems associated with the mid-latitude trough. It is noted that problems, particularly related to direction of arrival measurements, disappear when propagation is via a sporadic E (F_s) layer, from which reflections would be predominantly specular.

Buchau *et al (Ref. 12)* used Alouette topside ionogram data as a basis for three-dimensional ray-tracing of radio-waves assumed to originate from the Polar Fox II over-the-horizon radar system, at the site indicated as a source of "rays" in Figure 4. The isoionic contours in this figure indicate the location of the (cross-hatched) mid-latitude trough. The figure gives some indication of strong north-south electron density gradients; ground-based and airborne measurements show that steepest gradients are, in fact, greater than the figure would suggest, being approximately 2 to 3 MHz per 100 km.

Figure 5 from Ref. 12 shows a set of curves, each of which is the locus of landing points of 5 MHz radio-waves transmitted in a particular azimuthal direction at various elevations. Zero azimuth corresponds to transmissions in a direction 45 deg E of N which is approximately along the trough. Figure 5 indicates, for instance, that rays directed at approximately 40 deg E of N (i.e. at -5 deg to the length of the trough) which land at skip distances of the order of 3000 km are some 1400 km or 28 deg off a great circle path as a result of the presence of the mid-latitude trough. This is taken to be a measure of the maximal error that might arise in attempting to locate a source of transmissions by measuring the direction of arrival of the signal, unless allowance is made for the presence of the mid-latitude trough.

4.3 Limitations in Ionospheric Data for the Southern Ocean

Ionospheric ray-tracing techniques at HF, with particular application to travelling ionospheric disturbances, are discussed in Ref. 35.

By means of the RADFIN computer program developed at DRCS, the location of a source of transmissions received via the ionosphere may be computed from measurements of the direction of arrival of signals. Ray-tracing techniques are applied to ionospheric data, within the limits of the most comprehensive data set available (Ref. 15). The extent, and limitations, of these CCIR data, which are employed in the calculation of world-wide F2 region ionospheric characteristics, are indicated by the following description from Ref. 15:

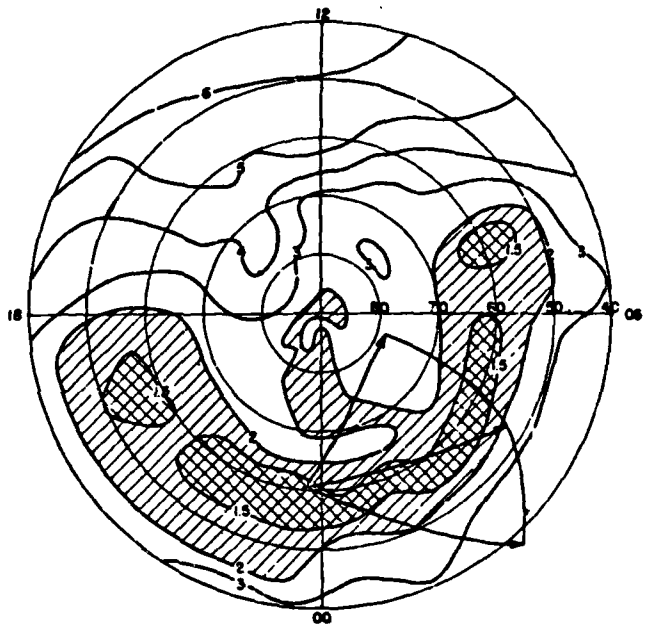

Figure 4. Contours of Median f_oF2 (in MHz) Derived from Alouette 1 Topside Soundings. Data base: Winter 1963, 0000 to 1200 UT, Kp 0 to 1+. The co-ordinate system is corrected geomagnetic latitude and corrected geomagnetic local time (from Buchau et al (1973), Ref. 12).

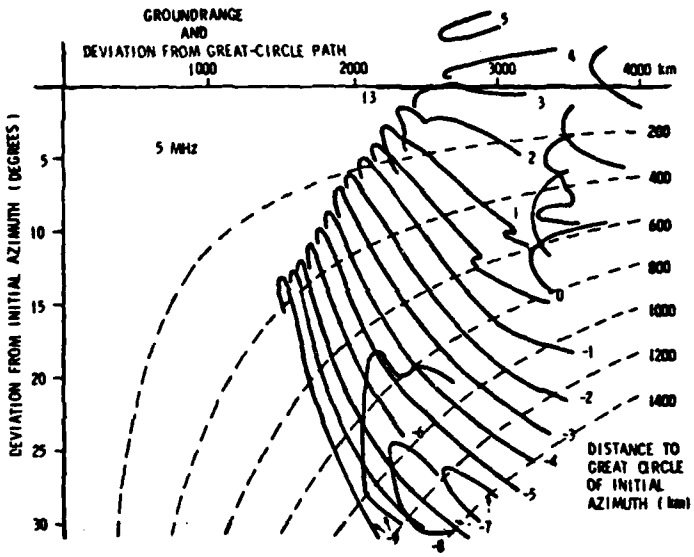

Figure 5. Raytracing Results for 5 MHz. Shown are the loci of the landing points as a function of the initial azimuths. Initial azimuths with respect to a central boresight of 45 deg east of north are indicated by the numbers to the right of the curves (from Buchau et al (1973), Ref. 12).

"Data for five years, 1954 - 1958, were analysed month by month. These years were typical of a period from solar cycle minimum to maximum. In addition to data from stations actually operating in those years, it was possible to use, as supplemental data, observations from stations that were in operation in other years, to fill some large gaps in world coverage. This is particularly helpful for 1954, a period of solar cycle minimum. The use of data from 1964, also a solar cycle minimum year, to supplement the 1954 data was necessary to provide sufficient data for mapping most of the Southern Hemisphere. The severe limitations in Southern Hemisphere data are particularly noted."

Although the CCIR data indicate a smoothed "average" position of the trough, as seen in Figures 6 and 7, they do not include steep ionisation gradients that are important in computing directions of arrival of signals refracted by the ionosphere.

Limitations in the accuracy of CCIR numerical maps are indicated by the following statement from Ref. 14. Comparisons made (Refs. 13 and 44) "between satellite observations of plasma frequencies and the numerical maps of f_oF2 reveal that average discrepancies are generally small, but that in some ocean regions, notably the South Pacific and in the Southern Hemisphere, and at some times, the predictions are in error by as much as a factor of 2".

In Ref. 16 it is commented that "the ionosonde network in existence when Report 340 (CCIR (1967)) was prepared has provided a reasonable sample of one-third of the Earth's surface. Since that time, approximately 15 new ionosondes have begun operation..."

However, the major source of error in ionospheric data for the Southern Ocean still arises from the lack of ionospheric sounding stations in this region south and south-west of Australia. This necessitates the extrapolation between data obtained at stations thousands of km apart, as seen in Figure 8. The limited accuracy of data for the Southern Ocean is highlighted by the absence of stations in an area bounded by the geographic latitudes of Hobart (42.9 S) and Antarctica (e.g. Wilkes 66.9 S; Mirny 66.5 S; Terre Adelie 66.7 S) and the longitudes of Macquarie Island (159.0 E) and Kerguelen (70.2 E) (Ref. 21). These stations are listed in Table 2 together with other adjacent stations.

4.4 Usefulness and Limitations of the Mid-latitude Trough Model

In order to make meaningful ray-tracing computations, a realistic model of the trough must be superimposed on the CCIR data. In the present context, this has been possible by adding to the RADFIN program subroutines obtained from the Pennsylvania State University (Mr. R.L. Divany) which are based on the mid-latitude trough model developed by Halcrow and Nisbet (Ref. 39).

In the present discussion, it is assumed that this model, derived for the Northern Hemisphere, can be applied directly to the Southern Hemisphere. Ref. 78 provided some measure of support for this assumption from Ariel III satellite observations at conjugate regions in the two hemispheres by showing that the low latitude boundaries of troughs in the two hemispheres coincided within ±1.2 deg of invariant latitude under a variety of conditions.

Other minor improvements to the model were recommended by Lockwood (Ref. 54); these are briefly considered later in this section.

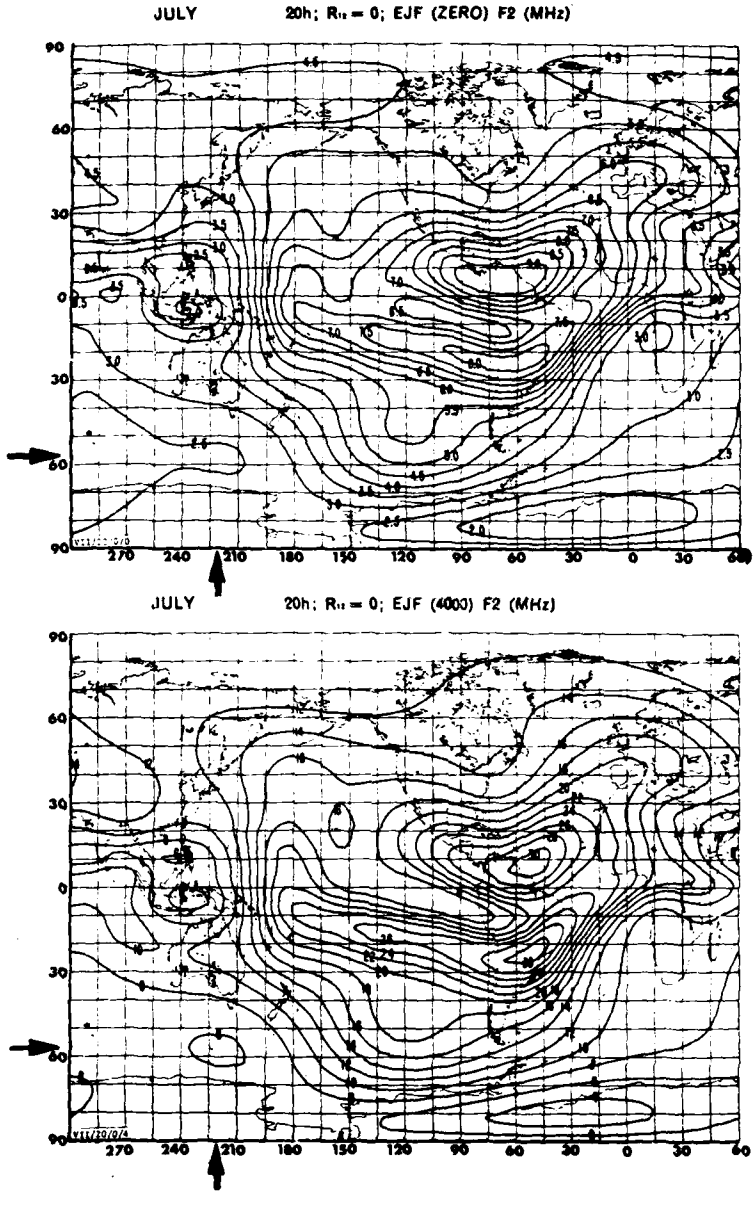

Figure 6. Arrows indicate the mid-latitude trough position (from CCIR REPORT 340 (1966), Ref. 15).

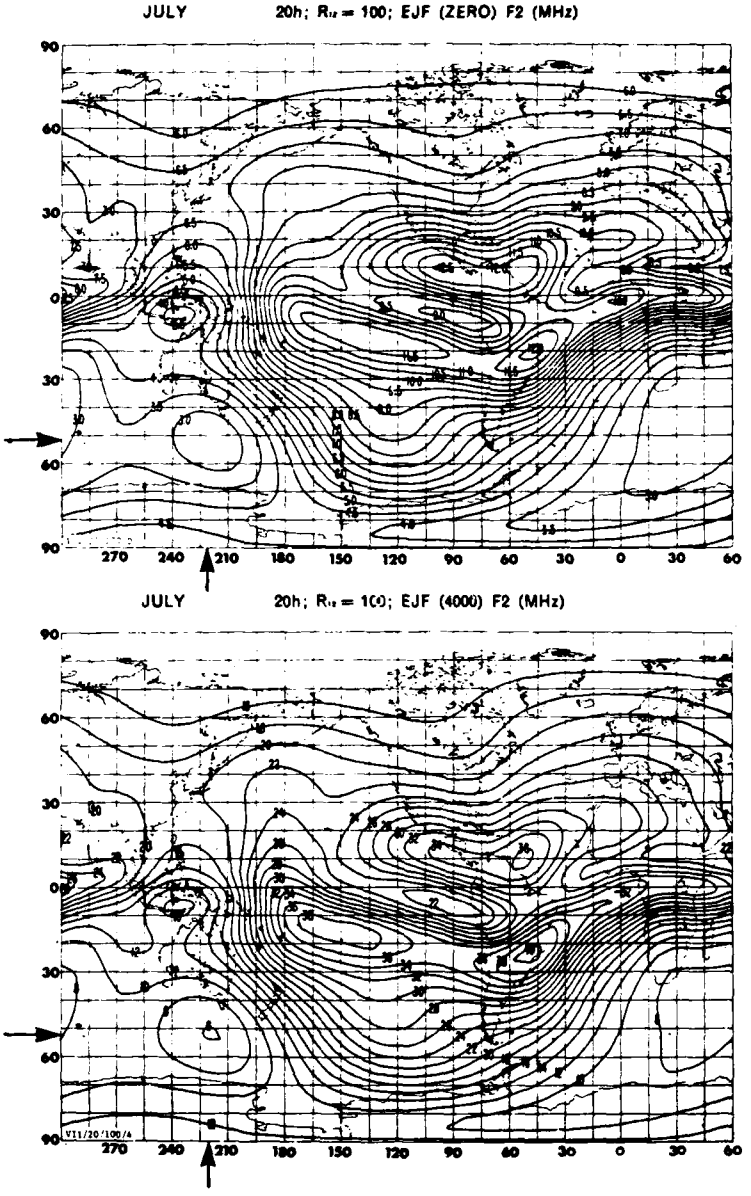

Figure 7. Arrows indicate the mid-latitude trough position (from CCIR REPORT 340 (1966), Ref. 15).

ERL-0449-SD

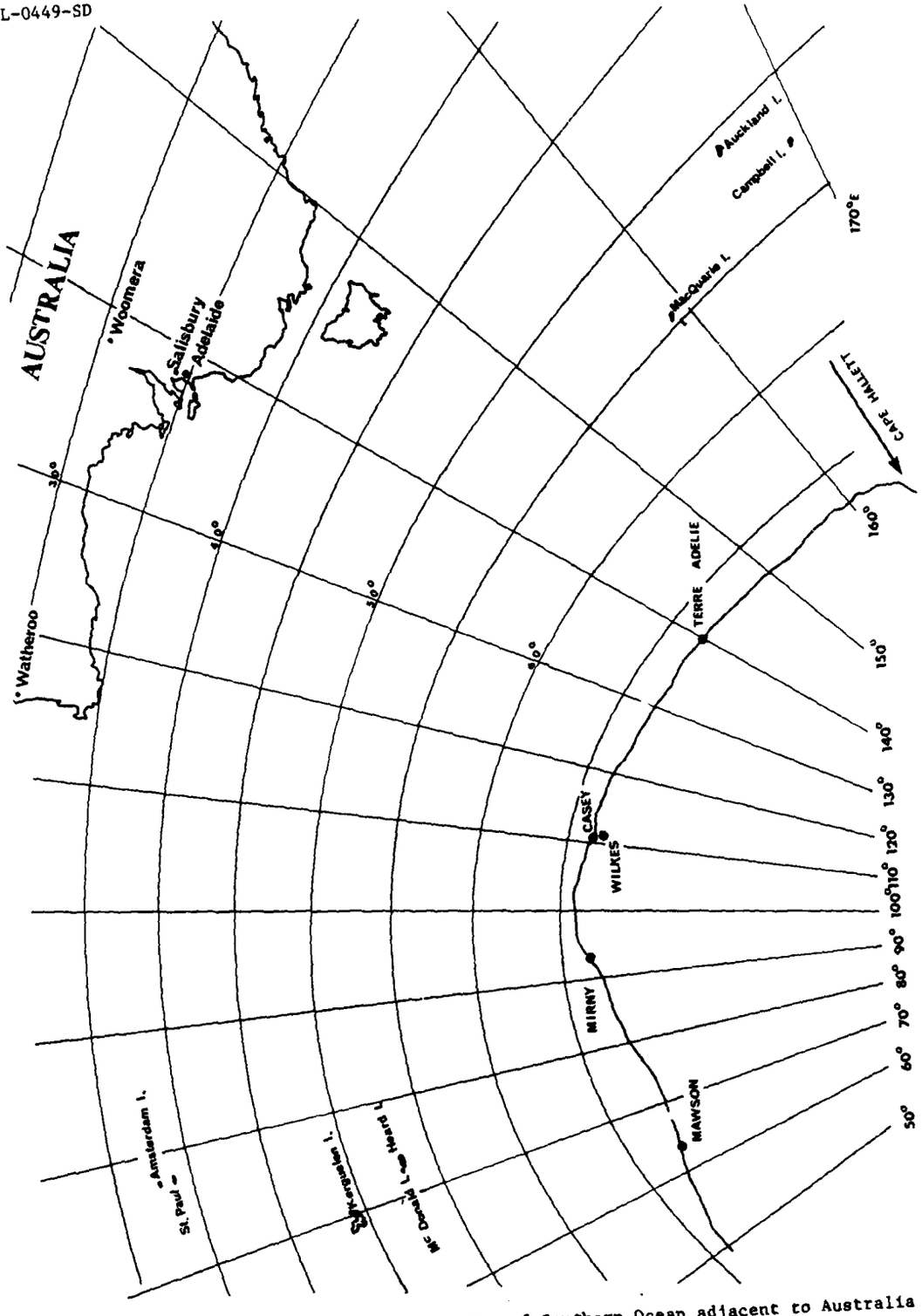

Figure 8 Map of Southern Ocean adjacent to Australia

TABLE 2. LOCATIONS OF HIGH-LATITUDE SOUTHERN STATIONS

(Data from Conkright and Brophy (1982), Ref. 21)

		LAT. deg S	LONG. deg E	RELEVANT IONOGRAM RECORDING PERIOD FOR CCIR (1966) DATA
Stations between Geographic Latitudes 40 and 70 S and Longitudes 70 and 170 E	Campbell Island	52.50	169.20	1954-58, 1964
	(Casey)	(66.28)	(110.53)	(2/1969-1975)
	Hobart	42.90	147.30	1954-58, 1964
	Kerguelen	49.35	70.24	1954-58, 1964
	Macquarie Island	54.50	159.00	1954-11/1958
	Mirny	66.50	93.00	4/1956-58, 1964
	Terre Adelie	66.66	140.02	1954-58, 1964
	Wilkes	66.90	110.50	7/1957-58, 1964
Other (Adjacent) Stations	Canberra	35.30	149.00	1954-58, 1964
	Cape Hallett	72.30	170.20	1957-58, 2/1964-12/64
	Christchurch	43.60	172.80	1954-58, 1964
	Little America	78.20	197.80	7/1957-58
	Mawson	67.60	62.90	2/1958, 1964
	Mundaring	31.99	116.31	1964
	Salisbury	34.70	138.60	1964
	Scott Base	77.90	166.80	3/1957-58, 1964
	Vostok	78.4	106.9	3/1958-12/58, 1964
	Watheroo	30.30	115.90	1954-58
	Woomera	31.00	138.6	1964

The position of the mid-latitude trough shows substantial temporal variations in latitude. Figures 9a and 9b are examples of true height versus latitude distributions (derived by G.D. Slade and I.P. Buttery from CCIR data using the RADFIN program). The trough appears in these figures as only a small change in height over a broad range of latitudes and centred roughly on the mean latitude expected for the trough.

To represent the iono here in the absence of the trough, Halcrow (Ref. 38) and Halcrow and Nisbet (Ref. 39) employed F2 layer peak electron densities (denoted $N_mF2(CCIR)$) derivable from tabulated CCIR data based on observations (Ref. 15).

In effect, this necessitated interpolating between data representing sunspot numbers 0 and 100. It is noteworthy that this procedure also introduced a potential source of error by neglecting the fact that the CCIR data already included the influence of the mid-latitude trough averaged over all latitudes where it occurred. The trough occurred, in fact, at lower latitudes for higher sunspot numbers, corresponding to enhanced geomagnetic activity. A comparison of the particular CCIR data in Figures 6 and 7 shows that the geographic latitude of the average trough position, south of Australia, for sunspot number zero was some 6 deg polewards of its average position for sunspot number 100. Figures 9a and 9b, which show true height as a function of geographic latitude, also indicate that the trough moved equatorward by several degrees of latitude as the sunspot number increased from 0 to 100.

Halcrow and Nisbet (Ref. 38) indicated that in their model, in the particular case of the spring equinox, the northern and southern bottom edges of the trough represent peak F2 region electron densities (N_mF2) which are 0.25 of the densities in the absence of the trough, as seen in Figure 10. They employed 29770 Northern Hemisphere observations of peak F2 layer electron densities, denoted N_mF2(observed), obtained by means of Alouette I and II (Refs. 4 and 5) satellite topside sounders from 1962 to 1970. They used the ratio:

$$\phi = N_mF2(\text{observed})/N_mF2(\text{CCIR})$$

at the intersection of invariant latitude lines and the 300 km altitude level, in defining the locations of the walls of observed troughs, as a basis for developing their trough model.

In Ref. 39, Halcrow and Nisbet stated that values of ϕ at the northern and southern bottom edges were similar to each other, and exhibited no significant variation with season, Kp, sunspot number or local time. In particular, they indicated that a constant value of $\phi = 0.25 \pm 20\%$ provided as satisfactory a fit to the available data as did more complicated expressions.

In order to obtain some estimate of the error involved in applying Halcrow and Nisbet's model (Ref. 39), the particular case of winter (July) and a local time corresponding to 20.00 U.T. at geographic longitude 225 W are considered. It is assumed that the model, which was derived for the Northern Hemisphere, also applies to the Southern Hemisphere. These conditions pertain to Figures 6 and 7 which include, in the top maps, contours of the F2 region extraordinary ray critical frequency (f_xF2) at vertical incidence. These show, in particular, that at geographic latitude 50 S, $f_xF2 \doteqdot 2.6$ MHz in both figures, whereas at 60 S, $f_xF2 \doteqdot 2.4$ MHz for sunspot number zero and $F_xF2 \doteqdot 3.0$ MHz for sunspot number 100. These latter values of f_xF2 at 60 S would correspond to an increase in electron density of

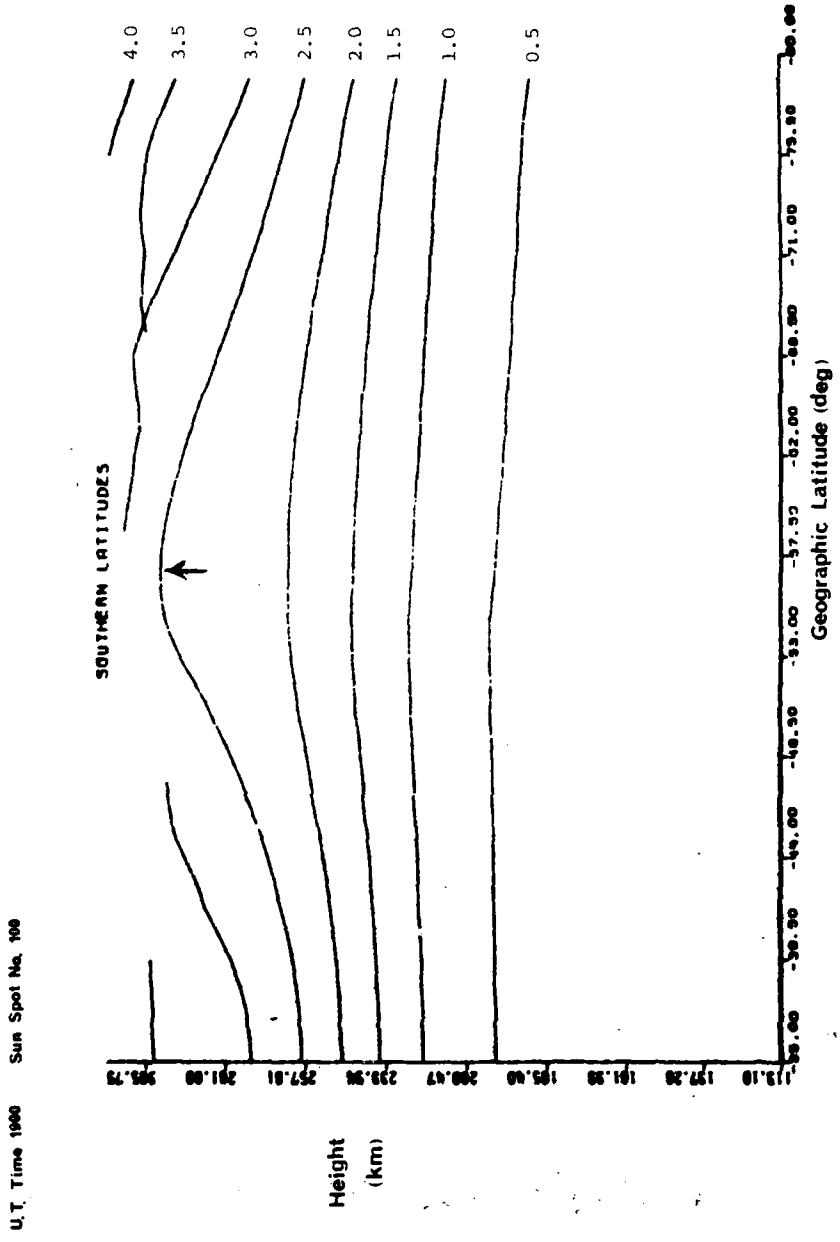

Figure 9a. Curves of constant ionisation density computed with the DRCS "RADFIN" program, by G.D. Slade and I.P. Buttery for the longitude of Adelaide, July. Plasma frequencies (MHz) of curves are indicated.

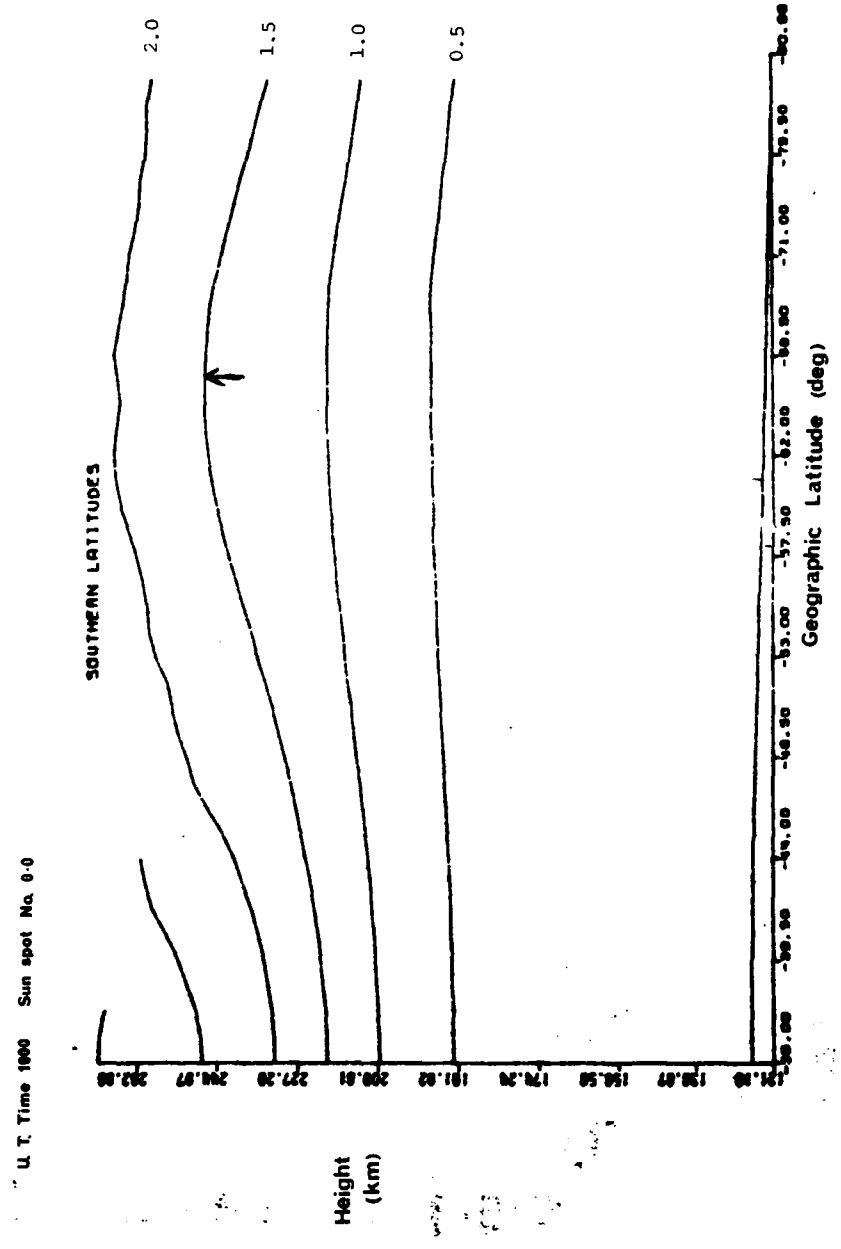

Figure 9b. Curves of constant ionisation density computed with the DRCS "RADFIN" program, by G.D. Slade and I.P. Buttery for the longitude of Adelaide, July. Plasma frequencies (MHz) of curves are indicated.

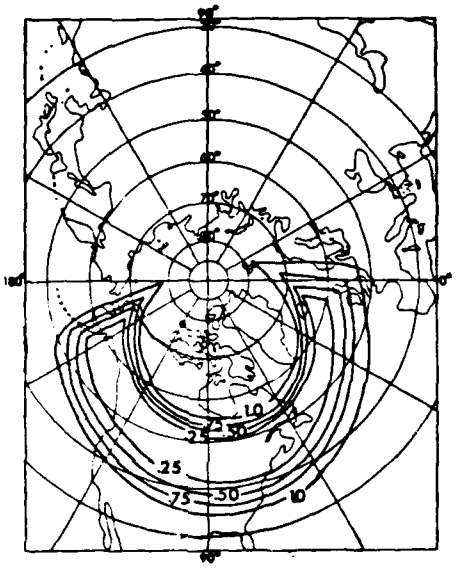

Figure 10. Main Trough Location and Associated Φ Values for Spring (from Halcrow and Nisbet (1977), Ref. 39).

approximately 50% as sunspot number changed from 0 to 100. It is concluded that variations in F2 region peak electron density associated with sunspot number variations can potentially cause considerable errors in trough positions computed on the basis of a constant value of $\phi = 0.25$. In particular, the possible error in ϕ of ±20% claimed in Ref. 39, might well be an optimistic underestimate.

Halcrow and Nisbet's model predicts values of ϕ which are used as multipliers in converting values of peak F2 region electron density observed when the trough is present. It is noted that this model provides ϕ values corresponding only to peak electron densities. In ray-tracing, e.g. in using the RADFIN program, it is necessary to generate an electron density profile representative of the F2 region trough extending below its peak, i.e. values of ϕ that are appropriate to various heights below the peak are produced, as discussed below in this section.

Examples of trough profiles are indicated in Figure 11 from Ref. 12; the corresponding directions of radar transmissions can be inferred from Figure 12, as can the fact that the second and third profiles in Figure 11 represent rays which passed twice through the trough. In Figure 11, the trough which has a critical frequency (f_oF2) of approximately 2 MHz, is about 100 and 300 km above the corresponding electron density contours on its equatorward and poleward sides, respectively. The trough may therefore be represented as having a height of about 200 km. Its altitude is approximately 450 km at its peak.

Figures 2, 13, 14 and 15 from Ref. 11 show that the height of the peak electron density occurred, on four occasions, approximately 450, 360, 450 and 350 km respectively above the level of a similar electron density at latitudes adjacent to the trough. A representative trough height of about 400 km therefore seems appropriate. The trough critical frequencies (f_oF2) range from 1.5 to 2.2 MHz, and the trough altitudes are approximately 630 km at their peaks.

Data from the Advanced Ionospheric Sounder (AIS) are presented in Ref. 63, including two representative troughs shown in Figure 16. These have heights of approximately 360 and 100 km and respective f_oF2 values of 2 and 1.5 MHz. The troughs have altitudes of approximately 600 and 430 km respectively at their peaks. Further AIS data are presented by Dudeney et al in Ref. 23, which includes Figure 17 representing a trough of height approximately 200 km, f_oF2 equal to 2 MHz, and an altitude of approximately 470 km at its peak.

Lockwood (Ref. 53) measured the Doppler shifts of 7.335 MHz signals transmitted over great circle paths of 5212 km such that double hop F2 echoes could be returned to ground from the trough in two regions approximately one-quarter and three-quarters of the distance from transmitter to receiver. Using a simple ray-tracing model, and assuming "reflection points at the low altitudes of 200 km", he was able to interpret his observations in terms of two-hop F2 echoes. Hence, he deduced that the height of the F2 region peak electron density within the trough was only of the order of 30-80 km above the height having this electron density outside the trough. This conclusion was in accord with Lockwood's further report (Ref. 54) on focusing gains, or losses, of up to 30 dB for double-hop F2 region reflections via the trough over these long paths.

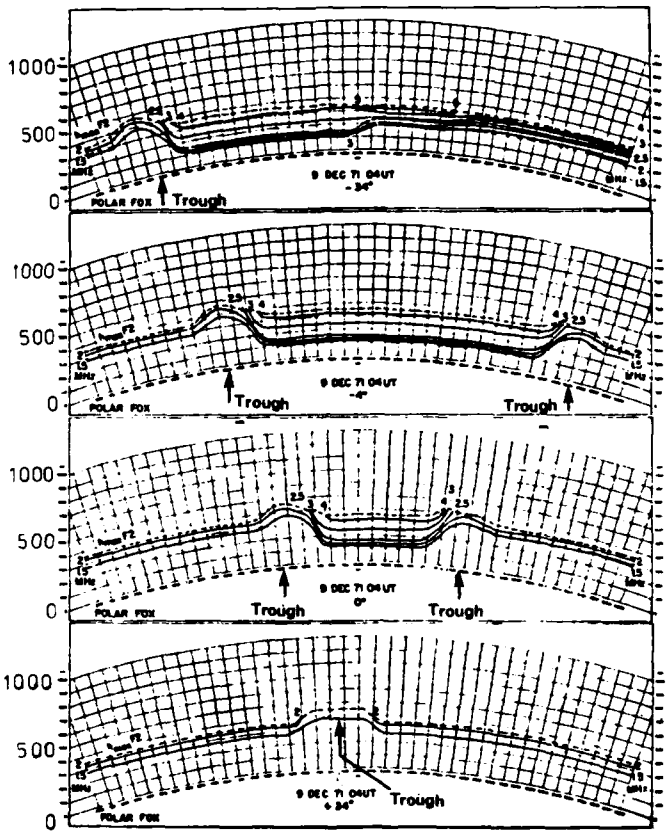

Figure 11. Ionospheric electron density profiles are shown, including profiles of the mid-latitude trough (after J. Buchau et al (1973), Ref. 12).

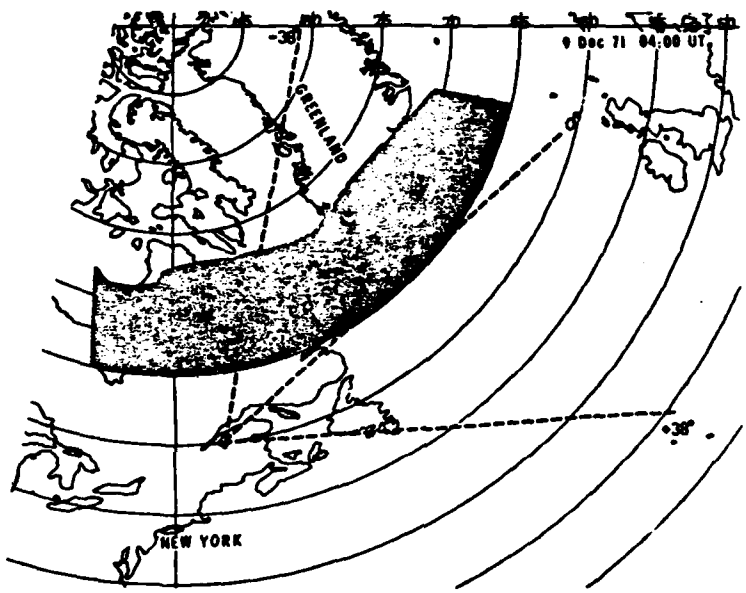

Figure 12. Continuous Aurora (shown in Fig. 4 of Ref. 12) Transferred into the Corrected Geomagnetic Co-ordinate System. Note extremely good representation of the aurora midnight sector in corrected geomagnetic co-ordinates. Black square indicates location of POLAR FOX II. The sector of the ionosphere studied lies between -38 deg and +38 deg azimuth with respect to the 0 deg boresight in 25 radial cross-sections (after J. Buchau et al (1973), Ref. 12).

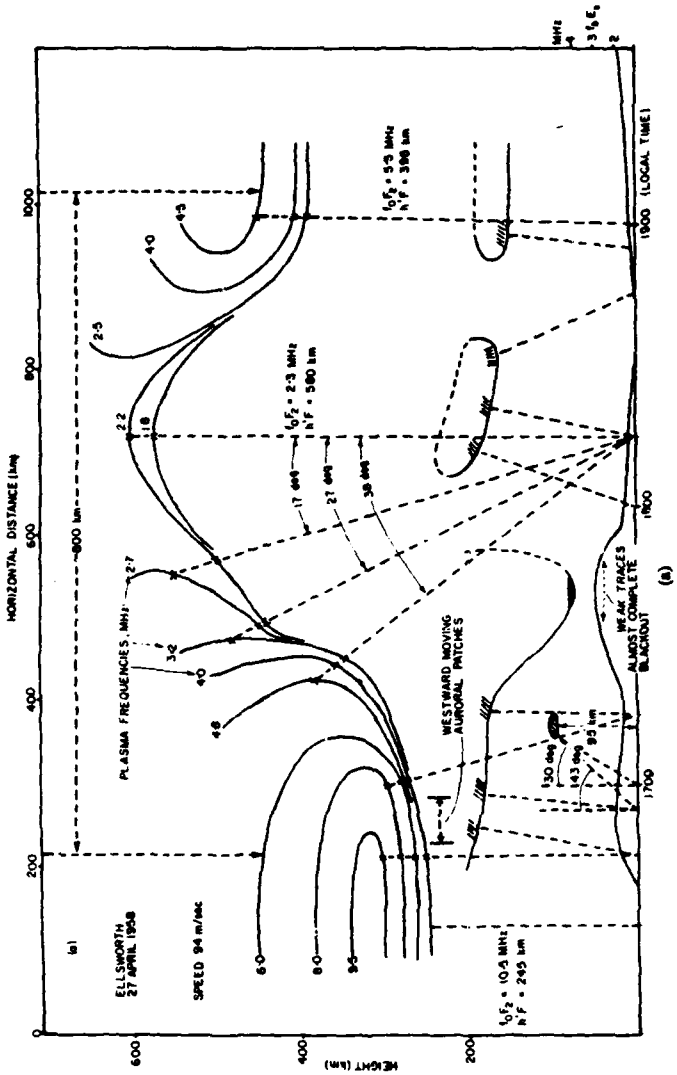

Figure 13. A Mid-latitude Trough (after Bowman (1969), Ref. 11).

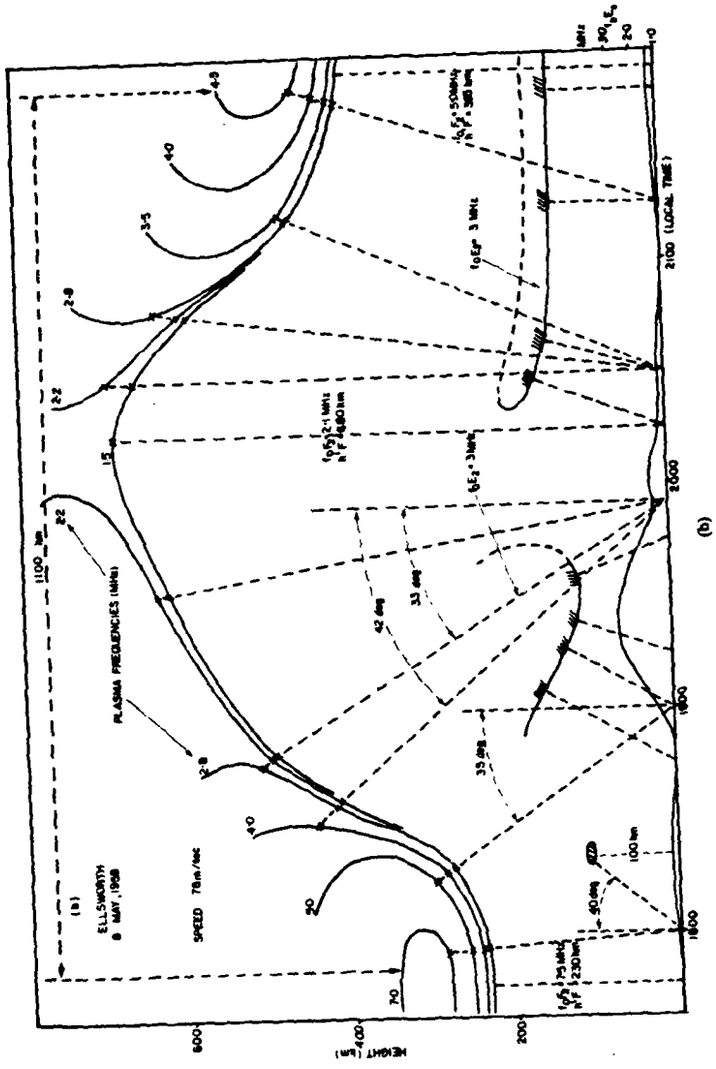

Figure 14. Distribution of Ionisation for Bottomside Trough (a) on 27 April, 1958, (b) on 8 May, 1958 (after Bowman (1969), Ref. 11).

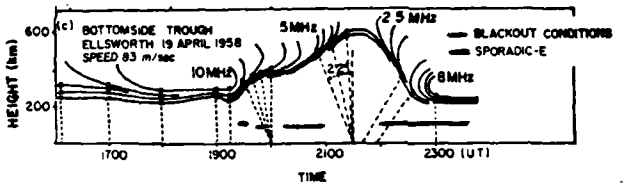

Figure 15. Ionisation Contours of a Bottomside Trough (after Bowman (1969), Ref. 11).

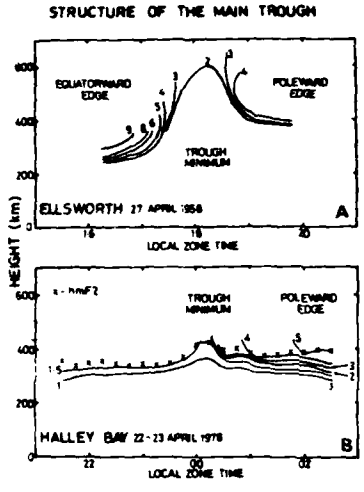

Figure 16. Iso-ionic Contours of Different Types of Mid-latitude Trough. Numbers associated with contours indicate plasma frequency in MHz (after Rodger and Pinnock (1980), Ref. 63).

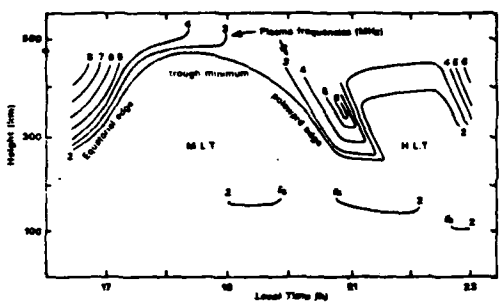

Figure 17. A Mid-latitude Trough (MLT) and High Latitude Trough (HLT) are shown (after Dudeney et al (1982), Ref. 23).

It is noted that at a frequency of f = 7.335 MHz and on Lockwood's (Ref. 53) assumption of a 200 km reflection altitude for two-hop echoes and a 5212 km path, the equivalent vertical frequency (f_{ev}) (e.g. Ref. 9) which equals the plasma frequency at the reflection height, would be, neglecting the earth's curvature:

$$f_{ev} = f\cos i$$

where $i = \cot^{-1}(200/1303)$ is the angle of incidence of the signal on the ionosphere. Hence, f_{ev} = 1.1 MHz which being below the values of f_oF2 expected for the trough, implies that the signal would be returned to earth.

From the foregoing examples of troughs, 450 km would seem to be a reasonable estimate for the altitude of the peak. On the assumption of 450 km as a possible reflection altitude for two-hop echoes, it would follow that $i = \cot^{-1}(450/1303)$, and hence f_{ev} = 2.4 MHz. However, the values of f_oF2 for the troughs ranged from 1.5 to 2.2 MHz, so that 7.335 MHz signals for which f_{ev} = 2.4 MHz would, in fact, have penetrated these troughs. This simple argument therefore casts doubt on Lockwood's (Refs. 53 and 54) estimate of 50 km for trough heights. It seems at least possible that his signals may have been reflected from the walls of troughs rather than from their peaks.

On the basis of his observations, Lockwood (Ref. 54) made the following minor modifications to Halcrow and Nisbet's (Ref. 39) model:

(1) To avoid the effects of discontinuities in the gradient of ϕ at the top and base of each wall, the linear walls were replaced by a cosinusoidal increase up to the constant maximum value of ϕ.

(2) Corresponding to the trough in the F2 region peak electron density, a similar increase was included in the height of the F2 region peak by raising it by an amount Δh inside the trough. The model variation of Δh was made the same as for ϕ; in particular, across the trough bottom, Δh assumed a maximum value of 50 km coincident with the maximum depletion in electron density for which Halcrow and Nisbet (Ref. 39) assumed that $\phi = 0.25 \pm 0.5$.

(3) The F2 layer semithicknesses were assumed to be constant across the trough.

Rush et al (Ref. 66) have published a simplified model of the high latitude ionosphere for telecommunications applications. It employs CCIR data to predict median monthly values of the critical frequency, height of the maximum electron density and semithicknesses of the E, F1 and F2 regions. It also predicts high latitude features including the F2 region ionisation trough, seen in Figure 18. In particular, the trough is placed immediately south of the auroral oval and is defined only from sunset to sunrise, the height of the F2 maximum ionisation (h_mF2) being 50 km higher in the trough than in its absence, as indicated in Figure 19. The location of the equatorward boundary and the depth of the trough can be varied so that f_oF2 values in the trough and its latitudinal extent can be made to agree with observations, when available. It is noted that Rush et al (Ref. 66) did not substantiate their choice of 50 km for the trough height.

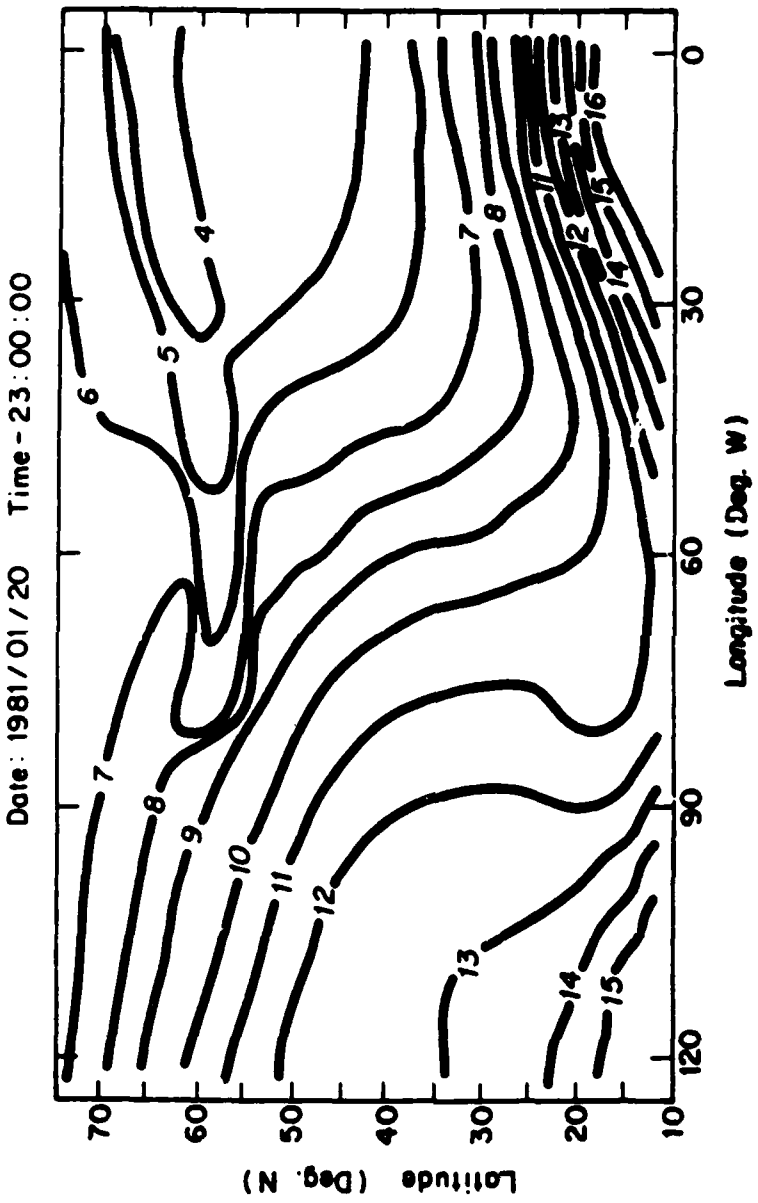

Figure 18. Contours of f_0F2 (in MHz) for 20 January, 1981, at 2300 UT (after Rush et al (1982), Ref. 66).

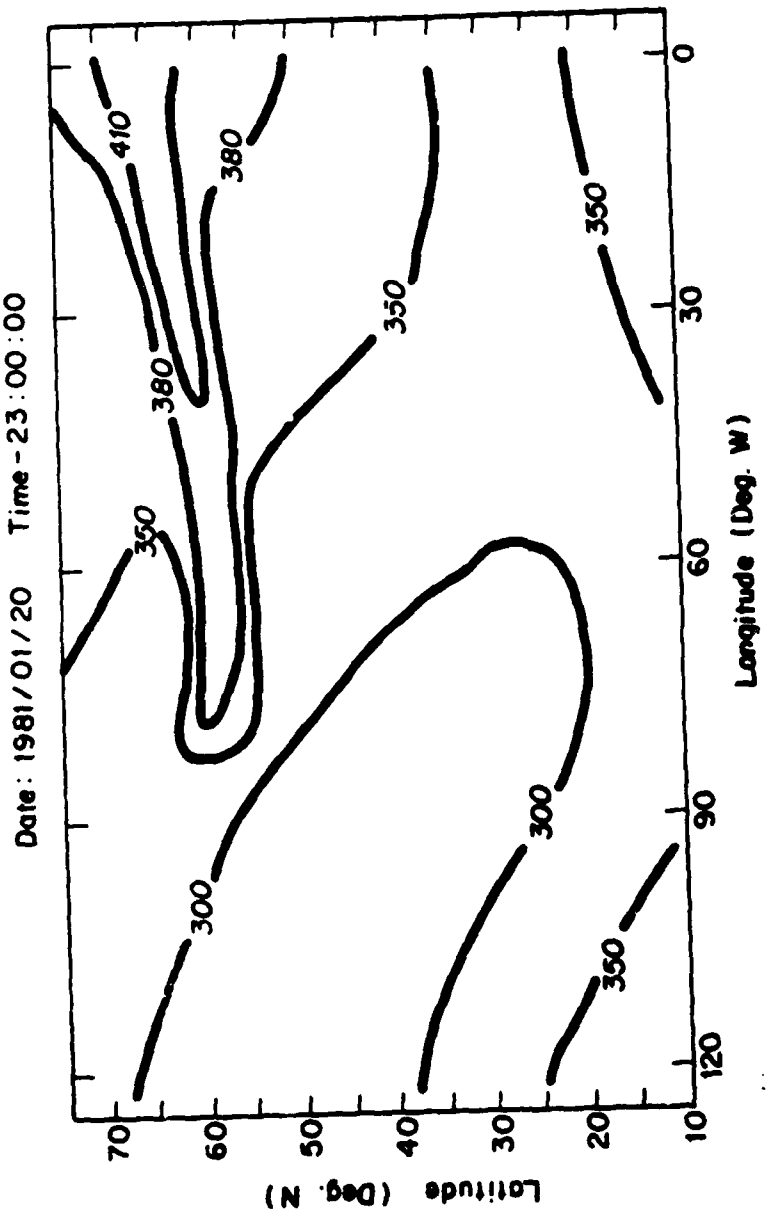

Figure 19. Contours of hmF2 (in km) for 20 January, 1981, at 2300 UT (after Rush et al (1982), Ref. 66).

In the light of the above-mentioned observations of trough height, which are summarised in Table 3, it seems unfortunate that Lockwood (Ref. 54) and Rush et al (Ref. 65) chose a representative trough height as small as 50 km. On the other hand, the entries in Table 3, except for Lockwood's, might well include the more "spectacular", i.e. easily identifiable, examples of troughs, i.e. include troughs with greater than average heights.

The above discussion underlines the lack of information available on the height of the mid-latitude trough. It clearly indicates the desirability of the continuation of observations of the trough by instruments such as the Advanced Ionospheric Sounder at Halley Bay (Rodger and Pinnock (Ref. 63); Dudeney et al (Ref. 23)).

TABLE 3.

REFERENCES	REPRESENTATIVE MID-LATITUDE TROUGH CHARACTERISTICS		
	Height (Δh) km	Altitude of Peak km	Critical Frequency (f_oF2) MHz
12. Buchau et al (1973)	200	450	2
11. Bowman (1969)	400	630	1.5-2.2
63. Rodger and Pinnock (1980)	360,100	600,430	2.0, 1.5
23. Dudeney et al (1982)	200	470	2
53,54. Lockwood (1980, 1981)	50	-	-

Nevertheless, the information in Table 3 is adequate to assign an approximate value of Δh = 200 km for the trough height, which is used in the present study in the application of Halcrow and Nisbet's (Ref. 39) model. Δh is the altitude of the electron density maximum within the trough minus the altitude of that value of electron density outside the trough.

4.5 Mid-latitude Trough Model

It is noted that Halcrow and Nisbet's model provides contours of peak F2 electron density only. In following ray-tracing procedures, it is also necessary to define electron density contours below the peak. The following guidelines, additional to those of Halcrow and Nisbet (Ref. 39), were applied in the present computations.

(1) The critical frequency (f_oF2) within the trough was obtained by multiplying the critical frequency in the absence of the trough by 0.5 ($= \phi^{\frac{1}{2}}$). (It is noted (e.g. Ref. 9) that:

$$f^2 \propto N$$

where f represents the plasma frequency, and
N the corresponding electron number density, so that:

$$\left[\frac{f_oF2(\text{trough present})}{f_oF2(\text{trough absent})}\right]^2 = \frac{N_mF2(\text{trough present})}{N_mF2(\text{trough absent})} = 0.25)$$

The above guideline therefore corresponds to the Halcrow and Nisbet procedure of multiplying the F2 region electron number density (N_mF2) in the absence of the trough by ϕ = 0.25 to obtain N_mF2 for the trough.

(2) It is assumed that while the trough's electron density is being depleted, the altitude of its maximum is increasing, and becomes approximately 200 km above the altitude at which electron density has the same value outside the trough; i.e. the trough height becomes approximately Δh = 200 km. Due to the reduction in electron density within the trough, it is seen from the schematic diagram in figure 20 that the actual altitude rise Δa of the depleted peak would be less than 200 km. For the sake of computation in Appendix 4, Δa was taken to have a notional value of 150 km, to sufficient accuracy for the present purposes.

(3) Figures 9a and 9b show curves of constant plasma frequency as true height versus latitude plots for specified sunspot numbers. Curves of this kind represent the averaging of many troughs which occurred over a wide range of latitudes. These troughs produced a broad peak centred on the particular latitude (e.g. 57.5 S in Figure 9) which, presumably, was the predominant mean trough position at the corresponding sunspot number. The height of a curve, i.e. the altitude of a curve at its peak (e.g. at latitude 57.5 S) compared with its altitude remote from that latitude, is, of course, much less than expected for individual troughs. However, the ratios of the heights of the various curves should be the same as for a representative individual trough. Absolute values for the heights of curves that would represent an individual trough can be computed on the assumption, from (2) above, that the height rise for the curve representing the critical frequency was such that Δh was approximately 200 km.

In Appendix 4, the above guidelines, modified for practical application, are employed in computing model mid-latitude troughs.

4.6 Planetary K-index (Kp) in an Ionospheric Model

Figure 21, derived from Ref. 82, gives the probability distribution, over several sunspot cycles, for Kp which is a measure of geomagnetic activity. For instance, it indicates that the occurrence probability of Kp > 1.5 is 50%, and for Kp > 3 it is 81%.

In the present discussion, the occasions when the trough has moved appreciably equatorwards from the polar regions are of most interest. At such times, the trough is more likely to be located between a distress signal source in the Southern Ocean and a receiving station, e.g. in Adelaide. Histograms denoted by asterisks in Figure 22 (adapted from Ref. 68) indicate the frequencies of occurrence of the equatorial boundaries of troughs at particular Northern Hemisphere invariant latitudes. It is assumed that similar invariant latitudes apply for the Southern Hemisphere, and Figure 22 indicates the corresponding southern geographic latitudes (for the longitude of Adelaide). The data in Figure 22 were obtained in the interval February-December, 1969, at a time of maximum sunspot activity when the excursions of geomagnetic activity, denoted by Kp, would also be maximal.

Figure 22(b) indicates that even during a year of maximum sunspot activity, there were times of reduced geomagnetic activity ($Kp \leq 3+$) when the equatorwards boundary of troughs would have been over southern Australia, i.e. at geographic latitudes equatorwards of 43 S. It may be inferred from these observations that during sunspot minimum, when Kp would normally have smaller values, there would often be occasions when the equatorwards boundaries of troughs would occur at geographic latitudes of southern Australia.

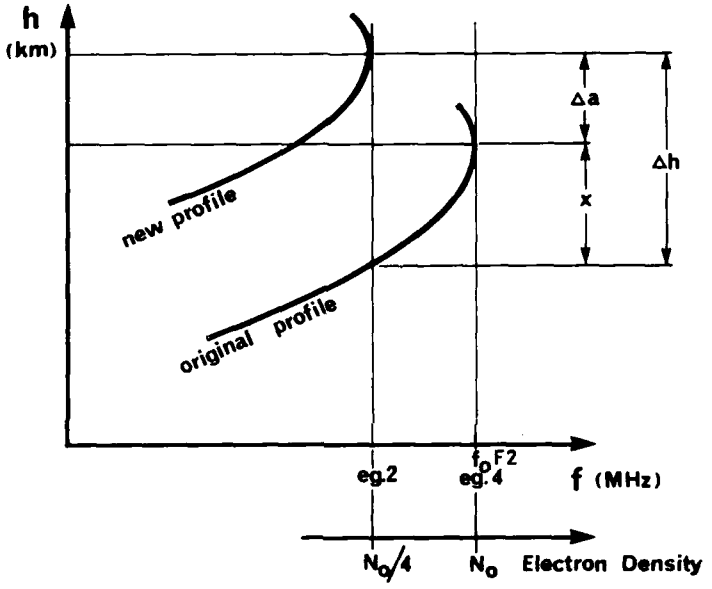

Figure 20. This schematic diagram indicates that if the peak electron density (N_o) at a given height is reduced in the formation of a trough, the new peak electron density, e.g. $N_o/4$, would be x km higher in altitude than the previous level at which electron density was $N_o/4$. (Outside the trough, electron density at this (lower) level is unaltered at $N_o/4$).
In addition, the whole electron density profile is raised Δa, so that the trough height becomes $\Delta h = \Delta a + x$.

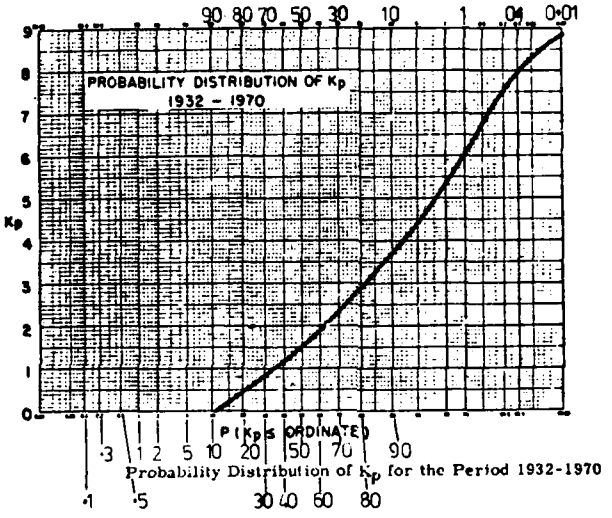

Figure 21. Kp Data (derived from Zawalick and Cage (1971), Ref. 83) are shown.

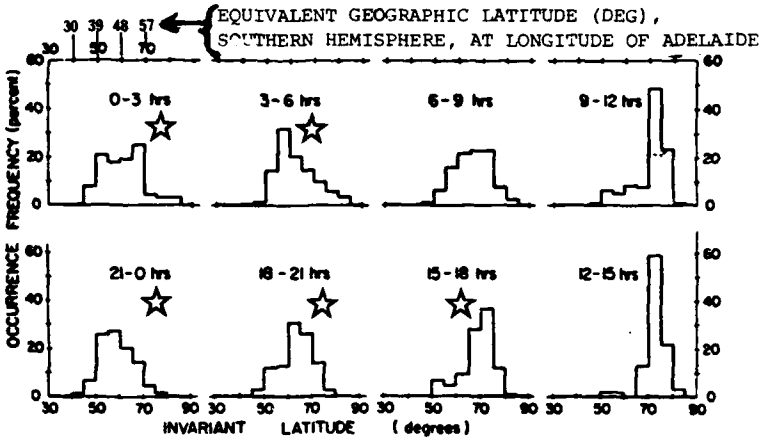

(a) Equatorial Boundary of the Ionization Irregularity Zone in the Northern Hemisphere (Kp $\leq$ 3+) as a Function of Local Time for Low Magnetic Activity.

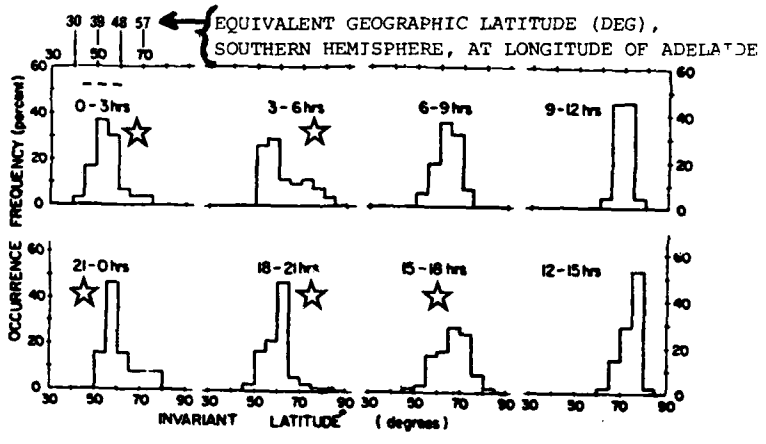

(b) Equatorial Boundary of the Ionization Irregularity Zone in the Northern Hemisphere (Kp $\geq$ 3+) as a Function of Local Time for High Magnetic Activity.

Figure 22. Stars indicate distributions which also represent the equatorial boundaries of mid-latitude troughs (from Sagolyn et al (1973), Ref. 68).

It is concluded that mid-latitude troughs can occur at unpredictable times at sufficiently low latitudes in the vicinity of Australia to necessitate making allowance for their presence in computing the location in the Southern Ocean of the sources of H.F. ionospherically-propagated radio signals received in southern Australia, e.g. in Adelaide.

In employing an ionospheric model, which includes a mid-latitude F region trough, reliable values of all parameters are readily available except for Kp which can vary rapidly and by large amounts in response to geomagnetic disturbances associated with solar activity.

In observations from September 1962 to March 1963, Muldrew (Ref. 59) found from 73 Alouette I topside soundings of troughs that unit increase in Kp was associated with approximately 3.5 deg equatorward movement of the trough in geographic latitude. (At the longitude of Ottawa, this corresponds to 3.4 deg reduction in invariant latitude.)

Kohnlein and Raitt (Ref. 46) employed approximately 300 observations of the trough obtained by means of the ESRO 4 satellite, from November 1972 to April 1974. They determined an empirical relationship for the mean invariant latitude Λ of the trough in terms of Kp and t (local time in hours, being positive after midnight and negative before) namely:

$$\Lambda = 65.2 - 2.1Kp - 0.5t \pm 2 \text{ deg}$$

The linear dependence of Λ on Kp is illustrated in Figure 23 (derived from Ref. 46) which also indicates the corresponding south geographic latitudes, assuming the longitude of Adelaide.

Earlier work by Rycroft and Burnell (Ref. 66) involving 39 topside observations from Alouette I, from April to August 1963, indicated a relationship:

$$\Lambda = 62.7 - 1.4Kp - 0.7t \pm 3.5 \text{ deg}$$

while 45 observations by Rycroft and Thomas (Ref. 67) indicated:

$$\Lambda = 64.6 - 1.8Kp - 0.5t \pm 2.6 \text{ deg}$$

The above data suggest that unit increase in Kp was associated with decreases in invariant latitude of 3.4, 2.1, 1.4 and 1.8 deg respectively, from which 2 deg decrease is taken to be representative of these topside trough observations.

From October 1964 to January 1966, ground level observations of the ionospheric electron content were made by Liszka (Ref. 52) employing a Faraday rotation technique at 40 and 41 MHz observing the S-66 satellite. Some of his observations are summarised in Figure 24, which indicates that a unit increase in Kp is associated with a reduction in geographic latitude of approximately 2.9 deg, which, at the longitude of Kiruna, corresponds to a reduction of approximately 3.1 deg in invariant latitude.

On the basis of much more extensive data, extending over 8 years of Alouette I and II topside sounding observations, Halcrow and Nisbet (Ref. 39) devised a trough model, examples of which are shown in Figure 25, and which at zero hours local time is represented as follows:

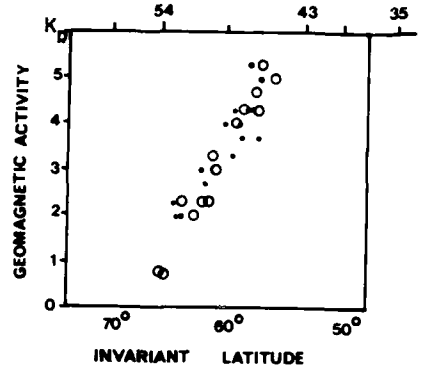

(a) Position of the Mid-latitude Trough: Invariant Latitude vs Geomagnetic Activity at 19.6 hr LT.

The dots refer to the Northern Hemisphere and the circles to the Southern Hemisphere.

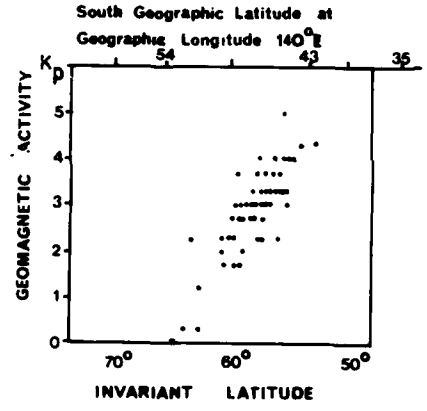

(b) Position of the Mid-latitude Trough: Invariant Latitude vs Geomagnetic Activity at 1.2 hr LT (Northern Hemisphere).

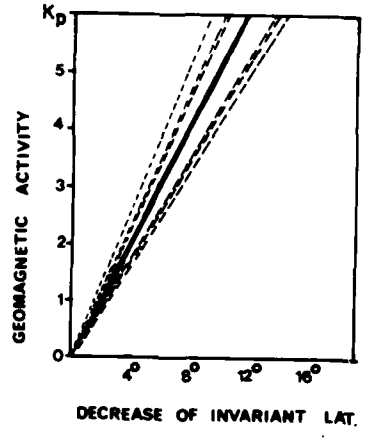

(c) Decrease of Invariant Latitude with Increasing Geomagnetic Activity.

----, Gradient at different local times.

—, Average gradient of all local times investigated.

KOHNLEIN AND RAITT (1977), Ref. 46

Figure 23.

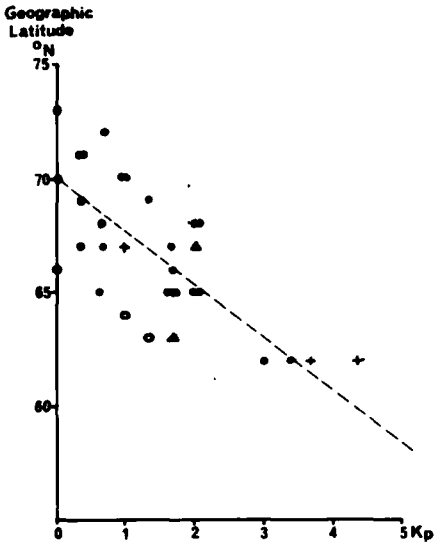

Figure 24(a). Dependence of the Trough Latitude on Geomagnetic Kp-index for all Observations During the Period 19.00-20.00 L.M.T. (from Liszka (1967), Ref. 52).

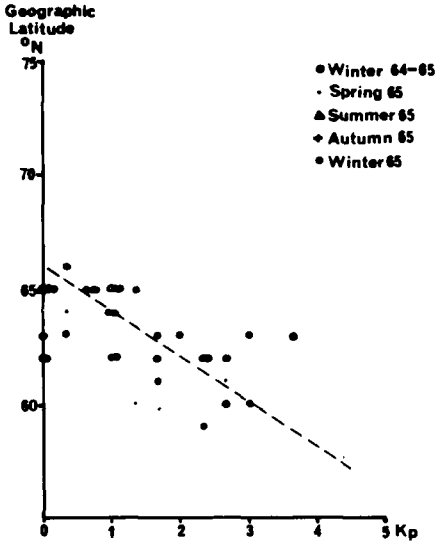

Figure 24(b). Dependence of the Trough Latitude on Geomagnetic Kp-index for all Observations During the Period 03.00-04.00 L.M.T. (from Liszka (1967, Ref. 52).

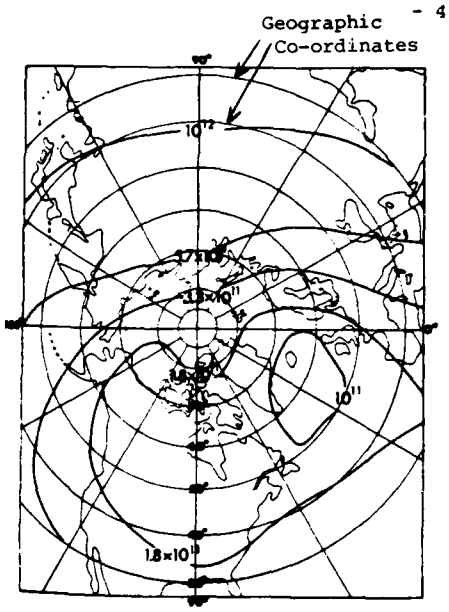

Figure 25(a). N_mF_2 Predicted by CCIR (1966) in m^{-3} for Spring Equinox; R_z = 50, Kp = 0+ (after Halcrow and Nisbet (1977), Ref. 39).

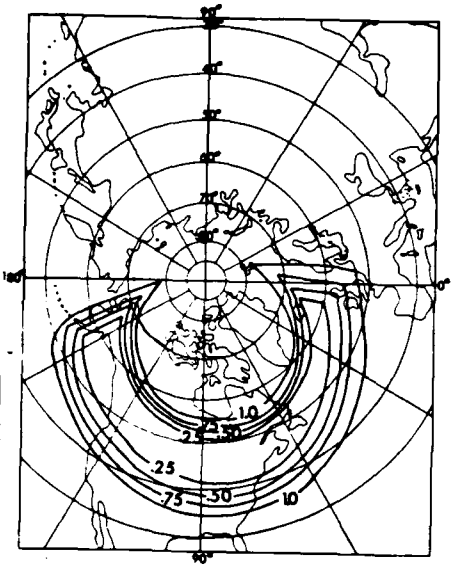

Figure 25(b). Main Trough Location and Associated Φ Values for Spring Equinox (after Halcrow and Nisbet (1977), Ref. 39).

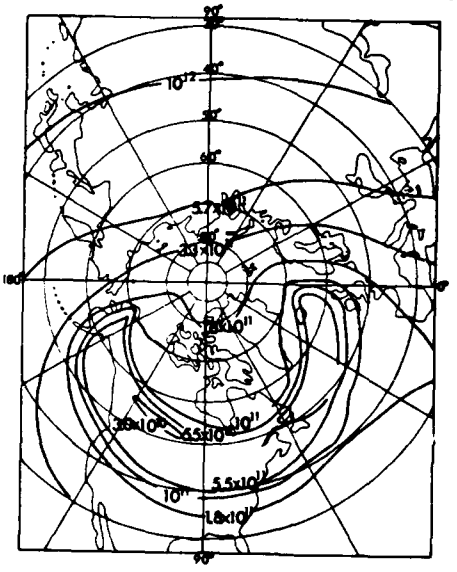

Figure 25(c). Modified CCIR Predicted N_mF_2 in m^{-3} for Spring Equinox; R_z = 50, Kp = 0+ (after Halcrow and Nisbet (1977). Ref. 39).

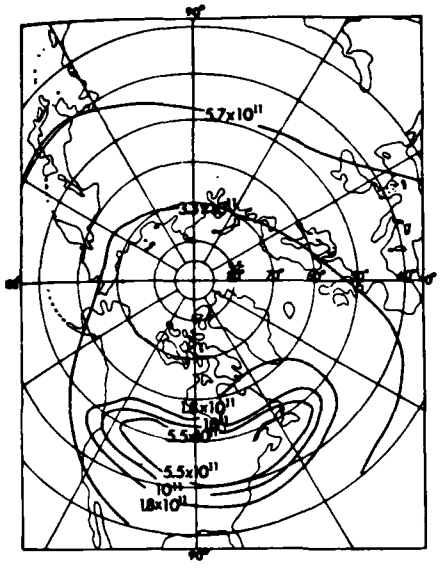

Figure 25(d). Modified CCIR Predicted N_mF_2 in m^{-3} for Summer Solstice; R_z = 50, Kp = 0+ (after Halcrow and Nisbet (1977), Ref. 39).

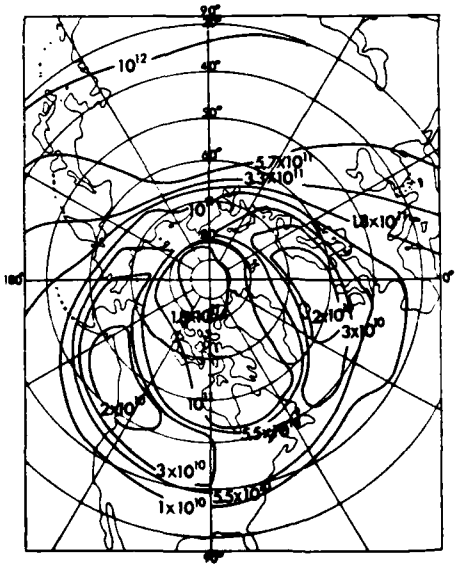

Figure 25(e). Modified CCIR Predicted N_mF_2 in m^{-3} for Winter Solstice; R_z = 50, Kp = 0+ (after Halcrow and Nisbet (1977), Ref. 39).

$$\Lambda_{ST} = 48$$

$$\Lambda_{SB} = 61 - 0.5(Kp - \tfrac{1}{3})$$

$$\Lambda_{NB} = 73 - 1.0(Kp - \tfrac{1}{3})$$

$$\Lambda_{NT} = 76 - 1.25(Kp - \tfrac{1}{3})$$

where Λ represents invariant latitude, the subscripts T, B, S and N represent top, bottom, equatorward and poleward respectively, and the non-fractional numbers represent degrees.

In particular, these formulae indicate a decrease of the order of 1 deg in invariant latitude per unit increase in Kp, which is a smaller decrease than those indicated from the earlier topside and bottomside observations mentioned above.

In the light of the above observations, it appears that Halcrow and Nisbet's (Ref. 39) model may well be improvable as regards the magnitude of the dependence of Λ on Kp. It highlights the importance of making direct observations of the position of the mid-latitude trough, preferably in as near to real time as possible for emergency procedures, rather than relying too heavily on a model that, of necessity, incorporates average values of the trough position. It also underlines the desirability of obtaining statistical data for the trough position in the Southern Hemisphere.

The question of how rapidly the ionosphere responds to a change in Kp requires consideration. Topside sounder data presented in Refs. 59 and 36 suggested that an increase in Kp preceded a reduction in the trough latitude by several hours, namely of the order of 5 hours and 17 hours respectively. These rough estimates are in qualitative agreement with Feinblum and Horan's (Ref. 32) more general conclusion that the F2 region critical frequency (f_oF2) was best correlated with Kp observed some 12 hours earlier.

In the present context, the several hours' delay between Kp and the F2 region response is of academic interest only. Information from the Geophysikalisches Institut at the University of Göttingen, Federal Republic of Germany, which provides an International Service of Geomagnetic Indices based on observations at many locations, indicated that there are 4 to 6 weeks' delay between geomagnetic observations being made and the derived Kp index being available. (Kp computations are based on local K (i.e. magnetic activity) observations at 13 stations, including Canberra in Australia and Eyrewell in New Zealand.)

The non-availability of Kp values in something approaching real time presented a dilemma. A possible solution was to obtain K values of geomagnetic variations from Australian observing stations, in order to compute a parameter comparable with Kp. Problems were anticipated in co-ordinating such a procedure, which would involve attempting, often outside of normal working hours, to obtain data by long-distance communication with observers. This suggested that a preferable alternative would be to observe the position of the mid-latitude trough directly.

A direct and convenient technique for locating the position of the trough would be to record, e.g. adjacent to a direction-of-arrival measuring station in Adelaide, the Doppler shift of dual-frequency H.F. transmissions from a circumpolar orbiting satellite. In this way, changes in total electron content along the continually changing satellite-to-receiver path could be determined, and the trough position identified. It would be desirable to use several such satellites,

so that the trough position could be monitored at intervals of no more than an hour or so. It would also be desirable for these satellites to transmit on the same pair of coherent frequencies. There are five U.S. Navy Navigational Satellites which satisfy this criterion and transmit coherently at 150 and 400 MHz in circumpolar orbits. The dual-frequency Doppler technique of measuring ionospheric electron content is described and discussed in Section 5.

Another requirement of a dual-frequency Doppler receiving facility is that it be immediately available for determining the trough location at times of emergency. Unfortunately, the existing TRANET satellite tracking facility at Smithfield, near Adelaide, does not satisfy this latter requirement, since its use is dedicated to United States Government purposes. However, dual frequency TRANET data would be available for statistical studies of the mid-latitude trough position, through courtesy of the U.S. Defense Mapping Agency.

4.7 *Scintillation Fading*

Lyon (Ref. 55) has indicated the potentially adverse effects of auroral ionospheric scintillations on Doppler frequency measurements using NNSS satellites, discussed in Section 5.3 below. In particular, to ensure continuous signal reception, a good phase-locked receiving system is required which will hold the signal through severe scintillations, allowing the fluctuations to be smoothed with the use of suitable time constants.

Similar sdverse effects are expected with the proposed SARSAT Satellite System (discussed in Section 5.2 below) which will receive VHF (121.5 MHz) distress transmissions through the ionosphere. At higher geomagnetic latitudes, scintillations due to ionospheric irregularities will degrade the signal by imposing rapid time fluctuations, an effect that is reduced at higher operating frequencies. It is concluded in Ref. 55 that in moderate scintillating conditions, a VHF signal will be acquired without large errors in estimating the position of a distress signal source; but in severe scintillation conditions, the signal will simply not be acquired at high geomagnetic latitudes. Table 4 includes data from Ref. 14 which emphasises the severity of scintillation fading at auroral latitudes, particularly at night under magnetically disturbed (high Kp) conditions.

The present project would afford an opportunity to gain additional data on scintillations at high invariant geomagnetic latitudes, as measured by the fading of NNSS satellite transmissions at 150 and 400 MHz.

4.8 Ground-Based Transmitting Stations

Further scintillation data are obtainable by recording at Adelaide, fixed frequency HF transmissions, e.g. from Mawson and Casey (by courtesy of the Australian Ionospheric Prediction Service) and Macquarie Island. However, a more important purpose in receiving such transmissions is to check their observed directions of arrival against the computed values. In short, a valuable check is provided on the suitability of Halcrow and Nisbet's (Ref. 39) Northern Hemisphere mid-latitude trough model as an addition to the RADFIN program of DRCS for Southern Hemisphere studies.

The present project could involve only one direction of arrival aerial system, which, in principle, should be sufficient. However, experiments in the reception of HF transmissions from ground-based stations may indicate that two or more such systems in southern

Australia are desirable to ensure (i) sufficient accuracy in locating the position of a distress signal source, and (ii) that adequate signal strengths are likely to be received by at least one system under conditions of severe ionospheric disturbance.

TABLE 4. PERCENTAGE OF OCCURRENCE OF SCINTILLATIONS*

(a) ⩾ 12 dB peak to peak at 137 MHz, sub-auroral and auroral latitudes

SITE	Kp	DAY (0500-1700 LT)	NIGHT (1700-0500 LT)
Sagamore Hill (Massachusetts)	0 to 3+	0	1.4
	> 3+	0.1	2
Goose Bay (Labrador)	0 to 3+	0.1	1.8
	> 3+	1.6	6.8
Narssarssuaq (Greenland)	0 to 3+	2.9	18
	> 3+	19	45

(b) ⩾ 10 dB peak to peak at 254 MHz, auroral latitudes

SITE	Kp	DAY (0600-1800 LT)	NIGHT (1800-0600 LT)
Goose Bay (Labrador)	0 to 3+	0.1	0.1
	> 3+	0.3	1.2
Narssarssuaq (Greenland)	0 to 3+	0.1	0.9
	> 3+	2.6	8.4

LT: Local Time * (Data from Ref. 14)

5. SATELLITES - SEARCH AND RESCUE CAPABILITIES

5.1 Geostationary Satellites

There are currently available several communications satellites in geostationary orbits (over the equator) with the capacity to provide assistance in recording distress signals. e.g. three geostationary MARISAT satellites (Ref. 20) are located over the Atlantic Ocean (15 W), the Indian Ocean (a "spare" satellite, 73 E) and the Western Pacific (176.5 E). These provide commercial communications services, via satellite, between ships and shore stations (at Southbury, Connecticut, for the Atlantic satellite, and Santa Paula, California, for the Pacific satellite) and thence to existing public teleprinter, telephone and facsimile communications systems. Figure 26 shows the service coverage of the MARISAT system, assuming elevation angles exceeding 5 deg from ship to satellite. The coverage of the Indian Ocean and Pacific satellites is seen to include most of the Southern Ocean south and south-west of Australia, which is of present concern.

The configuration of the MARISAT Communications System incorporates, as an objective, the provision of "improved safety and distress services", and permits, as a feature, the "handling of emergency calls on a priority basis over other traffic". However, the expense of the comparatively sophisticated ship-board equipment on L-band,

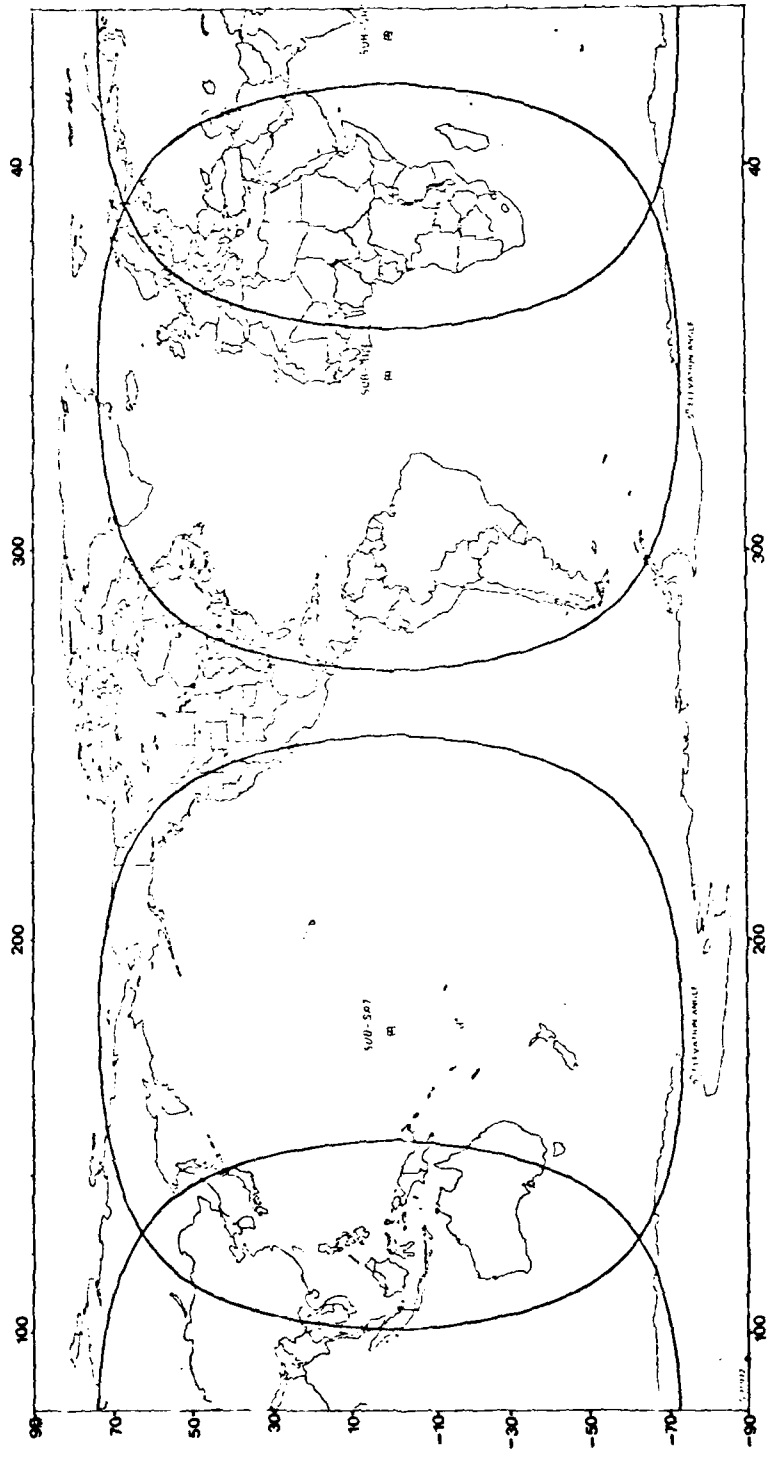

Figure 26. Ground "Coverage" of MARISAT Satellites (COMSAT General Corporation (1977), Ref. 20).

at 1638.5-1642.5 MHz, for transmission, and 1537-1541 MHz, for reception, together with a steerable antenna to be directed towards the satellite, would preclude such installations from any but the best-equipped ships, e.g. many overseas, and some Australian, tankers.

Furthermore, it is expected that ships using the MARISAT system will provide regular updates of their exact positions to shore stations. The location of a ship in distress could therefore be accurately estimated from a previous position without the need to take bearings on it. Transmit/receive aerials on the MARISAT satellites are "despun and earth oriented", i.e. stationary relative to the earth's surface; thus, even though the satellites could detect an "unknown" distress signal on the appropriate frequency, its bearing could not be determined.

Each MARISAT satellite also has three ultra-high frequency (UHF) channels in the 250-300 MHz band reserved for U.S. Navy use; these would be subject to some adverse ionospheric effects in the form of scintillation fading. The fact that these frequencies are similar to the VHF international distress frequencies, 121.5, 156.8 and 243 MHz indicates the suitability, in principle, of geostationary satellites such as MARISAT to record VHF distress signals.

Ship and 'plane communication has traditionally been below 250 MHz, i.e. at VHF and lower. 'Planes, and the majority of shipping, would not be equipped to exploit, in times of emergency, GHz frequencies available commercially with MARISAT. Nevertheless, the advantages of the wide coverage of the earth's surface and the lack of gross ionospheric fading effects at GHz frequencies supports the trend to their increasing usage in geostationary satellites.

The MARISAT system was described above as an example of a geostationary satellite system; its advantages and limitations in land/sea rescue procedures were indicated.

The INMARSAT system, which is intended to take the place of MARISAT, will involve the use of six satellites (orbiting and stationary) and include the facility for real time sea distress radio transmissions (Ref. 26).

5.2 Orbiting Satellites - Proposed SARSAT System

It is reported (Ref. 26) that the U.S.A., Canada and France are currently co-operating on a proposed SARSAT (Search and Rescue Satellite System) which will employ three weather satellites of the TIROS-N (Television Infrared Radiation Observation Satellite) system. These will have almost circular near-polar orbits with a 98.7 deg inclination to the equatorial plane at a height of 834 km, giving a period of 101.5 min. The satellites will each be equipped with a SARSAT transponder, and utilise, initially, emergency position indicating radio beacons (EPIRB) operating at the 121.5 and 243 MHz international distress frequencies at transmitted powers of the order of 100 mW. With this system, positions of EPIRB's are claimed to be determinable within 10 to 20 km. It is proposed that, later, beacons (being developed) will be employed at 406 MHz and allow positions to be determined within 2 to 5 km. In all cases the emergency transmission is received at the satellite in an on-board repeater, translated to a kHz band of frequencies which is transmitted to a ground station as phase modulation on a 1544.5 MHz down-link. Because of the satellite motion, the received emergency transmissions are Doppler shifted, and the information on emergency transmitter location

is contained in the Doppler signature in the usual manner for a Doppler navigation system, such as the Transit or Global Positioning Systems mentioned in Sections 5.3 and 5.4 below. Data processing for position location is carried out at the ground stations. (Appendix 2 summarises the techniques of Doppler measurement of range.)

Lyon (Ref. 55) has shown that in locating the emergency transmitter at a single frequency of 121.5 MHz, errors as great as 35 km in ground range can arise due to horizontal gradients in the mid-latitude trough (described in Section 6) or high latitude trough (Section 6.1) in F region electron density. The ionospheric contribution to the Doppler frequency change is, however, inversely proportional to frequency so that errors arising from the Doppler effect would be correspondingly reduced at a higher frequency, e.g. 406 MHz. Lyon (Ref. 55) also indicated that at high latitudes, rapid fading (scintillations) due to ionospheric irregularities will degrade the emergency signal. He suggested that with severe scintillations, the signal will not be acquired at high latitudes. (Clearly, EPIRB transmissions at two frequencies, e.g. 121.5 and 406 MHz could be employed, in principle, to locate EPIRB's to appreciably greater accuracy by employing a differential Doppler technique analogous to that described in Chapter 5.)

5.3 Orbiting Satellites - NNSS

The Navy Navigational Satellite System (NNSS) or Transit system, also called the NAVSAT system, has been operational since 1964, available for commercial use since 1967 and is expected to provide valuable service as a navigation aid for shipping until at least 1995, after which phase-over to a Global Positioning System (GPS) of navigation (described in Section 5.4 below) is expected to be complete (Ref. 79). The NNSS is operated by the Navy Astronautics Group with headquarters at Point Magu, California, and is under subsidy from the United States Navy. At any time there are a maximum of 6 (currently 5) operational satellites in circular polar orbits at about 1075 km altitude and having periods of 107 min. The orbits form a "bird-cage" (Figure 27) within which the earth rotates carrying an earth observer past each orbit in turn. In principle, an observer can obtain a position "fix" whenever a satellite is above the horizon. (The Doppler technique for position-fixing is outlined in Appendix 2.)

In practice, passes are accepted between 8 and 70 deg of elevation. Tropospheric refraction produces excessive errors (over-estimates) in range below 8 deg (Stansell (Ref. 76); his Figure 44). At elevations above 70 deg, limitations in knowledge of the observer's altitude above the geoid can result in excessive error in a "fix" of the observer's longitude (Stansell (Ref. 76); his Figure 46). This longitude error arises as follows for a satellite in polar orbit. Figure 28 depicts a satellite moving perpendicular to the page and at its closest approach to stations X, Y and Z at altitude 1. Stations X', Y' and Z' at altitude 2 would have respectively the same ranges and rates of change of range as for X, Y and Z. In particular, both longitude and altitude affect the range and its rate of change in similar ways. In computing an accurate longitude fix, it is therefore necessary to have prior knowledge of the receiving station's altitude.

With five satellites, the average time interval between fixes varies from about 32 min at 70 deg latitude to about 97 min at the equator, and is 81 min at 35 deg latitude (Stansell (Ref. 77); his Figure 32).

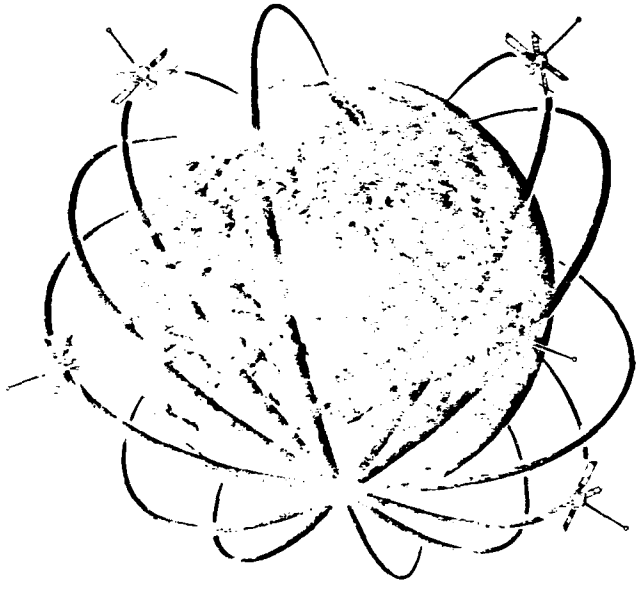

Figure 27. Transit Satellites Form a "Birdcage" of Circular, Polar Orbits About 1075 km Above the Earth (after Stansell (1978), Ref. 77).

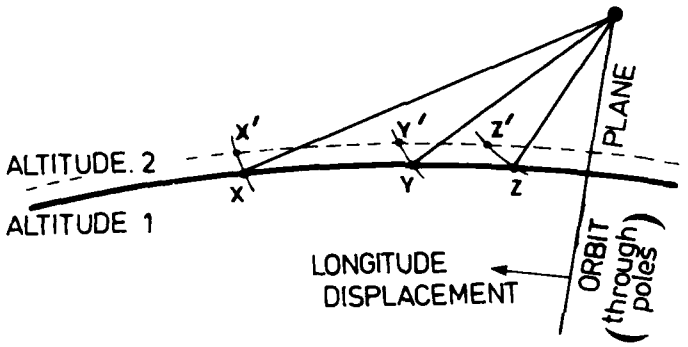

Figure 28. Effect of Altitude Estimate on Position Fix (after Stansell (1978), Ref. 77).

In the context of the present report, NNSS satellites would be used for finding the real time position of the F region mid-latitude trough. This would involve differential Doppler measurements of ionospheric electron density using 150 and 400 MHz transmissions at powers of approximately $\frac{3}{4}$ W and 1 W respectively. Prior knowledge is assumed of the location of a receiving station, e.g. near Adelaide, and of the particular received satellite at any instant.

5.4 Orbiting Satellites - Global Positioning System

Currently, the Global Positioning System (GPS) of navigation involves six satellites.

The GPS NAVSTAR system will be a new satellite constellation consisting of 18 satellites distributed uniformly within six orbital planes, each at 55 deg inclination to the equator; the first satellite is scheduled for launching in 1983, the eighteenth in 1988. The satellites orbit at about 17,400 km above the earth, completing an orbit cycle every 12 hours. They use frequencies of 1575.42 and 1227.6 MHz (Refs. 76 and 10).

The objective of NAVSTAR is to provide direct line-of-sight signals continuously from at least four satellites to all users on a world-wide basis. A ground control network tracks the satellite signals, determines the orbits precisely, and transmits an appropriate orbit definition to the memory system of each satellite. By this means, the satellites can provide users with an accurate description of their positions as a function of time. To obtain a position fix, the user must be equipped with a receiver capable of tracking signals from four satellites, either simultaneously or sequentially. Each set of four time-of-arrival measurements of signals made by the user permits four independent variables to be determined, namely clock time offset, latitude, longitude and altitude. Hence, the following accuracies are achievable: position, 16 m; velocity, 0.1 ms^{-1}; time, 100 ns. GPS provides near real-time determinations of three-dimensional position and velocity; (the TRANSIT system, described in Section 5.3 above, permits two-dimensional determinations only).

A future phase proposed for the GPS system involves an additional 28 satellites in three orbital planes. These would be Space Shuttle launched, commencing in 1986.

In the present context, the frequencies (1575.42 and 1227.6 MHz) employed by GPS would be too high to provide differential Doppler measurements of electron density with accuracy comparable to that achievable using the TRANSIT system. Nevertheless, the 55 deg inclination of NAVSTAR satellite orbits means that they would pass over geographic latitudes as high as 55 deg which, at the longitude of Adelaide, corresponds to 68 deg south invariant latitude; see Figure 3. The GPS satellites therefore traverse latitudes sufficiciently high that satellite transmissions received in Australia could pass through the mid-latitude trough under moderately disturbed geomagnetic conditions.

The GPS system would therefore provide the potential for real-time measurements of the total electron density in the trough, but with reduced accuracy due to the higher (GHz) frequencies employed.

6. IONOSPHERIC F REGION MID-LATITUDE TROUGH

6.1 General Features

The mid-latitude electron density trough was discovered by Muldrew (Ref. 59), and is a major but incompletely understood feature of the sub-auroral ionosphere. It has very significant effects on radio-wave propagation (Refs. 81, 39 and 23). It is most prominent in the winter night-time ionosphere, and consists of a circumpolar depletion of the plasma concentration (the "trough minimum") corresponding to electron densities at the F2 region maximum which are less by an order of magnitude than maxima elsewhere.

Although the present concern is mainly with the mid-latitude trough, it should be noted that there is also a polar trough which is a feature of very high invariant latitudes (defined in Appendix 1) greater than about 80 deg (e.g. Ref. 23). Both troughs are most clearly evident on winter nights. At other seasons, solar photo-ionisation tends to reduce their prominence.

6.2 Observations of Location and Extent of the Trough

(i) Topside Soundings and Other Satellite Techniques

Since Muldrew's (Ref. 59) initial description of the "ionospheric trough" appeared, based on topside soundings from the Alouette I satellite, it has been extensively studied by satellite techniques in attempting to understand its spatial and temporal variations, e.g. Refs. 18, 67 and 79. The main data gathering instruments were satellite-borne ion traps (e.g. Ref. 73) and electrostatic probes (e.g. Refs. 80 and 68) to measure the ion density, ion mass and the ratio of ion mass to ion temperature, as well as topside ionosonde sounding. Sagolyn et al's (Ref. 68) observations indicate that mid-latitude troughs occurred on 27% of all orbits at all times; furthermore, their equatorward edges had mean invariant latitudes of some 56 to 72 deg which at Adelaide's longitude (138.6 E) would correspond to mean geographic latitudes of 44 to 54 S. They also showed that either troughs or single gradient depressions (i.e. appearing at the equatorial boundary but not followed by a poleward increase) occurred on 51% of all orbits at all times. Figure 29 shows a significant diurnal variation in the frequency of trough occurrence. Troughs were rarely observed in daylight between 6 and 16 hrs local time; maximum occurrence was around 4 hrs local time.

From observations of approximately 3500 orbits of Isis 1, over some 12 months, Sagolyn et al (Ref. 68) found that the scale sizes of mid-latitude troughs typically ranged from 140 to 1500 km in latitudinal extent; some examples are shown in the top diagrams of Figure 29. The latitudinal extent of mid-latitude troughs is also indicated in the models in Figures 10 and 24 (Ref. 39) and Figure 30 (Ref. 54) discussed previously in Section 2.4. The trough can extend through almost as much as 180 deg of longitude. The overall invariant latitude width of the reduced electron density region can be about 10 deg including the trough edges.

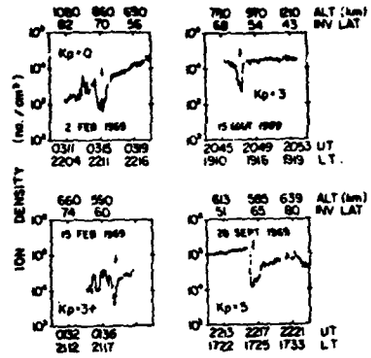

Figure 29(a). Examples of Ionisation Troughs (Sagolyn et al (1973), Ref. 68).

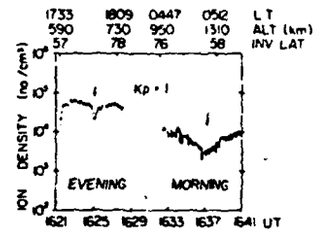

Figure 29(b). A Transpolar Orbit Showing Nightside and Dayside Trough (Sagolyn et al (1973), Ref. 68).

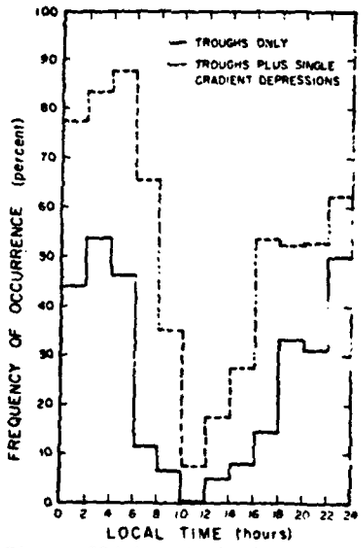

Figure 29(c). Variation with Local Time of the Occurrence Frequency of the Trough (Sagolyn et al (1973), Ref. 68).

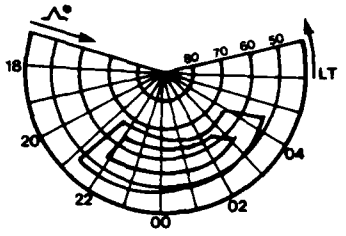

Figure 30(a). Invariant Latitude A, Local Time (LT) Plot of the Positions of the Predicted Trough Walls for the Night of May 18-19, 1976 ($\overline{Kp}$ = 1.1). (Lockwood (1981), Ref. 54)

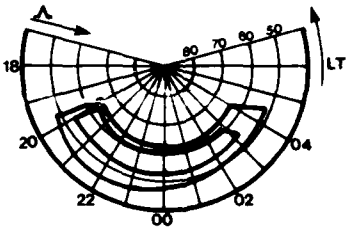

Figure 30(b). A-LT Plot of Mean Trough for $\overline{Kp}$ = 2.75, May 1976. (Lockwood (1981), Ref. 54)

The mid-latitude trough is bounded on the high latitude side by a steep "wall" of ionisation, the poleward "edge", which is approximately 2-4 deg of latitude wide, and is created primarily by soft (<1 keV) electron precipitation from the magnetosphere (Ref. 62). In the low latitude boundary (the "equatorial edge") which is approximately 3-8 deg of latitude wide, the electron concentration is highly variable and is an extension of the mid-latitude ionosphere (Ref. 24). The mean position of the trough is at about 60 deg of invariant latitude (which gives a good approximation to the actual geomagnetic field, as discussed in Appendix 1). The trough is most pronounced at the maximum of the F2 layer ionisation, but has been detected up to 2500 km.

In the particular case of night-time in winter, when the trough was most pronounced, Mendillo and Chako (Ref. 57) studied Northern Hemisphere topside ionospheric sounder observations obtained with the Isis 2 satellite during a period of very low magnetic activity. They showed (Figure 31) that at the altitude of maximum electron density, the poleward wall of the trough could be represented as having an invariant latitudinal width of about 2 deg, a trough minimum approximately 13 deg wide and an equatorward edge of the order of 7 deg width, i.e. a structure (at a geographic longitude of some 70 W) having an overall invariant latitude width of the order of 22 deg. (Mendillo and Chako's (Ref. 57) data were given in corrected geomagnetic latitude, considered briefly in Appendix 1).

Feinblum and Horan (Ref. 32) observed the trough width to be a variable feature depending on local time, the trough being narrow near midnight, and wide near dawn and dusk. Furthermore, the trough width decreased as the planetary magnetic activity index, Kp, increased. The width of the equatorward wall, in particular, decreased with increasing Kp. The depth of the trough also varied with local time and Kp; typically, electron densities in the trough were a factor of about 5-10 lower than those found on either the poleward or equatorward side of the trough. The trough tended to be deepest near midnight, with the depression in electron density being about a factor of 8 to 10. Past midnight, the trough filled in slightly, and the walls became less steep. Near dawn and dusk the trough became less pronounced owing to photoionisation.

(ii) Bottomside Soundings

Bottomside ionogram observations of the trough are rarely reported. This is because a trough that is directly above a transmitter will return off-vertical reflections from its steep "sides" (contours of equal ionisation) in directions some tens of degrees off-vertical (Figure 2) with critical frequencies close to those that would prevail in the absence of the trough (Bowman (Ref. 11)). As these reflections produce ionograms with critical frequencies and ranges (200-300 km) similar to those prevailing in the absence of the trough, they are readily mistaken for normal F2 region echoes. However, since the troughs are deep, as seen in Figure 2, the vertically incident signals produce traces with ranges around 500 km and critical frequencies several times smaller than those of the lower traces; vertical reflections from the trough therefore tend to be "lost" amongst other reflections. As a result of such effects,

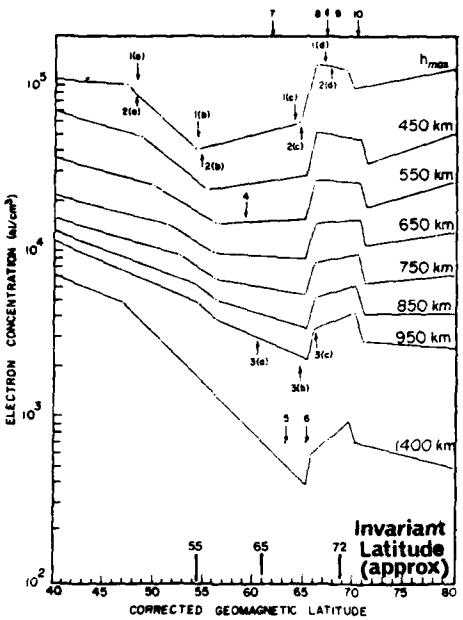

Figure 31. A representation of the mid-latitude trough at eight heights is shown. It was obtained from topside sounding observations from 22 satellite passes (Mendillo and Chako (Ref. 57)).

only an exceptionally wide trough can be resolved by means of usual ionosonde techniques. (This corresponds to very quiet geomagnetic conditions, or else a location where the invariant latitude lines are exceptionally far apart.) Alternatively, special techniques must be used to identify the bottomside trough; e.g. Bowman (Ref. 11) employed an ionosonde with direction-finding capabilities.

Rodger and Pinnock (Ref. 63) have identified five types of trough on ionograms recorded with a normal ionosonde at Halley Bay. Their classifications are associated with time of occurrence, Kp and relationship, or otherwise, with sporadic E and/or spread F ionisation. They made the interesting observation that the level of magnetic activity, measured by Kp, required for a particular trough sequence to be observed at Halley Bay was slightly lower at sunspot maximum compared with sunspot minimum. They suggested that, in principle, if Kp is known, the time of occurrence of the trough (e.g. at Halley Bay), its shape and movement can be predicted. This could lead to a significant improvement in the predictability of radio-wave propagation in the vicinity of the trough.

Preliminary observations at Halley Bay with an Advanced Ionospheric Sounder have demonstrated its suitability for recording the trough and tracking its diurnal motion by locating its echoing region in range, azimuth and elevation (Dudeney et al (Ref. 23)).

The mid-latitude trough, along with the auroral oval, is asymmetrically located with respect to the geographic polar axis, as suggested in Figure 32, but is fixed in space relative to the sun. Consequently, as the earth rotates, a fixed observer on the earth's surface records a diurnal motion of the trough which moves equatorwards in the early evening hours (local time), and afterwards moves polewards. Trough velocities relative to a fixed observer are of the order of 50-150 m/s (Bowman (Ref. 11)). The mid-latitude trough therefore assumes the appearance of a very large-scale travelling ionospheric disturbance.

Lietinger et al (Ref. 51) made differential Doppler measurements of transmissions from Navigation satellites at four middle to high latitude European stations. During some winter nights they observed F region ionospheric troughs (indicated in Figure 33) with poleward boundaries near the equatorward edge of diffuse aurorae coinciding with the precipitation of soft electrons (<400 eV). They commented that these electron content observations permitted F layer investigations to be made under disturbed conditions when ionograms failed or were very difficult to interpret.

In making differential Doppler measurements of NNSS satellite transmissions at 150 and 400 MHz, Evans and Wand (Ref. 31) observed that the trough did occur in the daytime, although it was mainly a night-time phenomenon. They found that on some magnetically disturbed winter days, deep troughs occurred in the afternoon and evening. These troughs are exemplified in Figure 34, and gave rise to the largest quasi-stationary refraction effects observed on UHF radar transmissions during a three-year study at Millstone Hill, Massachusetts.

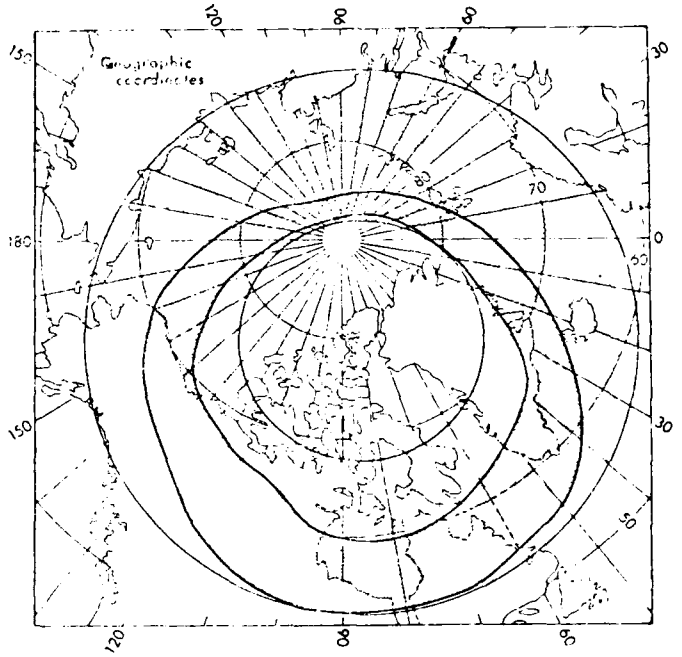

Figure 32. Location During Moderate Activity (Q = 4) of the Auroral Oval. Dark shading indicates the oval at 0800 UT, while light shading indicates the area swept over by the oval during the day. (The figure is taken from Knecht (Ref. 46) who reports that it is "based on data of Feldstein, as plotted by Feldstein and Starkov, 1967, and Akasofu, 1968").

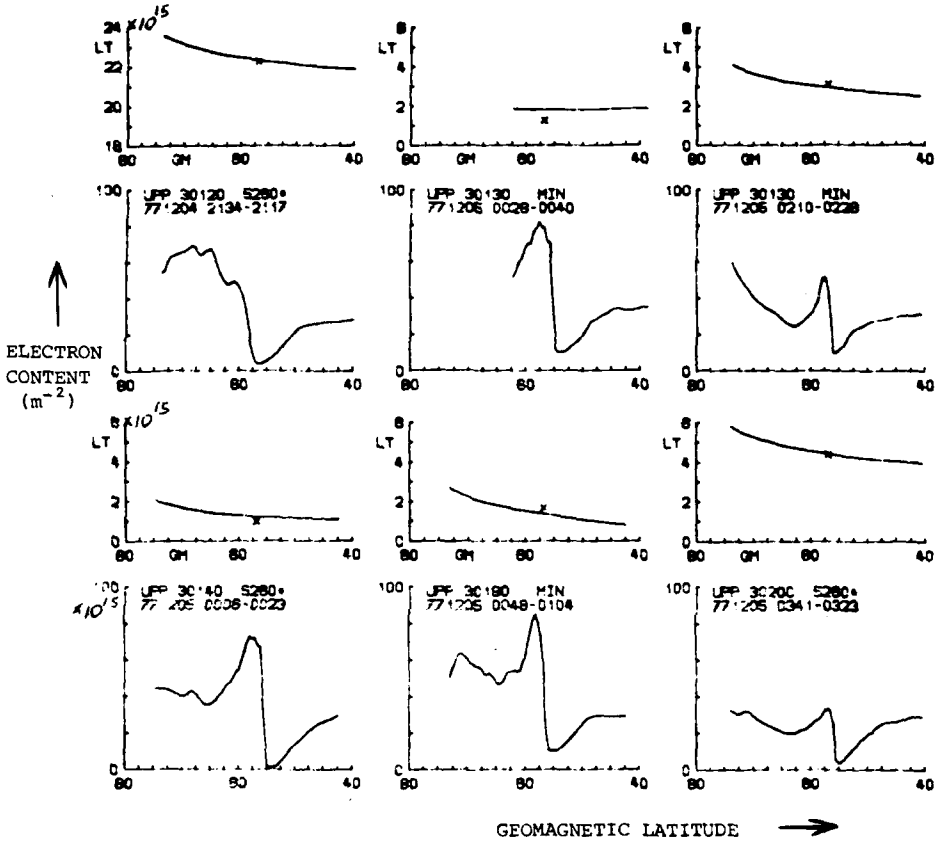

Figure 33. The Latitude Dependence of Ionospheric Electron Content is shown, for Data Recorded at Uppsala (Lietinger et al, Ref. 51).

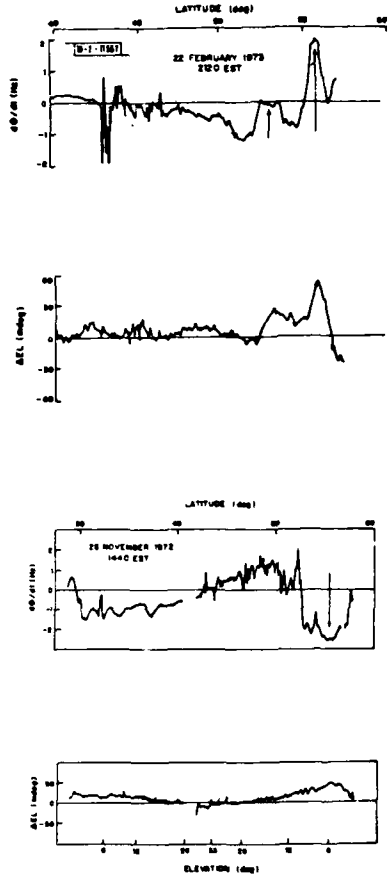

Figure 34. The figure shows examples of correlated differential-Doppler and refraction error perturbations. The arrows mark the location of Doppler excursions caused by gradients in the high-latitude ionosphere (Evans and Wand (1981), Ref. 31). $\Delta\Phi$ represents differential phase, and ΔEL represents elevation change.

The above discussion indicates that the trough is predominantly a night-time phenomenon. However, Ahmed and Sagolyn (Ref. 1) and Ahmed et al (Ref. 2) reported from topside observations (1969-1972) using ISIS I and INJUN V satellites that in the 560-3600 km range, i.e. extending to altitudes well above the peak, the trough had a strong likelihood of being present at any time: its occurrence frequency was 95% at night, 60% near dawn and dusk, and 48% near local noon. They also found negligible seasonal variation in trough location at a given local time, except near sunrise.

(iii) Equatorward Displacement of Auroral Phenomena

It is noted in Figure 3, from Evans et al (Ref. 28), that the Invariant South Geomagnetic Pole is displaced in the direction of Australia by some 16 deg of geographic latitude from the South Geographic Pole. As a result, at the longitude of Adelaide (138.6E) an invariant latitude of 60 S corresponds to a geographic latitude of approximately 48 S, i.e. the mean trough position would coincide approximately with the southern tip of New Zealand. Other invariant (southern) latitudes (with geographic latitudes indicated in brackets) are:

Hobart, 53.6 (42.9); Macquarie Island, 64.0 (54.3); Mawson, 70.0 (67.4). (The co-ordinates of many other southern stations are listed by Dudeney and Piggott (Ref. 24).

It is also noted that at a longitude of approximately 142 E, the South Geomagnetic Dip Pole is displaced 23 deg of geographic latitude from the South Geographic Pole in the direction of Australia.

Coupled with the displacement of the south magnetic pole towards Australia is the occurrence above the Southern Ocean of higher latitude ionospheric phenomena than might otherwise be expected. In particular, the mean position of the mid-latitude trough occurs as far north as Hobart in magnetically-disturbed conditions (Kp ≈ 5). The trough commonly occurs at higher latitudes where there is, unfortunately, a lack of ionospheric data.

6.3 Formation of the Mid-latitude Trough

The mid-latitude trough corresponds to a narrow region of very low electron density. It is situated just equatorward of the nocturnal auroral oval (Figure 32) within which auroral activity is largely confined, and which arises from diffuse auroral particle precipitation.

Like the auroral oval, the position of the trough for a particular degree of magnetic activity is "fixed" in space relative to the sun while the earth rotates beneath it.

The trough is primarily a feature of the night-time ionosphere; it can be very pronounced in winter and autumn, and less evident in summer and spring.

The electron density depression in the trough is generally deepest near local midnight suggesting that the processes which are acting to destroy the ionospheric plasma should be strongest at this time (Schunk et al (Ref. 71)).

The poleward edge of the trough is located ≈3 deg equatorward of the equatorial edge of the auroral oval (e.g. Sagolyn et al (Ref. 68)).

At this geomagnetic latitude occurs the plasma-pause which coincides with the boundary between the inner geomagnetic field co-rotating with the earth and the magnetospheric field resulting from the geomagnetic and interplanetary magnetic fields. These are indicated in Figures 35 and 36, from Dudeney (Ref. 22), and Figure 37, from Knecht (Ref. 46). The envelope of the magnetospheric field is blown by the solar wind to point away from the sun.

The plasmapause coincides with an abrupt step in the concentration of charged particles in the atmosphere. At lower latitudes than the plasmapause the atmospheric plasma is relatively cool and dense; at higher latitudes the plasma is hot (i.e. energetic) and tenuous. In the immediate vicinity of the plasmapause is the F region mid-latitude trough, a relatively stable region where the concentration of ionisation is greatly reduced. To date, no explanation proposed for the mid-latitude trough is fully consistent with the observational evidence.

The fact that the poleward wall of the mid-latitude trough lies just equatorward of the boundary of diffuse auroral precipitation suggests that the poleward wall is caused by ionisation produced by the soft component of auroral particles, namely <1 keV electrons, precipitated from the magnetosphere. The ionisation is produced at altitudes around 100-150 km, and moved upwards along geomagnetic field lines by the effects of auroral heating. Thus, the observed magnetic field-aligned wall of ionisation is formed corresponding to a steep horizontal ionisation gradient (as suggested in Figure 36).

Statistically, the centre of the mid-latitude trough lies near the ionospheric projection of the geomagnetic field line from the equatorial magnetospheric plasmapause, sometimes called the magnetopause (Kohnlein and Raitt (Ref. 49) as suggested in Figure 36. However, at any instant, the two do not coincide in a consistent way; Grebowsky et al (Ref. 36) explained this lack of coincidence as follows.

The trough is coupled to the plasmapause in ways not fully understood. A very complex dynamic interaction, in fact, occurs. This involves (i) the redistribution of plasma under the action of electric fields of magnetospheric origin and thermospheric winds, (ii) plasma production due to particle precipitation and solar U.V. radiation, as well as (iii) plasma loss through charge exchange and recombination processes (Dudeney et al (Ref. 23)).

Some further detail on the formation of the mid-latitude trough is given in Appendix 3.

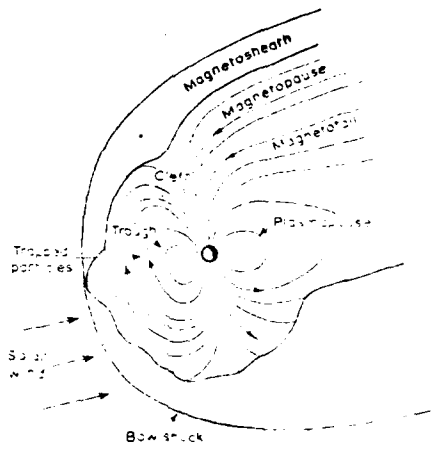

Figure 35. Magnetic Field Configuration Near the Earth (after Dudeney (1981), Ref. 22).

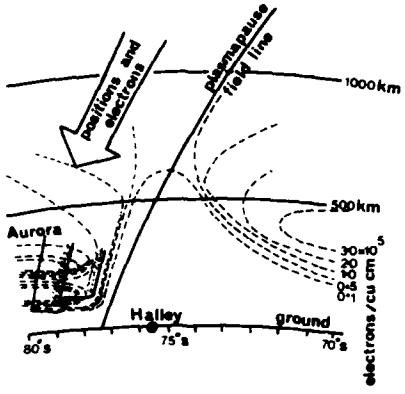

Figure 36. The F-region Trough, Before Midnight, Showing the Region of Reduced Ionisation (in terms of electrons/cm^3) and its Location Relative to Halley Station (from Dudeney (1981), Ref. 22).

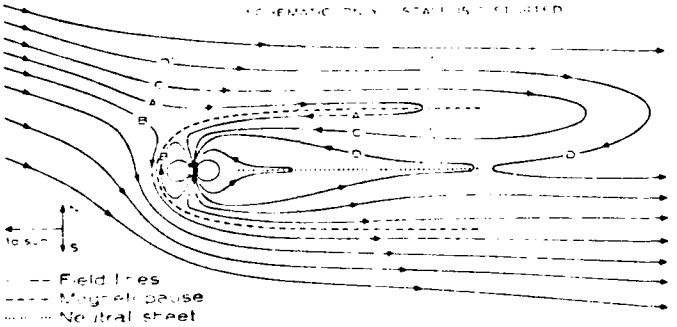

Figure 37. Reconnection of Magnetospheric and Interplanetary Field Lines, Shown Schematically (Not to Scale) for the Earth in a Sector of the Interplanetary Field which is Outward with a Southward Component (after Knecht (1972), Ref. 46).

7. DOPPLER ELECTRON CONTENT MEASUREMENTS - LOCATING THE TROUGH IN REAL TIME

The differential Doppler technique may be used in measuring the spatial (and temporal) variations in total electron content in the ionosphere between an orbiting satellite (e.g. a NNSS satellite) and a ground station. The change in phase difference between coherent 150 and 400 MHz transmissions is measured at the ground station, and is directly interpretable as the change in electron content along the ray path from satellite to ground station as the satellite moves in its orbit. (It is noted that phase changes are measured, and not absolute values of phase path length along the ray path; i.e. phase changes are measured relative to a minimum phase, usually occurring at closest approach of the satellite to the receiving station. Thus there is always an unknown constant = $2\pi m$ (where m is an integer) to be added to the measured phase difference to obtain an absolute value of phase.)

Guier and Weiffenbach (Ref. 37) described the Differential Doppler technique in proposing its use in a satellite Doppler navigation system. The technique is summarised e.g. by Essex and Day (Ref. 27).

The differential Doppler technique involves the measurement of the difference in phase path length of radio signals received from a satellite at two harmonically related frequencies f and f', where $f' = mf (m > 1)$. Phase path expressed as a number of wavelengths may be written:

$$P = \frac{f}{c} \int_0^S n\,ds$$

where n is the refractive index of the medium at a specified frequency,
c is the free space speed of light, and
s is the geometric path length from satellite to receiver.

Signals received at the two frequencies exhibit Doppler phase path shifts, i.e. rates of change of phase path length, of dP/dt and dP'/dt respectively, caused chiefly by the satellite motion.

Changes in phase path length arising from the line of sight motion of the satellite (and also phase delays introduced by the troposphere which are frequency independent) are removed in calculating the differential Doppler frequency defined to be:

$$F = m \frac{dP}{dt} - \frac{dP'}{dt}$$

(Specifically, F is the difference between the time rates of change of the two phase paths, measured in a length unit equal to the shorter wavelength.)

Provided that both frequencies greatly exceed f_oF2 (the F2 layer critical frequency), the refractive index of the ionosphere at a specified frequency f has the form:

$$n = \left[1 - \left(\frac{f_N}{f}\right)^2\right]^{\frac{1}{2}}$$

to sufficient accuracy for $f > 100$ MHz

where $f_N = \left(\frac{Ne^2}{4\pi^2 m'}\right)^{\frac{1}{2}}$

is the ionospheric plasma frequency,
N being the local electron concentration, and
e and m' the electron charge and mass respectively.

In particular, approximately:

$$n = 1 - a\frac{N}{f^2}$$

where a is approximately 4.5×10^{-9} MKS units.

It follows that the differential Doppler frequency (Hz) is:

$$F = \left(m - \frac{1}{m}\right)\frac{a}{cf}\frac{d}{dt}\int_o^{h_s} N\sec\psi\, dh$$

where ψ is the local zenith angle, and
h_s the satellite altitude.

Hence:

$$\int F dt = \left(m - \frac{1}{m}\right)\frac{a}{cf}\int_o^{h_s} N\sec\psi\, dh + c$$

It follows that by integrating with respect to time the differential Doppler frequency represented by F, it is possible in principle to determine the total electron content (corresponding to the integral on the right hand side of the above equation) along the ray path up to the satellite provided that the constant c of integration can be determined.

Essex and Day (Ref. 27) refer to several methods for determining c, including the use of local ionosonde data or combining differential Doppler data recorded at stations separated by several hundred km or the use of transmissions from a geostationary satellite. However, in the present context, spatial changes in total electron content corresponding to the presence of a mid-latitude trough or an atmospheric disturbance can be determined by differential Doppler observations at different times (denoted 1 and 2) at a single station. In particular, the phase (number of "cycles") change in the differential Doppler signal during a specified time interval is denoted:

$$\int F_2 dt - \int F_1 dt = \left(m - \frac{1}{m}\right)\frac{a}{cf}\int_o^{h_s} (N_2\sec\psi_2 - N_1\sec\psi_1)\, dh$$

where the integral on the right hand side corresponds to the total electron content change observed when the satellite was in position 2 compared with position 1.

Figure 38 shows examples of differential Doppler frequency (and phase) versus latitude graphs obtained by Essex and Day (Ref. 27). Fluctuations on the frequency versus latitude curves correspond to ionospheric irregularities.

Lyon (Ref. 55) also shows graphs (Figure 39) of electron content (along a ray path) versus time, recorded over the approximately 10 min intervals during which NNSS satellites are visible for an earth observer. The comparatively smooth variations of electron content in his graphs indicate the presence of peaks and troughs of ionisation, similar to those attributable to large travelling ionospheric disturbances or the mid-latitude trough. They suggest the suitability of differential Doppler observations to record time variations in electron content expected for the mid-latitude trough, as proposed in the present project.

Variations in total ionospheric electron content from receiver to satellite are the major cause of the differences in phase variations observed at two frequencies, as discussed above. These are the only variations relevant to the present discussion which deals with gross changes in electron

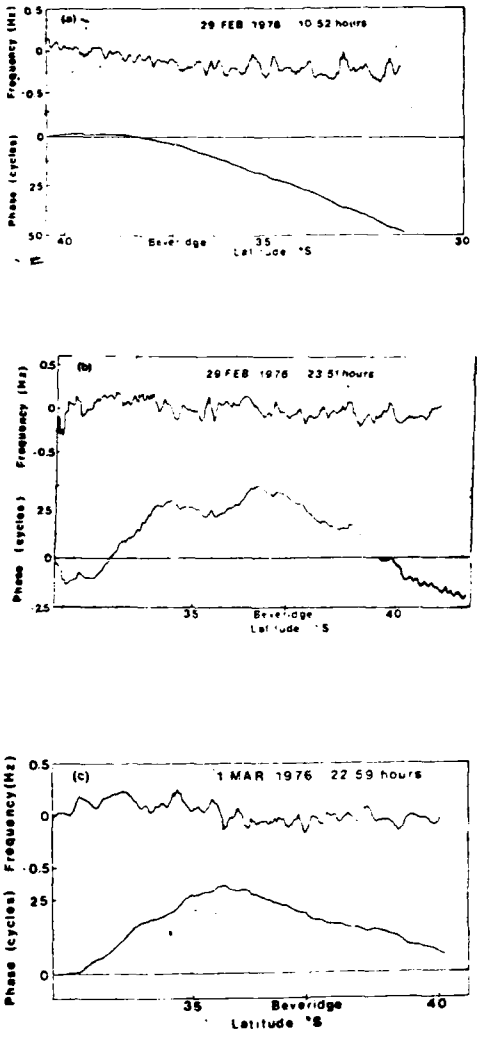

Figure 38. Examples are shown of differential Doppler frequency and phase versus latitude for three passes of the NNSS satellites during the period 29 February to 1 March, 1976. Sampling frequency is 2 Hz. The times indicated are the times of closest approach of the satellite (after Essex and Day (Ref. 27)).

density arising from the mid-latitude trough; this effect corresponds to the second order dependence of n on f, i.e. $n \propto 1/f^2$. Clynch and Renfro (Ref. 19), however, mention other minor variations in phase, namely:

(a) a third order term which involves the geomagnetic field through the electron gyrofrequency (electron cyclotron frequency) ≈ 1.4 MHz; this effect is inappreciable at frequencies remote from the gyro-frequency, and

(b) a fourth order term which becomes appreciable at low elevation angles.

CCIR (Ref. 16) remarks that "maps of total electron content (TEC) are needed for predicting ionospheric effects on the satellite-Earth links. Measurements of total electron content have been made at many stations by observations of the Faraday rotation or the Doppler effect on signals from low orbiting and geostationary satellites". Amayenc et al (Ref. 6) and Klobuchar (Ref. 45) have prepared maps of electron content for the mid-latitude ionosphere. Experiments of the kind described in the present report would provide additional TEC data on the ionosphere at high invariant latitudes (Mendillo and Klobuchar (Ref. 58)).

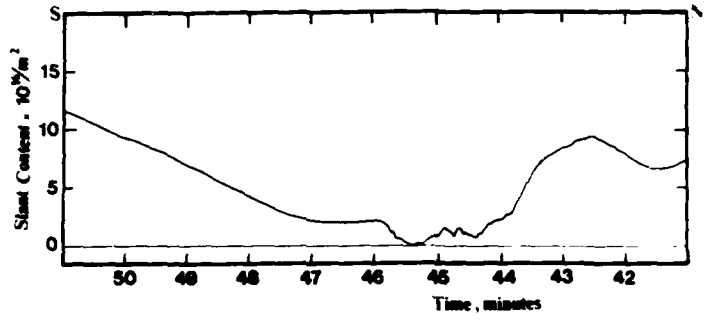

Measured Slant Content for NNSS Satellite Pass at La Ronge, Saskatchewan on 18 February, 1981, 0759 UT

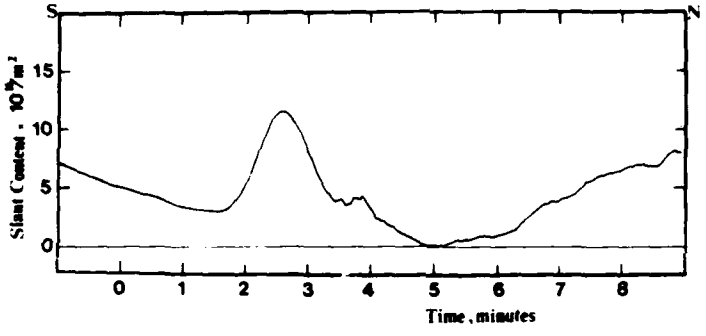

Measured Slant Content for NNSS Satellite Pass at La Ronge, Saskatchewan on 18 February, 1981, 0341 UT

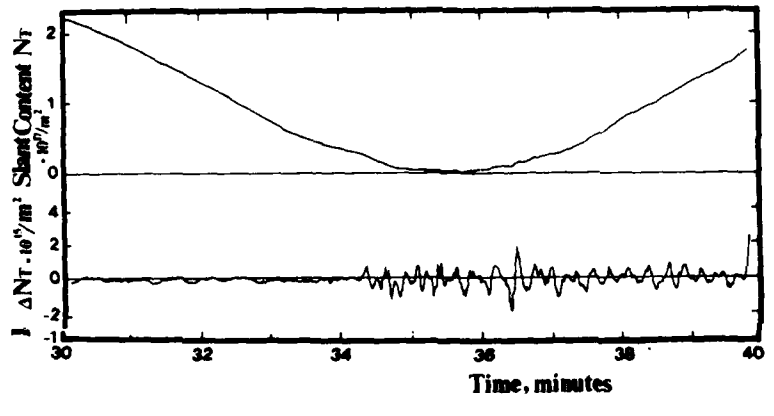

Measured Slant Content and Content Fluctuations for NNSS Satellite Pass at London, Ontario on 21 June, 1981, 0234 UT

Figure 39. From Lyon (Ref. 55).

APPENDIX 1

INVARIANT LATITUDE

The invariant geomagnetic latitude Λ is defined:

$$\Lambda = \cos^{-1}(L^{-\frac{1}{2}})$$

and is based on the parameter L, defined by McIlwain (Ref. 56) as follows (Filz et al (Ref. 33)).

If the geomagnetic field were a pure dipole, L would be equal to R_o which is the maximum distance from the centre of the geomagnetic field to the farthest point on the magnetic field line around which trapped charged particles would be constrained to move.

It can be shown that in a pure dipole field, the following relationship would hold:

$$\frac{R_o^3 B_m}{M} = f\left(\frac{I^3 B_m}{M}\right) \qquad \ldots\ldots\ldots\ldots\ldots\ldots\ldots\ldots \text{(A1.1)}$$

where B_m is the magnitude of the magnetic field strength at the mirror point of the charged particle and is an adiabatic invariant of the particle motion,

M is the magnetic moment of the dipole,

f indicates a function, and

I is the longitudinal invariant which has no clear physical or geometrical meaning.

I is defined as the integral with respect to distance (from one mirror point to its conjugate) of the term:

$$\left[1 - \left(\frac{B}{B_m}\right)\right]^{\frac{1}{2}}$$

where B is the magnitude of the magnetic field strength.

In the geomagnetic field, the relationship (A1.1) does not hold. McIlwain (1961) replaced R_o by L which he defined as follows:

$$\frac{L^3 B_m}{M} = f\left(\frac{I^3 B_m}{M}\right)$$

where the units of L are earth radii (R_E), and

$M = 0.311653$ (in units of gauss-R_E^3).

Because the geomagnetic field is nearly a dipole, $L \approx R_o$, as seen in Figure 40 from Knecht (Ref. 46).

The locus of all points with a given L value is called an L-shell.

Invariant latitude Λ is a convenient geomagnetic co-ordinate which gives a good approximation to the actual geomagnetic field, and a good indicator of the behaviour of charged particles in the upper atmosphere.

e.g. For an invariant latitude:

$$\Lambda = \cos^{-1}(L^{-\frac{1}{2}}) = 60 \text{ deg},$$

it is seen that:

$$L^{-\frac{1}{2}} = \frac{1}{2}$$

i.e. $L = 4$

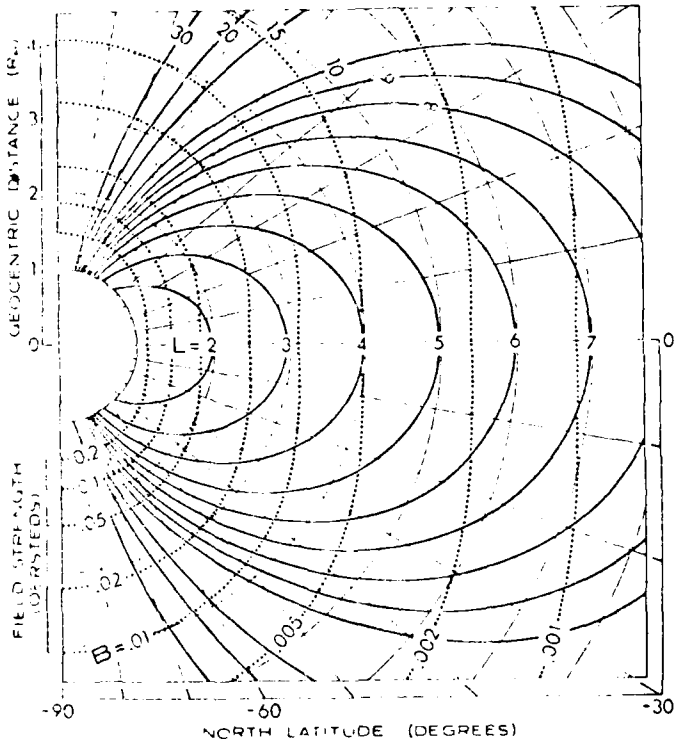

Figure 40. The B-L Co-ordinate System. The curves are the intersection with a magnetic meridian plane of surfaces of constant B and constant L. The departure of these curves, plotted for a dipole field, from those of the actual field is too small to be apparent in a figure of this scale (Knecht (Ref. 46)).

It follows that the geomagnetic field lines which emerge from the earth's surface at an invariant latitude of 60 deg, extend, very closely, to four earth's radii from the earth's centre.

Some papers e.g. Mendillo and Chako (Ref. 57) employ corrected geomagnetic co-ordinates. These are defined (Knecht (Ref. 46)) by analogy with geographic co-ordinates and represent the best earth-centred dipole approximation to the geomagnetic field with its axis tilted 11.5 deg to the rotation axis so as to intersect the (currently approximate) position of the geomagnetic north pole at geographic co-ordinates 78.5 N, 291 E.

APPENDIX 2

THE DOPPLER MEASUREMENT OF RANGE

The following description of the Doppler technique in measuring the receiver-to-satellite range, and hence in determining the receiver position, is similar to that given by Stansell (Ref. 76).

By receiving the navigation message, the Transit system user learns the position of the satellite as a function of time. Thus, to obtain a position fix he must relate his position to the known satellite orbit. This relationship is established by measuring the Doppler shift, which is a unique function of the observer's position and motion relative to the known satellite orbit.

Figure 41 illustrates the Doppler measurement technique. The frequency f_R being received from the satellite consists of the frequency being transmitted f_T plus a Doppler frequency shift of up to ±8 kHz due to relative motion between the satellite and the receiver. Note that the transmitted frequency is offset low by about 80 parts per million (32 kHz at 400 MHz) to prevent f_R from crossing 400 MHz.

The navigation receiver is equipped with a stable reference oscillator from which a 400 MHz ground reference frequency f_G is derived. Oscillator stability must be adequate to assume a constant frequency throughout the satellite pass. As shown by Figure 41, the navigation receiver forms the difference frequency $f_G - f_R$, and each Doppler measurement is a count of the number of difference frequency cycles occurring between time marks received from the satellite. Because every message bit effectively represents another time mark, the Doppler counting intervals are formed with respect to the particular message format. For example, each line of the message lasts about 4.6 seconds, and the commonly used Doppler count interval of 23 seconds is formed by starting a new count at the end of every fifth line.

Each Doppler count is composed of two parts: the count of a constant difference frequency $f_G - f_T$, minus the count of the number of Doppler cycles received during that time interval. It is the Doppler cycle count which is physically meaningful. The count of the difference frequency is an additive constant which is eliminated by the position fix calculation.

In Figure 41 it is emphasised that the distance between the satellite and the observer changes throughout the satellite pass. It is this change, in fact, which causes the Doppler frequency shift. As the satellite moves closer, more cycles per second must be received than were transmitted to account for the shrinking number of wavelengths along the propagation path. For each wavelength the satellite moves closer, one additional cycle must be received. Therefore, the Doppler frequency count is a direct measure of the change in distance between the receiver and the satellite over the Doppler count interval. In other words, the Doppler count is a geometric measure of the range difference between the observer and the satellite at two points in space, accurately defined by the navigation message.

This is a very sensitive measure because each count represents one wavelength, which at 400 MHz is only 0.75 metre.

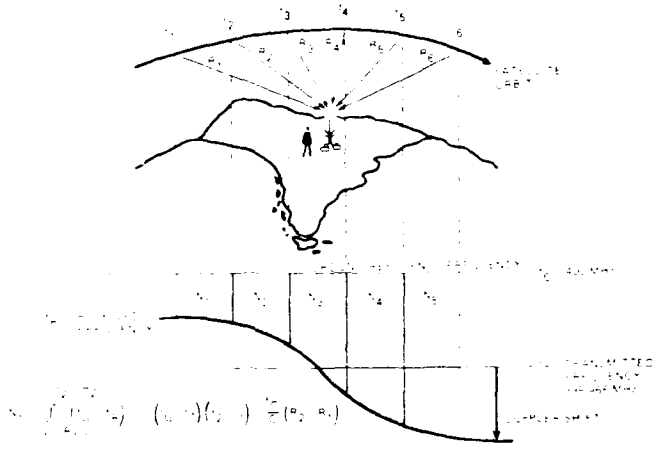

Figure 41. Each Doppler Count Measures Slant Range Change (Stansell (Ref. 76)).

The equation defining the Doppler count of $f_G - f_R$ is the integral of this difference frequency over the time interval between receipt of time marks from the satellite. For example:

$$N_1 = \int_{t_1 + R_1/C}^{t_2 + R_2/C} (f_G - f_R)dt$$

Note that $t_1 + R_1/C$ is the time of receipt of the satellite time mark that was transmitted at time t_1. The signal is received after propagating over distance R_1 at the velocity of light C.

The above equation represents the actual measurement made by the satellite receiver, but it is helpful to expand this equation into two parts:

$$N_1 = \int_{t_1 + R_1/C}^{t_2 + R_2/C} f_G dt - \int_{t_1 + R_1/C}^{t_2 + R_2/C} f_R dt$$

Because the first integral in this equation is of a constant frequency f_G, it is easy to integrate, but the second integral is of the changing frequency f_R. However, the second integral represents the number of cycles received between the times of receipt of two timing marks.

By a "conservation of cycles" argument, this quantity must equal identically the number of cycles transmitted during the time interval between transmission of these time marks. Using this identity, this equation can be written:

$$N = \int_{t_1 + R_1/C}^{t_2 + R_2/C} f_G dt - \int_{t_1}^{t_2} f_T dt$$

Because the frequencies f_G and f_T are assumed constant during a satellite pass, the integrals in this equation become trivial, resulting in:

$$N_1 = f_G\left[(t_2 - t_1) + \frac{1}{C}(R_2 - R_1)\right] - f_T(t_2 - t_1)$$

Rearranging the terms in this equation gives:

$$N_1 = (f_G - f_T)(t_2 - t_1) + \frac{f_G}{C}(R_2 - R_1)$$

This final equation clearly shows the two parts of the Doppler count. First is the constant difference frequency multiplied by a time interval defined by the satellite clock. Second is the direct measure of slant range change measured in wavelengths of the ground reference wavelength C/f_G. It happens that the wavelength of f_G is the proper scale factor because received time marks are used to start and stop the Doppler counts. If a ground clock is used to control the count intervals, the wavelength of f_T would become the appropriate scale factor.

A usable satellite pass will be above the horizon between 10 and 18 minutes, which determines the number of Doppler counts acquired. Typically 20 to 40 counts will be collected by modern equipment. The Doppler counts and the satellite navigation message are passed to a small digital computer for processing. For simplicity, a stationary receiver is assumed as shown in Figure 41 in order to establish the basic position fix concept.

APPENDIX 3

MID-LATITUDE TROUGH FORMATION - DETAILED CONSIDERATIONS

This appendix is intended to discuss in some detail the formation of the mid-latitude trough as an extension of its description given in Section 4.4.

Observations of the trough have mainly been carried out by means of ionospheric topside investigations. During August 1972, Grebowsky et al (Ref. 36) employed Explorer 45 and ISIS 2 topside data, obtained with a magnetic ion mass spectrometer in studying the movement of ions, particularly H^+, along geomagnetic field lines associated with the mid-latitude trough. They proposed an explanation for the short-term differences between the positions of the trough and plasmapause which involved the movement of ions at supersonic speeds for part of their paths along geomagnetic field lines. In this case, ion densities would be enhanced near the equatorial plane by means of the (observed) upward transport of light ions from the ionosphere; nevertheless, to agree with observation the ionospheric ion densities on the same field lines must remain undisturbed. In this way the plasmapause boundary can be formed at L co-ordinates (see Appendix 1) which, in the equatorial plane, are higher than the ionosphere. In supersonic ion flows, ion acoustic waves cannot propagate "upstream". Information about ion density increases occurring at altitudes above where the ion upward flow becomes supersonic cannot therefore be propagated down to ionospheric heights. In order to account at all local times for the separation between trough and plasmapause, Grebowsky et al (Ref. 36) concluded that supersonic flows must persist on the outer field lines of the plasmasphere for at least one day following a storm depletion of ionisation in the trough. They concluded that upward accelerated H^+ flows, possibly to supersonic speeds during the refilling of the magnetic flux tubes in the outer plasmasphere, could produce an equatorial plasmapause with magnetic field lines which mapped into the ionosphere at latitudes poleward of the H^+ density increase.

Schunk, Banks and Raitt (Ref. 70) concluded that there is no single cause for the observed troughs, but that at various times, different mechanisms act together to create electron density depressions of substantial magnitude. Some of the proposed mechanisms are considered briefly below.

One proposal (Nishida (Ref. 61)) was that the F region depletion could be a consequence of the escape of ionisation along open geomagnetic field lines.

Knudsen (Ref. 47) proposed that a factor in the formation of the trough was a slow plasma convection across the pole. This enhanced the rate of the ion-atom interchange reaction of O^+ with N_2^* (discussed below) resulting in a depletion of ionisation (Schunk et al (Ref. 70)).

The plasma convection pattern is illustrated in Figure 42 from Lockwood (Ref. 53). Thermospheric neutral winds, transporting vibrationally excited N_2 molecules (denoted N_2^*) equatorwards from the auroral zone, would also enhance the conversion of O^+ to NO^+ (Schunk and Banks (Ref. 69)). These factors, coupled with the normal lack of night-time maintenance of the F region, through recombination, could contribute appreciably to the observed reduction by an order of magnitude in the peak electron densities observed in the trough (Banks et al (Ref. 8); Schunk, Raitt and Banks (Ref. 71)).

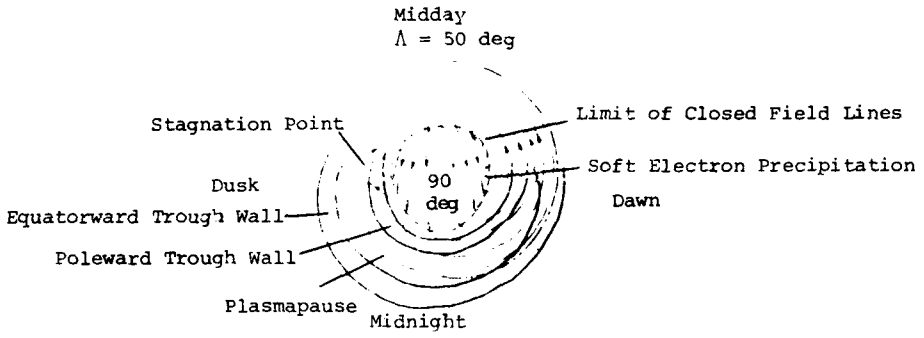

Figure 42. The diagram is derived from Lockwood (Ref. 53) and shows invariant latitude: local time plots of the model plasma convection pattern above 200 km (from Knudsen (Ref. 48)) and the mean positions of the walls of the trough in the F2-peak density at low Kp (between the solid lines) obtained from regression equations by Halcrow and Nisbet (Ref. 39).

Through various processes, discussed by Schunk and Banks (Ref. 69), N_2^* is produced in the nocturnal auroral oval. (These processes include the excitation of N_2 by precipitating electrons, thermal electrons and excited atomic oxygen (O), and the reaction of N with NO.) The presence of N_2^* substantially increases the rate at which O^+ is lost via the reaction:

$$O^+ + N_2^* \rightarrow NO^+ + N \quad \ldots\ldots\ldots\ldots\ldots\ldots\ldots\ldots \text{(A3.1)}$$

Owing to the action of the thermospheric winds (having equatorwards components) and diffusion, N_2^* does not remain at its point of origin, but is transported equatorwards to regions outside the auroral oval where it can act to reduce substantially the F-region electron density, following the above reaction and the one below (Spiro et al (Ref. 75)):

$$NO^+ + e \rightarrow N + O$$

As N_2^* leaves the precipitation region, there occurs a gradual loss of vibrational quanta and a consequent gradual decrease in the enhanced N_2 vibrational temperature (T_v). This decrease is primarily due to a "quenching" reaction of excited O with N_2, producing N_2^*. In the vicinity of the F2 region peak electron density around 200 km altitude, where the quenching and diffusion time constants are equal, the characteristic time (τ_d) for the decay of T_v is probably determined by the N_2^* - O quenching rate. (The loss of N_2^* by the reaction (A3.1) above is negligible compared with atomic oxygen quenching.) It follows that τ_d is ~ 5000 s at altitudes above 200 km, and if the equatorward component of the neutral wind is ~ 100 m/s, the vibrating N_2 molecules travel approximately 4 deg of latitude before quenching is likely. As the N_2^* ions drift over this distance, which is about the average width of a trough, T_v (previously enhanced in the auroral region) will cause an enhancement in the O^+ loss rate in reaction (A3.1) above. This can lead to a substantial reduction in the F region ion density.

It is noted that the above process involving N_2^* undoubtedly acts jointly with other mechanisms. Thus it can be expected that within the trough, transport processes will involve convection produced by electric fields (discussed below) and thermospheric winds with equatorward components. In addition, within the trough the O^+ loss rate will be increased owing to changes in the reaction rate of equation (A3.1) associated with electric fields and N_2 vibrational excitation, as well as increased N_2^* densities arising from enhanced auroral bombardment in the auroral oval (Schunk and Banks (Ref. 69)).

The mid-latitude trough can arise through a depletion of ionisation involving both ionic reactions, such as those mentioned above, and plasma transport.

Knudsen (Ref. 47) emphasised a different aspect of the nature of high-latitude plasma convection. In his view, the low ion concentrations observed within the trough resulted not from the enhanced recombination in this region, but from the longer time available for recombination to occur.

Spiro et al (Ref. 75) also proposed that the low ion concentrations observed within the trough resulted from the long time spent by plasma in passing through this region, rather than enhanced recombination in the region. Plasma flow in the high latitude ionosphere is characterised by a two-cell convection pattern (seen in Figures 42 and 43) that results from a viscous-like interaction of the wind with the earth's magnetospheric boundary (Axford and Hines (Ref. 7)). In particular, this interaction establishes a magnetospheric polarisation electric field.

(Another electric field can possibly arise in the magnetosphere from the bulk motion with velocity $\underset{\sim}{V}$ of the solar wind past the earth of magnetic induction $\underset{\sim}{B}$, creating a "$\underset{\sim}{V} \times \underset{\sim}{B}$" electric field. A further electric field can arise from a merging of magnetic field lines in the magnetospheric tail, creating an electric field through the motion of the magnetic field lines (Dungey (Ref. 25)). By considering the motion of plasma in the electric fields and the geomagnetic field, the "tear-drop" shape of the equatorial cross-section of the plasmapause (Figure 44) has been explained (e.g. Kavanagh et al (Ref. 43)).

In summary, Knudsen (Ref. 47) appears to have been the first to offer an explanation for the formation of an ionospheric trough on the night-side of the earth. According to this model, magnetic flux tubes are convected from the dayside to the nightside across the polar cap as a result of the impressed magnetospheric electric field. These tubes return to the dayside by subsequently drifting westwards or eastwards. Tubes drifting westwards must travel faster than earth rotation if they are to re-emerge in sunlit regions and some fail to do so, allowing the ionisation in them to fall to very low levels as it recombines. In this model, the trough then is the locus of flux tubes which spend a long period in darkness owing to the competing effects of the convection electric field motion and earth rotation. This model has been refined further through numerical studies (Knudsen et al (Ref. 48)) and a more realistic electric field convection pattern has been proposed by Spiro et al (Ref. 75) based upon Atmospheric Explorer C data. According to the latter, no special convection electric field pattern is required, only that the electric fields fall reasonably smoothly as geomagnetic latitude decreases. There then is always a region on the nightside where convection and corotation exactly balance, creating a stagnation line. Incoherent scatter studies of the convection electric field have been made from Millstone Hill (Evans et al (Ref. 30); Evans et al (Ref. 29)) which appear to support the explanation offered by Spiro et al (Ref. 75) for the night-time trough as it is a region in which the drift velocities appear to be extremely low.

Equatorward of approximately 55 deg invariant latitude, the ionsophere is effectively shielded from the influence of this magnetospheric electric field. At these lower latitudes, a corotation electric field dominates. This field arises through the rotation of the dipole geomagnetic field which produces a radial electric field falling off as $1/R^2$, R being the earth's radius (Hones and Bergeson (Ref. 42)). Plasma flux tubes within this region corotate eastward with the earth under the control of the corotation electric field.

Spiro et al's (Ref. 75) observations of total ion concentration involved the use of a retarding potential analyser on the Atmospheric Explorer C satellite. Their data showed that in the premidnight local time sector, the plasma in the poleward portion of the trough drifts generally westward whie the low-latitude portion rotates eastward. They explained these observations in terms of a plasma drift velocity expressed as:

$$\underset{\sim}{V} = \frac{\underset{\sim}{E} \times \underset{\sim}{B}}{B^2}$$

where B represents the earth's magnetic field strength, and
$\underset{\sim}{E}$ the local electric field.

The reversal of plasma drift velocity would arise through the corotating electric field (effective at lower latitudes) having a direction opposite to the magnetospheric electric field. The long time spent by plasma in the trough region arises as follows. In the premidnight sector, plasma convection in the poleward portion of the trough is mainly westward along the length of the trough with only a small equatorward component. In contrast in the equatorward portion, convection is mainly eastward

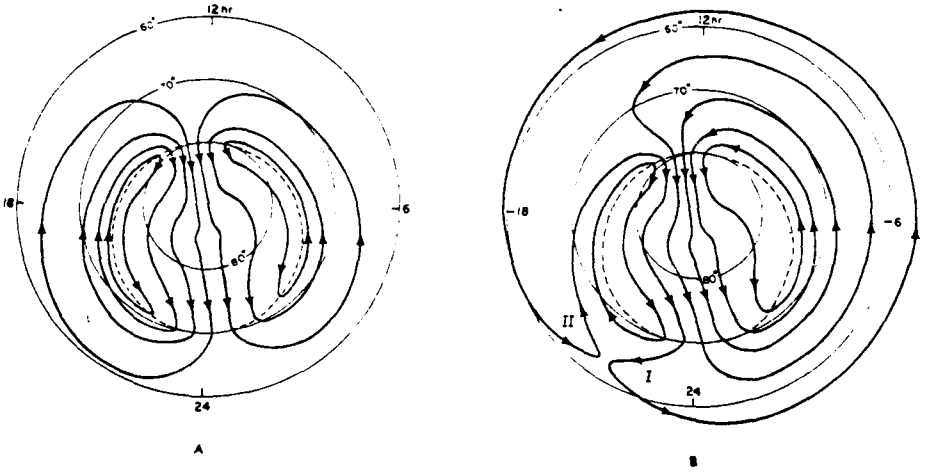

Figure 43. The diagrams are from Spiro et al (Ref. 75). A illustrates the "basic" convection pattern. B indicates the result of adding corotation to the pattern of A. The flow stagnation point is then located at ~22 hours MLT rather than at 18 hours MLT as would otherwise be the case.

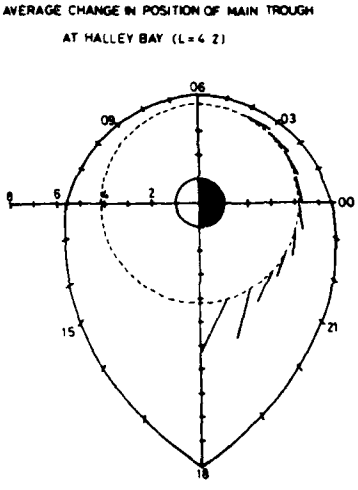

Figure 44. The diagram is from Rodger and Pinnock (Ref. 63). Bars show the mean velocity of main trough in the local hour immediately preceding the time when the poleward edge of the main trough is established over Halley Bay (L = 4.2), the locus of which is shown by the broken line. The radial axis indicates the L shell positions. The locus of the 'tear-drop' model of the plasmapause for quiet magnetic activity is indicated by the continuous line.

along the trough length. In summary, Spiro et al (Ref. 75) indicated that low ion densities within the trough arise where corotation and convective electric fields oppose each other, giving long periods of time in which the plasma decays.

Particle precipitation and the subsequent redistribution of the resulting plasma by the action of the convection electric field were shown to be of primary importance in the formation of the poleward edge of the mid-latitude trough (Pike et al (Ref. 62); Knudsen (Ref. 47); Spiro et al (Ref. 75); Soika et al (Ref. 74)). The location of the plasmapause is mainly controlled by the magnitude of the convection electric field (Lemaire (Ref. 50)) but often there is also significant particle precipitation on or near the geomagnetic field lines which thread the plasmapause where favourable conditions exist for gyro-resonance (Gendrin (Ref. 34)). Rodger and Pinnock (Ref. 63) indicate that, for these reasons a close relationship might be expected between the positions of the trough edge and the plasmapause. They observed similarities in their movements and positions on a time-scale of one hour or more during periods of low geomagnetic activity. However, there were dissimilarities during periods of high geomagnetic activity, as was also observed by Grebowsky et al (Ref. 36). The similarities probably reflect the importance of the convection electric field and particle precipitation on the formation of the plasmapause and the poleward edge of the trough.

Schunk et al (Ref. 72) have combined a simple plasma convection model with an ionospheric-atmospheric composition model incorporating ideas of the kind outlined above in this section, in order to simulate high-latitude ionospheric behaviour which is found to be in reasonable agreement with observation.

APPENDIX 4

COMPUTATION OF THE LOCATION, HEIGHT AND LATITUDINAL EXTENT OF THE MID-LATITUDE TROUGH

This appendix describes the results of preliminary computations of the location, height and latitudinal extent of the mid-latitude trough, and briefly indicates the reasoning (following that in Section 4.5) which led to the computations which were performed by Mr. G.D. Slade.

A modified version of the DRCS RADFIN program was employed. The latitudinal extent of the trough was determined using a subroutine developed by B.W. Halcrow and J.S. Nisbet based on their paper (Ref. 39).

The height of the F2 layer in the region where the trough exists was determined by modifying the CCIR Worldwide Numerical Map Data (Ref. 15). From the discussion in Section 4.4, the height h_m of the contour of maximum F2 region electron density within the trough was assumed to be 200 km above the height h_c of an equal electron density contour in the CCIR (i.e. "normal") data:

$$\text{i.e.} \quad h_m = h_c + 200 \text{ km}$$

As indicated in Section 4.5, the ratios of the heights of other electron density contours within the trough were taken to be the same as the ratios for the corresponding electron density contours derived from Ref. 15. (In this context the "height" was taken to be the altitude of a contour within the trough minus the altitude of the contour remote from the trough.)

An example of preliminary computations made on this basis is shown in Figure 45.

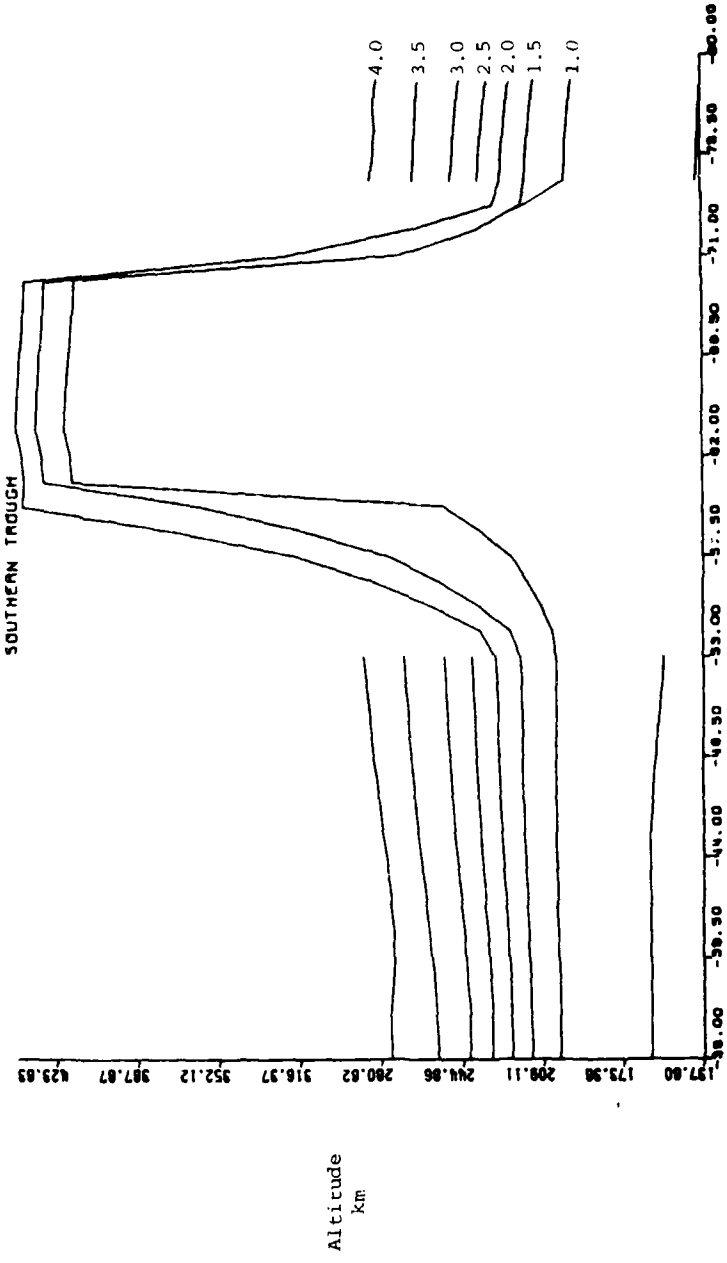

Figure 45. A computed mid-latitude trough is shown superimposed on contours of constant electron density (having plasma frequencies (MHz) as indicated) derived from data in Ref. 15 for the longitude of Adelaide at 11.00 UT in July and zero sunspot number.

REFERENCES

No.	Author	Title
1	Ahmed, M. and Sagolyn, R.C.	"Topside Ionospheric Trough Morphology at Mid- and High-Latitudes", Compilation of papers presented by the Space Physics Division at the Ionospheric Effects Symposium, Air Force Geophysics Lab., Hanscon AFB, Massachusetts, Report AFGL-TR-78-0080, April 1978.
2	Ahmed, M., Sagolyn, R.C., Wildman, P.J.L. and Burke, W.J.	"Topside Ionospheric Trough Morphology: Occurrence Frequency and Diurnal, Seasonal and Altitude Variations", J.Geophys.Res., 84, 489, 1979.
3	Alfvén, H.	"Some Properties of Magnetospheric Neutral Surfaces", J.Geophys.Res., 73, 13, 1968.
4	Alouette I	"Alouette I Ionospheric Data - Interpolated N(h)", 1-6, Department of Communications, Defense Research Telecommunications, Ottawa, Canada, 1968.
5	Aluoette II	"Alouette II Ionospheric Data - Interpolated, N(h)", 1-2, Department of Communications, Defense Research Telecommunications, Ottawa, Canada, 1970.
6	Amayenc, P., Bertin, F. and Papet-Lepine, J.	"Sur l'Evolution Latitudinal de Contenu Electronique de l'Ionosphere", Ann.de Géophys., 27, 345, 1971.
7	Axford, W.I. and Hines, C.O.	"A Unifying Theory of High-Latitude Phenomena and Geomagnetic Storms", Can.J.Phys., 39, 1433, 1961.
8	Banks, P.M., Schunk, R.W. and Raitt, W.J..	"NO^+ and O^+ in the High-Latitude F-region", Geophys.Rev.Lett., 1, 239, 1974.
9	Belrose, J.S.	"The Lower Ionospheric Regions", Chapter 3 of "Physics of the Earth's Upper Atmosphere", ed. Hines, C.O., Paghis, J. Hartz, T.R. and Fejer, J.A., 1965
10	Bowman, G.G.	"Directional Characteristics of Ionosonde Interference Patterns from the Filchner Ice Shelf", J.Atmos.Terr.Phys., 30, 1115, 1968.
11	Bowman, G.G.	"Ionization Troughs Below the F2-layer Maximum", Planet.Space Sci., 17, 777, 1969.

No.	Author	Title
12	Buchau, J., Pike, C.P. and Wong, M.	"Detailed Specification of the Arctic Ionosphere and an Application of Three-Dimensional Raytracing", Air Force Cambridge Research Laboratories, Report No. AFCRL-TR-73-0726, November 1973.
13	Burge, J.D., King, J.W. and Slater, A.J.	"Mapping of f_0F2 by Means of Topside Sounder Satellites", Telecommunication Journal, 40, 356, 1973.
14	C.C.I.R. (International Radio Consultative Committee)	Recommendations and Reports of the C.C.I.R., "Propagation in Ionized Media", vol. VI, XIVth Plenary Assembly (Kyoto), Geneva, 1978.
15	C.C.I.R. (International Radio Consultative Committee)	Report 340 concerning the C.C.I.R. Atlas of Ionospheric Characteristics (Oslo 1966), International Telecommunication Union, Geneva, 1967.
16	C.C.I.R. (International Radio Consultative Committee)	15th Plenary Assembly (Document 6/1004-E), Geneva, 1982.
17	Chako, C.C. and Mendillo, M.	Report No. AFGL-TR-78-0092(I), Air Force Geophysics Labs., Hanscomb, Massachusetts, 1967.
18	Chan, K.L. and Colin, L.	"Global Electron Density Distributions from Topside Soundings", Proc. IEEE, 57, 990, 1969.
19	Clynch, J.R. and Renfro, B.A.	"Evaluation of Ionospheric Range Error Model", Proc. Third International Geodetic Symposium on Satellite Doppler Positioning, Vol. 1; Sponsor: Dense Mapping Agency and National Ocean Survey; Host: Physical Science Lab. of New Mexico State Uni., Las Cruces, 497, February, 1982.
20	COMSAT General Corporation	"MARISAT System Description", prepared by C.G.C. as Manager of the MARISAT Joint Venture, March 1977.
21	Conkright, R.O. and Brophy, H.J.	Catalog of Ionosphere Vertical Soundings Data, Report UAG-85, World Data Center A for Solar-Terrestrial Physics, U.S. Dept. of Commerce, National Oceanic and Atmospheric Administration Environmental Data and Information Service, Boulder, Colorado, U.S.A., 80303, July 1982.
22	Dudeney, J.R.	"The Ionosphere - a View from the Pole", New Scientist, September 17, 1981.
23	Dudeney, J.R., Jarvis, M.J., Kressman, R.I., Pinnock, M., Rodger, A.S. and Wright, K.H.	"Ionospheric Troughs in Antarctica", Nature, 295, 307, 1982.

No.	Author	Title
24	Dudeney, J.R. and Piggott, W.R.	"Antarctic Ionospheric Research", Antarctic Research Series (American Geophysical Union), 29, 200, 1978.
25	Dungey, J.W.	"Interplanetary Magnetic Field and the Auroral Zones", Phys.Rev.Letters, 6, 47, 1961.
26	ERNO Raumfahrttechnik GMBH	"SARSAT, Ein Rettungssystem für Schiffe und Flugzeuge", Report 80-054, Bremen, West Germany, October 1980. (English translation: NASA Technical Memo., NASA TM-76391, "SARSAT: A Rescue System for Ships and Airplanes".
27	Essex, E.A. and Day, T.W.	"The Differential Doppler Technique and its Use in Measuring the Spatial and Temporal Variation of Irregularities in the Ionosphere", Monitor - Proc. of the IREE Aust., 104, 1978.
28	Evans, J.E. Newkirk, L.L. and McCormac, B.W.	"North Polar, South Polar, World Maps and Tables of Invariant Magnetic Co-ordinates for Six Altitudes: 0, 100, 300, 600, 1000 and 3000 km", Final Report DASA 2347 (N-9A-69-1) to the Defense Atomic Support Agency, Washington D.C. from Lockheed Palo Alto Research Laboratory, October, 1969.
29	Evans, J.V., Holt, J.M., Oliver, W.L. and Ward, R.H.	"Millstone Hill Incoherent Scatter Observations of Auroral Convection over 60 deg $\leq$ Invariant Latitude $\leq$ 75 deg, 2. Initial Results", J.Geophys.Res., 85, 41, 1980.
30	Evans, J.V., Holt, J.M., and Wand, R.H.	"Millstone Hill Incoherent Scatter Observations of Auroral Convection over 60 deg $\leq$ Invariant Latitude $\leq$ 75 deg, 1. Observing and Data Reduction Procedures", J.Geophys.Res., 84, 7059, 1979.
31	Evans, J.V. and Wand, R.H.	"Anomalous Ionospheric Refraction Associated with the Auroral Zone", article in "Effect of the Ionosphere on Radiowave System" (editor-in-chief J.M. Goodman) based on Ionospheric Effects Symposium at Old Town, Alexandria, Vancouver, sponsored by Naval Res. Lab. Office of Naval Res. and Air Force Geophys. Lab., April 1981.
32	Feinblum D.A. and Horan, R.J.	"HILION - A Model of the High-Latitude Ionospheric F2 Layer and Statistics of Regular Ionospheric Effects at Fort Churchill, 1968", Joint Radar Propagation Study of Bell Laboratories, Western Electric and Lincoln Laboratory, Massachusetts Institute of Technology, for U.S. Army Safeguard System Command under Contract DAHC60-71-C-0005 and for Advanced Ballistic Missile Defence Agency under Contract F19628-73-C-0002, 1973.

No.	Author	Title
33	Filz, R.C., Katz, L., Kuck, G.A., Shea, M.A. and Smart, D.F.	"Corpuscular Radiation", A revision of Chapter 17, "Handbook of Geophysics and Space Environments", Air Force Cambridge Research Labs., AFCRL-68-0666, Air Force Surveys in Geophysics, No. 208, December 1968.
34	Gendrin, R.	'Is the Plasmapause a Preferential Region for Proton Precipitation?", Annls.Geophys., 31, 127, 1975.
35	George, P.L.	"HF Skywave Aspects of Trunk-Area Communications ESM", Department of Defence, Defence Science and Technology Organisation, Electronics Research Laboratory, Defence Research Centre, Salisbury, Tech. Memo, ERL-0234-TM (unclassified), April 1982.
36	Grebowsky, J.M., Hoffman, J.H. and Maynard, N.C.	"Ionospheric and Magnetospheric Plasma-pauses", Planet.Space Sci., 26, 651, 1978.
37	Guier, W.H. and Weiffenbach, G.C.	"A Satellite Doppler Navigation System", Proc. I.R.E., 507, 1960.
38	Halcrow, B.W.	"F2 Peak Electron Densities in the Main Trough Region of the Ionosphere", Report No. PSU-IRL-IR-55, Contract: NASA NGL 39-009-003, Ionosphere Research Lab., Pennsylvania State Uni., May 1976.
39	Halcrow, B.W. and Nisbet, J.S.	"A Model of F2 Peak Electron Densities in the Main Trough Region of the Ionosphere", Radio Sci., 12, 815, 1977.
40	-	"Handbook for Radiotelephone Ship Station Operators", ISBN 0-642-01431-0 (Australian Government Printing Service, Canberra), 1981.
41	Heaps, M.G.	"Accounting for Ionospheric Variability and Irregularity in High Frequency Direction Finding", article in "Effect of the Ionosphere on Radiowave Systems" (editor-in-chief J.M. Goodman) based on Ionospheric Effects Symposium at Old Town, Alexandria, Vancouver, sponsored by Naval Res. Lab. Office of Naval Res. and Air Force Geophys. Lab., April 1981.
42	Hones, E.W. and Bergeson, J.E.	"Electric Field Generated by a Rotating Magnetized Sphere", J.Geophys.Res., 70, 4951, 1965.
43	Kavanagh, L.D. Freeman, S.W. and Chen, A.J.	"Plasma Flow in the Magnetosphere", J.Geophys.Res., 73, 5511, 1968.

No.	Author	Title
44	King, J.W.	"The Determination of F_0F2 and h_mF2 from Satellite-borne Probe Data", Telecommunication Journal, 40, 364, 1973.
45	Klobuchar, J.A.	"Total Electron Content Studies of the Ionosphere", Report TR-73-0098, Air Force Cambridge Research Labs., Bedford, Massachusetts, U.S.A., 1973.
46	Knecht, D.J.	"The Geomagnetic Field (A Revision of Chapter 11, Handbook of Geophysics and Space Environments", Air Force Surveys in Geophysics No. 246, AFCRL-72-0570, September 1972.
47	Knudsen, W.C.	"Magnetospheric Convection and the High-Latitude F2 Ionosphere", J.Geophys.Res., 79, 1046, 1974.
48	Knudsen, W.C., Banks, P.M. Winningham, J.D. and Klumpar, D.M.	"Numerical Model of the Convecting F2 Ionosphere at High Latitudes", J.Geophys.Res., 82, 4784, 1977.
49	Kohnlein, W. and Raitt, W.J.	"Position of the Mid-Latitude Trough on the Topside Ionosphere as Deduced from Esro 4 Observations", Planet.Space Sci., 25, 600, 1977.
50	Lemaire, J.	"The Mechanisms of Formation of the Plasma-pause", Annls.Geophys., 31, 175, 1975.
51	Lietinger, R., Hedberg, A. and Tanskanen, P.	"The Electron Content of the Ionosphere and the Southern Boundary of Diffuse Aurora", J.Atmos.Terr.Phys., 44, 369, 1982.
52	Liszka, L.	"The High-Latitude Trough in Ionospheric Electron Content", J.Atmos.Terr.Phys., 29, 1243, 1967.
53	Lockwood, M.	"The Bottomside Mid-Latitude Ionospheric Trough", J.Atmos.Terr.Phys., 42, 605, 1980.
54	Lockwood, M.	"A Simple Model of the Effects of the Mid-Latitude Total Ion Trough in the Bottomside F layer on HF Radiowave Propagation", Radio Science, 16, 3, 385, 1981.
55	Lyon, G.F.	"Ionospheric Effects of the SARSAT System", Canad.Aeronaut.Space Journal, 27, 327, 1981.
56	McIlwain, C.E.	"Co-ordinate for Mapping the Distribution of Magnetically Trapped Particles", J.Geophys.Res., 66, 11, 3681, 1961.
57	Mendillo, M. and Chako, C.C.	"The Baselevel Ionospheric Trough", J.Geophys.Res., 82, 5129, 1977.

No.	Author	Title
58	Mendillo, M. and Klobuchar, J.A.	"Investigations of the Ionospheric F-region Using Multi-station Total Electron Content Observations", J.Geophys.Res., 80, 643, 1975.
59	Muldrew, D.B.	"F-layer Ionization Troughs Deduced from Alouette Data", J.Geophys.Res., 70, 15, 3635, 1965.
60	Mundo, C., Tami, L. and Larsen, G.	"Final Report Program Plan for Search and Rescue Electronics Alerting and Locating System", DOT-TSC-OST-73-42, February 1974.
61	Nishida, A.	"Average Structure of the Storm-time Change in the Polar Topside Ionosphere at Sunspot Minimum", J.Geophys.Res., 72, 6051, 1967.
62	Pike, C.P., Whalen, J.A. and Buchau, J.	"A 12-hour Case Study of Auroral Phenomena in the Midnight Sector", J.Geophys.Res., 82, 3547, 1977.
63	Rodger, A.S. and Pinnock, M.	"The Variability and Predictability of the Main Ionospheric Trough", from C.S. Deehr and J.A. Holder (eds.), "Exploration of the Polar Upper Atmosphere" (D. Reidel Publ. Co.), 463, 1980.
64	Rodger, A.S. and Pinnock, M.	"Movements of the Mid-Latitude Ionospheric Trough", J.Atmos.Terr.Phys., 44, 985, 1982.
65	Rush, C.M., Rosich, R.K., Brooks, C.B. and Leise, D.L.	"A Simplified Model of the High Latitude Ionosphere for Telecommunications Applications", NTIA Report 82-94, U.S. Dept. of Commerce, National Telecommunications and Information Service, Boulder, Colorado, January 1982.
66	Rycroft, M.J. and Burnell, S.J.	"Statistical Analysis and Movements of the Ionospheric Trough and the Plasmapause", J.Geophys.Res., 75, 5600, 1970.
67	Rycroft, M.J. and Thomas, J.O.	"The Magnetospheric Plasmapause and the Electron Density Trough at the Alouette I Orbit", Planet.Space Sci., 18, 65, 1970.
68	Sagolyn, R. Bredesen, S. and Wildman, P.	Article in "An Empirical Model of the Polar Ionosphere", ed. T.J. Elkins, Air Force Surveys in Geophysics No. 267, AFCRL-TR-73-0331, May 1973.
69	Schunk, R.W. and Banks, P.M.	"Auroral N_2 Vibrational Excitement of the Electron Density Trough", Geophys.Res.Letters, 2, 6, 239, 1975.
70	Schunk, R.W., Banks, P.M. and Raitt, W.J.	"Effects of Electric Fields and Other Processes Upon the Night-Time High-Latitude F-layer", J.Geophys.Res., 81, 3271, 1976.

No.	Author	Title
71	Schunk, R.W., Raitt, W.J. and Banks, P.M.	"Effect of Electric Fields on the Day-time High-Latitude E and F regions", J.Geophys.Res., 80, 3121, 1975.
72	Schunk, R.W., Raitt, W.J. and Sojka	"High-Latitude Ionospheric Model: First Step Towards a Predictive Capability", article in "Effect of the Ionosphere on Radiowave Systems" (editor-in-chief J.M. Goodman) based on Ionospheric Effects Symposium at Old Town, Alexandria, Vancouver, sponsored by Naval Res. Lab. Office of Naval Res. and Air Force Geophys. Lab., April 1981.
73	Sharp, G.W.	"Mid-Latitude Trough in the Night Ionosphere", J.Geophys.Res., 71, 1345, 1966.
74	Soika, J.J., Raitt, W.J. and Schunk, R.W.	"Theoretical Predictions for Ion Composition in the High-Latitude Winter F-region for Solar Minimum and Low Magnetic Activity", J.Geophys.Res., 86, 2206, 1981.
75	Spiro, R.W., Heelis, R.A. and Hanson, W.B.	"Ion Convection and the Formation of the Mid-Latitude F Region Ionization Trough", 83, A9, 4255, 1978.
76	Stansell, T.A.	"The Transit Navigation Satellite System", Magnavox Government and Industrial Electronics Co., R-5933, October 1978.
77	Thomas, J.O. and Dufour, S.W.	"Electron Density in the Whistler Medium", Nature, London, 206, 567, 1965.
78	Tulunay, Y.K.	"Magnetically Symmetric Detection of the Mid-Latitude Electron Density Trough by Ariel III Satellite", J.Atmos.Terr.Phys., 34, 1547, 1972.
79	Tulunay, Y.K. and Grebowsky, J.M.	"The Noon and Midnight Mid-Latitude Trough as seen by Ariel IV", J.Atmos.Terr.Phys., 40, 845, 1978.
80	Tulunay, Y.K. and Sayers, J.	"Characteristics of the Mid-Latitude Trough as Determined by the Electron Density Experiment of Ariel III", J.Atmos.Terr.Phys., 33, 1737, 1971.
81	Wrenn, G.L. and Raitt, W.J.	"In Situ Observations of Mid-Latitude Ionospheric Phenomena Associated with the Plasmapause", Ann.Geophys., 31, 17, 1975.
82	Zawalick, E.J. and Cage, A.L.	"Frequency Tables of the Geomagnetic Index Kp, 1932-1970", J.Geophys.Res., 76, 7009, 1971.

DISTRIBUTION

Copy No.

EXTERNAL

In United Kingdom

	Cnt Sht Only
Counsellor, Defence Science, London	
British Library, Document Supply Centre (UK)	1
Institution of Electrical Engineers	2
British Antarctic Survey, Natural Environ Res Council	
(Attention: Dr J.R. Dudeney)	3
(Attention: Dr W.R. Piggott)	4
University of Leicester, Ionospheric Physics Group	
(Attention: T.B. Jones)	5
Rutherford-Appleton Laboratory	
(Attention: Dr J.W. King)	6
University College London, Mullard Space Sci Lab	
(Attention: Dr W.J. Raitt)	7
University of Southampton, Dept of Physics	
(Attention: Dr M.J. Rycroft)	8
University College of Wales, Physics Dept	
(Attention: Prof L. Thomas)	9

In United States of America

	Cnt Sht Only
Counsellor, Defence Science, Washington	
NASA Scientific and Technical Information Office	10
Regis College	
(Attention: Dr M. Ahmed)	11
Pennsylvania State University, Ionospheric Res Lab	
(Attention: Dr R.L. Divany)	12
SAMSO	
(Attention: Dr B.W. Halcrow)	13
Lockheed Palo Alto Res Lab	
(Attention: Dr W.C. Knudsen)	14
Boston University, Dept of Astronomy	
(Attention: Dr M. Mendillo)	15
Pennsylvania State University, Ionospheric Res Lab	
(Attention: Dr J.S. Nisbet)	16
Air Force Cambridge Res Lab, Ionospheric Physics Lab	
(Attention: Dr R.C. Sagolyn)	17

University of California at San Diego, Dept Applied Phys
(Attention: Dr R.W. Schunk) 18

Magnavox Gov and Indust Electronics
(Attention: Mr T.A. Stansell) 19

In Canada

University of Western Ontario, Physics Dept
(Attention: Prof G.F. Lyon) 20

In Germany

University of Bonn, Astronomical Institute
(Attention: Dr W. Kohnlein) 21

In Turkey

Technological University
(Attention: Dr Y.K. Tulunay) 22

In New Zealand

University of Auckland, Radio Res Centre
(Attention: Dr M. Lockwood) 23

In Australia

Chief Defence Scientist

Assistant Chief Defence Scientist (Policy) 24

Assistant Chief Defence Scientist (Operations)

Joint Intelligence Organisation (DSTI)
(Attention: HST-AF) 25

Defence Signals Directorate 26

Director General, Joint Communications and Electronics
(Attention: DJCE(PP)) 27

Director, Naval Intelligence and Security
(Attention: DDNI) 28

Director, Electronic Warfare - Navy 29

Director, Military Intelligence
(Attention: SO1(EW)) 30

Director General, Operational Requirements - Air Force
(Attention: OREW) 31

Director, Air Force Intelligence and Security
(Attention: ISINT) 32

Director, Communications and Electronics - Air Force
(Attention: CERCOM2) 33

Document Exchange Centre,
Defence Information Services Branch for:

Microfiche copying	34
United Kingdom, Defence Research Information Centre	35 - 36
United States, Defense Technical Information Center	37 - 48
Canada, Director, Scientific Information Services	49
New Zealand, Ministry of Defence	50
National Library of Australia	51

Director General, Army Development (NSO), Russell Offices
for ABCA Standardisation Officers

UK ABCA representative, Canberra	52
US ABCA representative, Canberra	53
Canada ABCA representative, Canberra	54
NZ ABCA representative, Canberra	55

Librarian, Technical Reports Centre, Defence Central Library, Campbell Park	56
Library, DSD, Melbourne	57
Library, Materials Research Laboratories	58
Library, RAN Research Laboratory	59
Library, Aeronautical Research Laboratories	60
Director, Industry Development, Adelaide	Cnt Sht Only
South Aust Inst of Tech, Physics Dept (Attention: Prof G.L. Goodwin)	61 - 62
University of Queensland, Physics Dept (Attention: Dr G.G. Bowman)	63
University of Adelaide, Physics Dept (Attention: Dr B.H. Briggs)	64
(Attention: Dr R.A. Vincent)	65
LaTrobe University, Div of Theoretical and Space Physics (Attention: Prof K.D. Cole)	66

INTERNAL

Director, Electronics Research Laboratory	67
Superintendent, Electronic Warfare Division	68
Superintendent, Communications Division	69
Principal Officer, Radio Wave Propagation Group	70

DOCUMENT CONTROL DATA SHEET

Security classification of this page : UNCLASSIFIED

1 DOCUMENT NUMBERS

AR Number : AR-005-365

Series Number : ERL-0449-SD

Other Numbers :

2 SECURITY CLASSIFICATION

a. Complete Document : Unclassified

b. Title in Isolation : Unclassified

c. Summary in Isolation : Unclassified

3 DOWNGRADING / DELIMITING INSTRUCTIONS

Limitation to be reviewed in March 1991

4 TITLE

LOCATING THE SOURCE OF LONG-DISTANCE RADIO DISTRESS SIGNALS FROM THE SOUTHERN OCEAN

5 PERSONAL AUTHOR (S)

G.L. Goodwin

6 DOCUMENT DATE

March 1988

7 7.1 TOTAL NUMBER OF PAGES 94

7.2 NUMBER OF REFERENCES 82

8 8.1 CORPORATE AUTHOR (S)

Electronics Research Laboratory

8.2 DOCUMENT SERIES and NUMBER

Special Document
0449

9 REFERENCE NUMBERS

a. Task :

b. Sponsoring Agency :

10 COST CODE

720350

11 IMPRINT (Publishing organisation)

Defence Science and Technology Organisation Salisbury

12 COMPUTER PROGRAM (S) (Title (s) and language (s))

13 RELEASE LIMITATIONS (of the document)

Approved for Public Release.

Security classification of this page : UNCLASSIFIED

Security classification of this page : UNCLASSIFIED

14 ANNOUNCEMENT LIMITATIONS (of the information on these pages)

No limitation

15 DESCRIPTORS		**16 COSATI CODES**
a. EJC Thesaurus Terms	Distress Signals Position (location) Radio signals Search and rescue Ionospheric propagation	0045C
b. Non - Thesaurus Terms	NAVSAT	

17 SUMMARY OR ABSTRACT
(if this is security classified, the announcement of this report will be similarly classified)

This report summarises a feasibility study and strategy appropriate to search and rescue operations for ships or aircraft in distress in the Southern Ocean. The use of high frequency ionospherically-propagated radio transmissions is justified. Measurement of the direction of arrival of a radio signal facilitates ray-tracing through the ionosphere Characteristics of the F2 region mid-latitude ionisation trough are considered in detail. Because the trough is displaced towards Australia, its position must be known as near as practicable in real time for sufficiently accurate ray-tracing to be performed quickly enough after receipt of a distress signal. The differential Doppler technique using e.g. 150 and 400 MHz tranmissions tram NAVSAT (NNSS) satellites is recommended in locating the trough position.

Security classification of this page : UNCLASSIFIED